Acetyl-CoA Carboxylase 1 (ACC1) Regulates Endothelial Cell Migration by Shifting the Membrane Lipid Composition

Dissertation
zur Erlangung des Doktorgrades
der Naturwissenschaften

vorgelegt beim Fachbereich 14
Biochemie, Chemie und Pharmazie
der Johann Wolfgang Goethe-Universität
in Frankfurt am Main

von
Daniel Karl Glatzel
aus Oldenburg

Frankfurt am Main, 2018
(D 30)

Vom Fachbereich Biochemie, Chemie und Pharmazie (FB 14) der
Johann Wolfgang Goethe-Universität als Dissertation angenommen.

Dekan: Prof. Dr. Clemens Glaubitz
1. Gutachter: Prof. Dr. Robert Fürst
2. Gutachter: Prof. Dr. Rolf Marschalek

Datum der Disputation: 18.04.2018

deeply grateful and with love dedicated to my mother, father and brother

TABLE OF CONTENTS

1 INTRODUCTION

1.1 The vascular endothelium

In the recent years, the understanding of the structure and function of the endothelium has been vastly extended. In the 1980s, the newly acquired knowledge has shifted the role of the endothelium from a simple barrier to a highly specialized, metabolically active player in the regulation of homeostasis and physiological or pathological processes like inflammation, vascular wall remodeling or thrombosis. This knowledge helped developing new strategies for the treatment of atherosclerosis and the inhibition of tumor growth by new antiangiogenic drugs (1, 2).

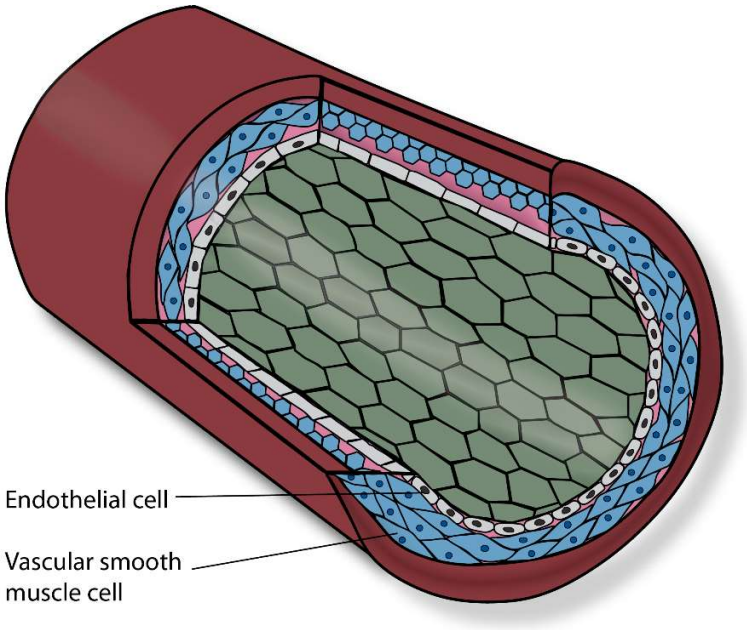

Figure 1: The vascular endothelium.
Endothelial cells are forming the inner lining of artery walls longitudinally, the outer layers are formed by vascular smooth cells circumferentially. Figure according to Hahn *et al.* (3).

The vascular endothelium consists of a monolayer of endothelial cells forming the inner lining of each blood vessel, ranging from the heart to the smallest capillaries (2, 4, 5) (see Figure 1). This layer provides a barrier that tightly controls the passage of fluids, solutes, macromolecules and cells from the blood to the underlying tissue (6, 7). Endothelial cells are sensitive to changes in the blood flow as well as blood composition and respond to these changes. This fluid-controlling role of the endothelium is mediated by membrane-bound receptors (8). Besides its function as a dynamic barrier, the vascular endothelium can also be regarded as a multifunctional paracrine

and endocrine organ within the cardiovascular system (7, 9). Thereby, the vascular endothelium regulates physiological processes, such as blood flow, homoeostasis and the vascular tone (7, 8) and also participates in the pathophysiology of cardiovascular diseases, such as chronic heart failure, chronic kidney failure, coronary artery disease, diabetes, hypertension, peripheral vascular disease and viral infections (e.g., viral hemorrhagic fever) (4, 10-17). Thus, the knowledge of the vascular endothelium regarding its physiology and its cell interactions is worth to be expanded (2).

One of the most common models for studying endothelial cell biology in general are human umbilical vein endothelial cells (HUVECs). These cells are an established, well characterized and widely accepted model used for scientific research *in vitro*. HUVECs are isolated by collagenase digestion of umbilical veins and have been cultured in 1973 for the first time (18). In this study, mainly the macrovascular HUVECs are used as a model organism for human endothelial cells. Besides macrovascular HUVECs, also the microvascular human dermal microvascular endothelial cell line (HMEC-1) was used in this study (see 2.2.2).

1.1.1 Endothelial cell migration

A very important function of endothelial cells is their ability to migrate. This fundamental process already plays a crucial role in the early phase of life. It is essential during the development in gastrulation cells to form the three layers of an embryo. Migration becomes also essential in forming tissues and organs as well as during wound healing, tissue regeneration and in maintaining the homeostasis (19, 20). Under physiological and pathological conditions, endothelial cell migration is necessary for the formation of new blood vessels, a process called angiogenesis (see 1.2.2) (20). A disturbed endothelial cell migration is part of the pathogenesis and progression of many severe disorders, such as ischemia reperfusion injury, diabetic angiopathy, macular degeneration, rheumatoid arthritis, wound healing defects, immunosuppression and cancer (19, 20). Consequently, pharmacological modulation of endothelial cell migration offers interesting therapeutic prospects.

Depending on the cell type, migrating cells can move randomly or directly towards a chemoattractant, organized in groups, sheets or individually. Nevertheless, certain characteristics in migration are typical for all cell types. Migrating cells have an asymmetric morphology, which consists of a leading and a trailing edge. Membrane protrusions on the leading edge attach to the

underlying substrate, while cellular attachments at the distal end are released by cellular contractions and traction forces (20).

Endothelial cell migration is an interplay of three different movement patterns: (i) chemotaxis, the directional movement towards a soluble, chemical stimulus; (ii) haptotaxis, the directional movement towards a gradient of immobilized ligands, namely extracellular matrix components such as collagen I and fibrin; and (iii) mechanotaxis, the directional movement via mechanical cues (19, 21-23). In this study, the focus is based on chemotaxis, whereas haptotaxis and mechanotaxis are not covered.

Chemotactic migration is regulated by a broad spectrum of different cytokines. The three major actors of chemotaxis during angiogenesis are vascular endothelial growth factor (VEGF), basic fibroblast growth factor (bFGF) and angiopoietins. Other promotors are: platelet-derived growth factor (PDGF), fibroblast growth factor (FGF-2), transforming growth factor-β (TGF-β), epidermal growth factor (EGF), tumor necrosis factor-α (TNF-α), platelet-activating factor (PAF), hepatocyte growth factor (HGF), interleukins, ephrins, soluble adhesion molecules, endoglin and angiogenin (19). In response to VEGF, the Ras/Raf/MEK/ERK1/2 pathway is known to be essential in regulating endothelial cell functions like proliferation and migration (24).

1.1.2 Actin remodeling during endothelial cell migration

During migration, the actin remodeling into stress fibers, lamellipodia and filopodia represents an integral function of endothelial cells (19). Stress fibers are bundles of actin filaments with inverted polarity. They are linked by myosin II and accessory proteins, such as tropomyosin. Lamellipodia are cytoplasmic protrusions, which consist of a thick cortical network of actin filaments. These protrusions are approximately 2 µm thick, 1 to 5 µm wide and are located at the leading edge of migrating cells (25). Filopodia consist of bundled, parallel actin filaments. These finger-like projections have important sensory and exploratory functions, especially in cell motility (26-29). The three different actin-structures are displayed in Figure 2.

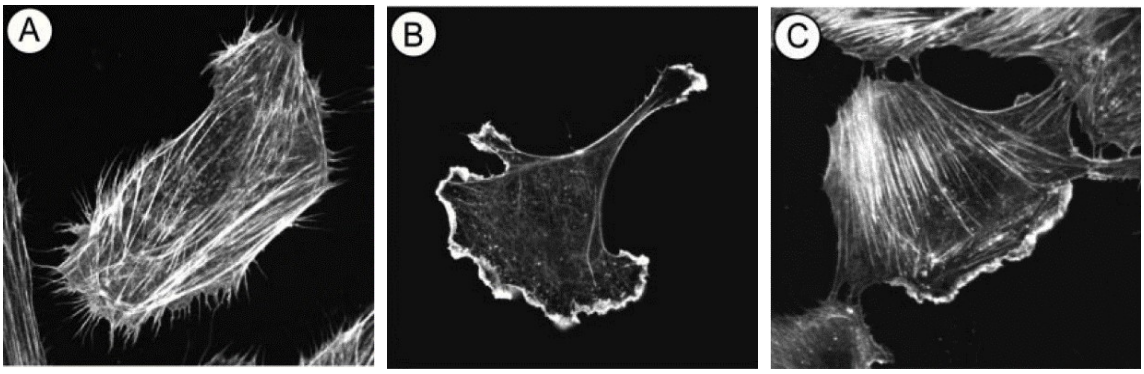

Figure 2: Actin remodeling involved in endothelial cell migration.
HUVECs treated with VEGF showing (A) filopodia, (B) lamellipodia or (C) stress fibers. The figure was adapted from Lamalice *et al*. (unpublished data from François, 2006) (19) and is reprinted with permission from Wolters Kluwer Health, Inc.

Lamellipodia, filopodia and stress fibers mediate the actin-based migration of endothelial cells. This process is divided into the following six steps and pictured in Figure 3: (i) In the first Cdc42 dependent step, filopodia sense motile stimuli; (ii) followed by cellular extension by the Rac-1 dependent development of lamellipodia. (iii) Part of the third step is the attachment of protrusions to the extracellular matrix of focal adhesions kinases (FAK) such as vinculin, talin or paxillin. (iv) In the fourth step, the cell body contraction *via* stress fibers results in forward progression and (v) the distal end is released by traction forces mediated trough stress fibers. Finally, (vi) the adhesive and the signaling components are recycled (19).

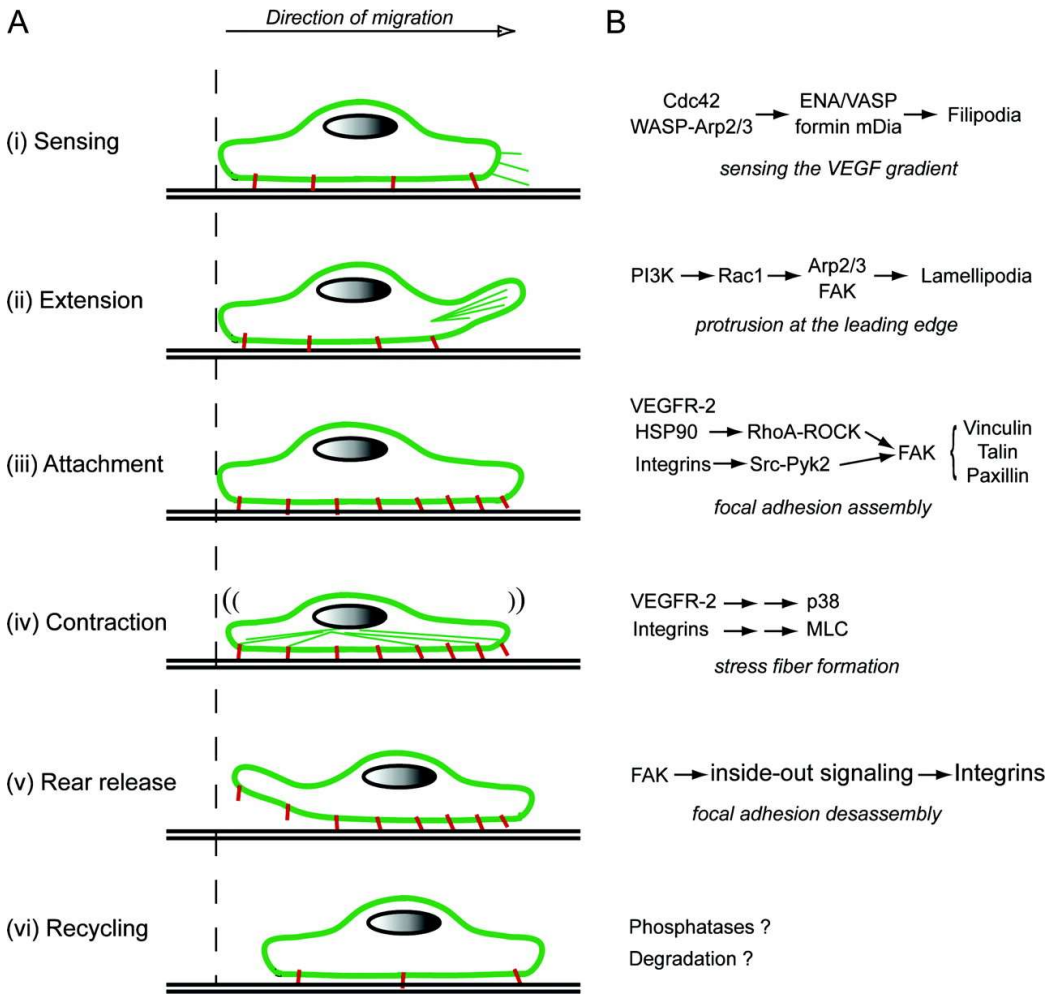

Figure 3: The six major phases of endothelial cell migration.
(A) Steps of migration. (B) Signaling events associated with the respective migration phase. The figure is reprinted from Lamalice *et al.* (19) with permission from Wolters Kluwer Health, Inc.

1.2 Neoangiogenesis

Blood vessels are needed to provide each cell of the body with blood containing oxygen and nutrients on the one hand and to deplete CO_2 and cellular waste on the other hand (30). Blood vessels are classified into three main types: arteries, veins and capillaries. Neoangiogenesis is defined as the formation of new blood vessels, which is proceeded in two steps during embryogenesis: During the process of vasculogenesis, endothelial cells derive from progenitor cells and during angiogenesis, new blood vessels are formed from existing vessels (31, 32) (see Figure 4). All blood vessels in the human body are created by these processes.

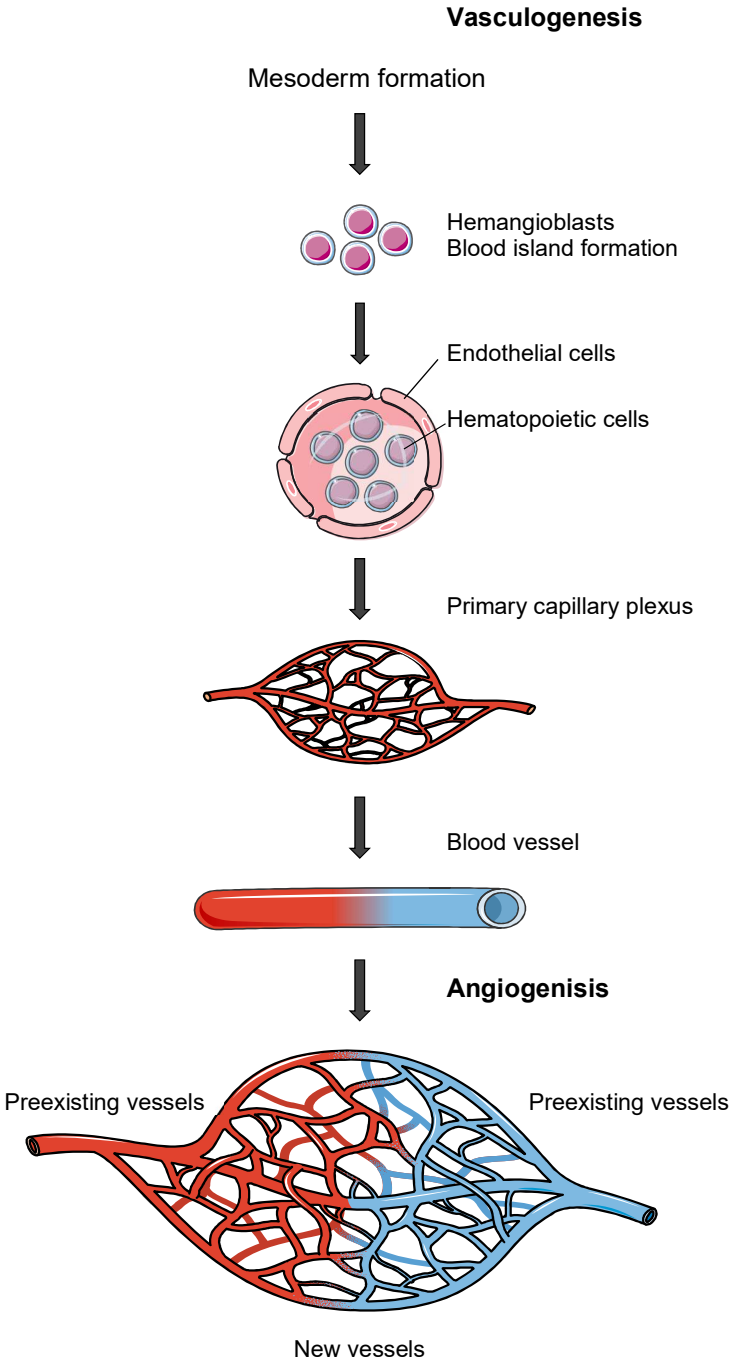

Figure 4: The origin of the vascular system.
Primitive blood islands are formed by differentiation of mesodermal cells into hemangioblasts, followed by differentiation of hemangioblasts into angioblasts. Migrating endothelial cells promote blood island fusion and their remodeling into tubular structures. By the process of vasculogenesis, the first primitive vascular plexus is remodeled into larger vessels. Angiogenesis is defined as the formation of new blood vessels out of preexisting ones. Figure according to Karkkainen *et al.* (33) and Lamalice *et al.* (19).

1.2.1 Vasculogenesis

Vasculogenesis is understood as the *de novo* organization of endothelial cells into vessels, which mainly occurs during the early phase of embryogenesis in the absence of any vascular system (8). In adults, vasculogenesis occurs during the processes of the female reproductive cycles namely ovulation, menstruation, implantation and pregnancy (31). The first vascular structures are shaped by endothelial cells, which are formed by differentiation from mesodermal cells into hemangioblasts (19). Hemangioblasts forming primitive blood islands differentiate to precursors of endothelial cells, named angioblasts (19, 34). After chemotactic and haptotactic activation, the first primitive vascular complex is formed by the migration of angioblasts and endothelial cells on a matrix consisting of collagen and hyaluronan. This results in the fusion of blood islands and their structural remodeling into tubular structures. Hereupon, the first vascular plexus is expanded into larger vessels *via* vasculogenesis leading to vascularization (19, 33).

1.2.2 Angiogenesis

In contrast to vasculogenesis, angiogenesis is understood as the expansion or the vascular network by endothelial sprouting from existing vessels. This process uses existing blood vessels as a structure to form new ones (19, 31). There are two different types of angiogenesis: sprouting angiogenesis and non-sprouting angiogenesis, also called intussusception. Sprouting angiogenesis arises both in the embryo and in the yolk sac. After proteolytic degradation of the extracellular matrix, chemotactic migration and proliferation of endothelial cells forms the lumen and drives the functional maturation of the endothelium. The action of splitting preexisting vessels is referred to as non-sprouting angiogenesis. Interstitial cellular columns are inserted into the lumen of preexisting vessels stabilizing, partitioning and remodeling the vascular tree (35).

Besides during embryogenesis, angiogenesis in general occurs in adults during wound healing, tissue regeneration and tumor metastasis or growth, which is called “neoangiogenesis” (19, 31, 36). A balance between pro- and antiangiogenic agents regulates the progression of angiogenesis. The “angiogenic switch” is activated when proangiogenic agents (e.g., vascular endothelial growth factor [VEGF], basic fibroblast growth factor [BFGF], matrix metalloproteinases, cytokines and integrins) overweigh the antiangiogenic agents (e.g., vascular endothelial growth factor receptors [soluble VEGFR1, VEGFR3], pigment epithelium-derived

factor [PEDF], angiostatin and endostatin) (31, 37-41). Proangiogenic signals cause motility, invasion of endothelial cells and the formation of filopodia. These motile endothelial cells are called tip cells and function as leading structures by guiding following endothelial cells and sensing their environment (42, 43). Tip cells are highly polarized, functionally specialized and located at the forefront of vessel branches. Filopodia sense their environment resulting in the migration towards a gradient of angiogenic factors. Tip cells are not able to form a vascular lumen and their proliferation rate is reduced to a minimum (44). Their molecular signature is characterized among other things by the expression of vascular endothelial growth factor receptors (VEGFR), such as VEGFR2 and VEGFR3 as well as platelet-derived growth factor-B (PDGF), neuropilin-1 (Nrp-1) and delta-like ligand 4 (Dll4) (44-48).

While following tip cells, stalk cells start proliferating to support the elongation of sprouts. Vessel loops are built by tip cells fusing with cells from neighboring sprouts. This process is depicted in Figure 5. New connections are stabilized by the formation of a basement membrane, the recruitment of mural cells and the establishment of blood flow. This sprouting process continues until proangiogenic signals are reduced (42).

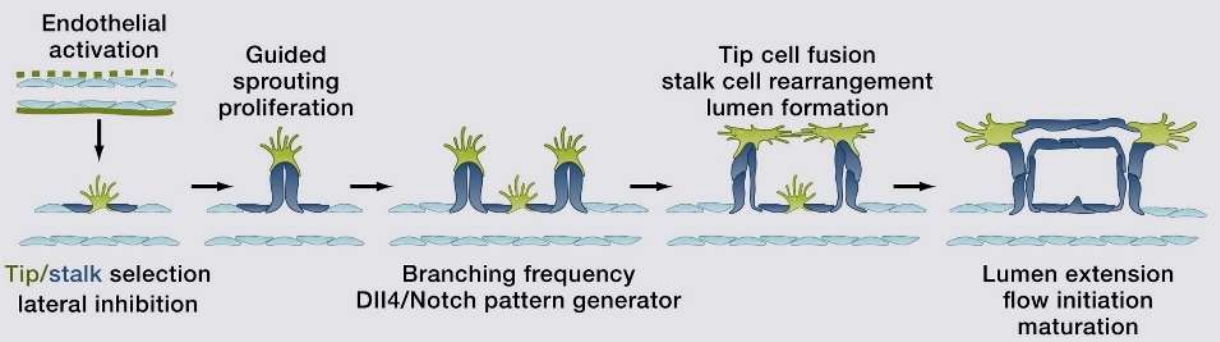

Figure 5: The different stages of vessel sprouting.
Vessel sprouting starts with the selection of tip and stalk cells, which is followed by tip cells navigating the proliferation of stalk cells. After the coordination of branching, stalk cell elongation, tip cell fusion, lumen formation, perfusion and vessel maturation follows. Figure is reprinted from Potente *et al.* (30) with permission from Elsevier.

In sprouting angiogenesis, the most important pathways considered in regulating tip cell migration and stalk cell proliferation are VEGF and Notch signaling. These pathways balance the formation of tip and stalk cells (49).

In tumors, endothelial cell migration and proliferation are mediated by enhanced expression of VEGF and bFGF and downregulated by antiangiogenic agents like thrombospondin-1 (50). Besides VEGF, bFGF and angiopoietin, several receptors for extracellular matrix ligands (e.g., $\alpha_v\beta_3$ and α_5 integrins) regulate cell migration and spreading (2).

1.3 Natural compounds

Natural products are defined as chemical compounds or substances produced by living organisms like microorganisms, plants or animals. These compounds are divided into two classes: the primary and secondary metabolites (51, 52). While the variety of primary metabolites is strongly limited (e.g., polysaccharides, proteins, nucleic and fatty acids), secondary metabolites stand out through their enormous chemical diversity (53). In contrast to primary metabolites, secondary metabolites have the extrinsic function to affect other organisms and are often able to modulate biochemical and signal transduction pathways (54). Due to this fact, a more restrictive definition limits natural products to secondary metabolites.

Until today, natural compounds still play an essential role in the discovery and development of new drugs against human diseases (55). Between 1981 and 2014 a large fraction of small-molecule drugs (43.6 % of antiinfective drugs and 40.7 % of anticancer agents) are based on natural products or their derivatives (56). Their high chemical diversity and biological reactivity offer an enormous spectrum for new therapeutically active agents. Some few unmodified natural compounds directly serve as pharmaceuticals. Most of compounds, however, are valuable lead structures for the design of new drugs. Besides their important function as drugs and leads, natural products are also extremely valuable tools to investigate complex biological processes and to identify new drug targets (57).

The “wonder drugs” such as the penicillins, aminoglycosides, cephalosporins, tetracyclines, macrolides, chloramphenicol and many others revolutionized the antibiotic and antifungal area (53). Other important secondary metabolites are enzyme inhibitors, such as cholesterol lowering agents (e.g., lovastatin, pravastatin), immunosuppressants for organ transplantation (e.g., ciclosporin, sirolimus, tacrolimus, mycophenolic acid) and antitumor agents (e.g., doxorubicin, daunorubicin, mitomycin, bleomycin). Natural products are also used as antiparasitic agents

(avermectins, narasin, lasalocid), bioherbicides (bialaphos), plant growth regulators (gibberellins), biopesticides (kasugamycin, polyoxins) and bioinsecticides (spinosins, nikkomycin) (53, 58).

1.3.1 Myxobacteria – factories of natural compounds

Soraphen A, which has been used in this work, has originally been isolated from myxobacteria (59). These rod-shaped bacteria are predominantly found in soil, dung of herbivores, bark and rotting wood (60). They belong to the group of gram-negative bacteria and exhibit the largest bacterial genome. *Minicystis rosea* and *Sorangium cellulosum*, which belong to the group of myxobacteria, have the largest (16.04 million nucleotides) and the second largest genome (13.03 million nucleotides) among bacteria, respectively (61-63).

A characteristic feature of myxobacteria is the ability to form fruiting bodies by directed cell movement upon stress conditions such as starvation (see Figure 6). Other unique behaviors differing from other bacteria are their movement by creeping or gliding over surfaces and the production of several extracellular enzymes to digest food. They also typically form swarms of many cells, which are kept together by intercellular signal molecules (64). The most interesting biotechnological aspect of myxobacteria is, that they are producers of extraordinary amounts of secondary metabolites such as linear and cyclic peptides, polyketides and heterocyclic molecules (65, 66). Due to their potent biological activity, many research groups identified promising metabolites with interesting benefits when used as pharmacological agents.

Figure 6: Light microscope images of *Sorangium cellulosum*.
Colonies (left) and fruiting bodies (right) of *S. cellulosum*. The figure was adapted from Schneiker *et al*. (61) and is reprinted under a Creative Commons license (Attribution-Noncommercial) from the Nature Publishing Group.

1.3.2 The natural compound soraphen A

The macrocyclic polyketide soraphen A belongs to the class of soraphens, which consist of at least 40 chemically related secondary metabolites. Originally, soraphen A was isolated from the myxobacteria strain *Sorangium cellulosum* (So ce26) in 1986 and was characterized as potent antifungal compound (59, 65, 67). This natural product contains an unsaturated 18-membered lactone ring with an extracyclic phenyl ring attached to it, two hydroxyl groups, three methoxy groups and three methyl groups (68, 69). The structure of soraphen A is illustrated in Figure 7. Soraphen A has been proven to be a potent inhibitor of the eukaryotic acetyl-coenzyme A carboxylase (ACC) (59, 65, 68, 70). It is known to interfere with the oligomerization of the biotin carboxylase (BC) domain of eukaryotic ACC1 and ACC2 by binding to this domain (71, 72). The oligomerization is required for the regular activity of the enzyme ACC (68, 73). Due to structural differences in the soraphen A binding site at the BC domain, bacterial ACC is not targeted by soraphen A (68). Crystallographic analysis revealed that the BC domain in complex with this natural product inhibitor is bound at an allosteric site, about 25 Ångström (Å) from the active site of the BC domain (68).

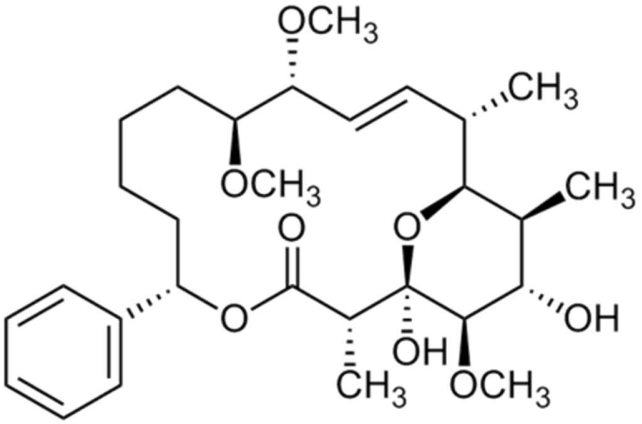

Figure 7: Chemical structure of soraphen A.

1.4 Acetyl-Coenzyme A carboxylase

The enzyme acetyl-CoA carboxylase (ACC) plays a crucial role in the metabolism of fatty acids. It regulates the first and rate limiting step in the biosynthesis of fatty acids by catalyzing the carboxylation of acetyl-CoA into malonyl-CoA (74-76).

This reaction is carried out in two steps (see Figure 8). In the first and ATP-dependent step, the biotin carboxylase (BC) activity carboxylates the N1 atom in the ureido ring. Bicarbonate acts as a donor of the carboxyl group in this conversion. To coordinate the ATP phosphates for catalysis, divalent cations (Mg^{2+} or Mn^{2+}) are needed (77, 78).

The second step is catalyzed by the carboxyltransferase (CT) domain of the enzyme and consists of transferring the activated carboxyl group from the N1 atom of biotin to the methyl group of acetyl-CoA (Figure 8). This step produces malonyl-CoA without additional energy input (68, 79).

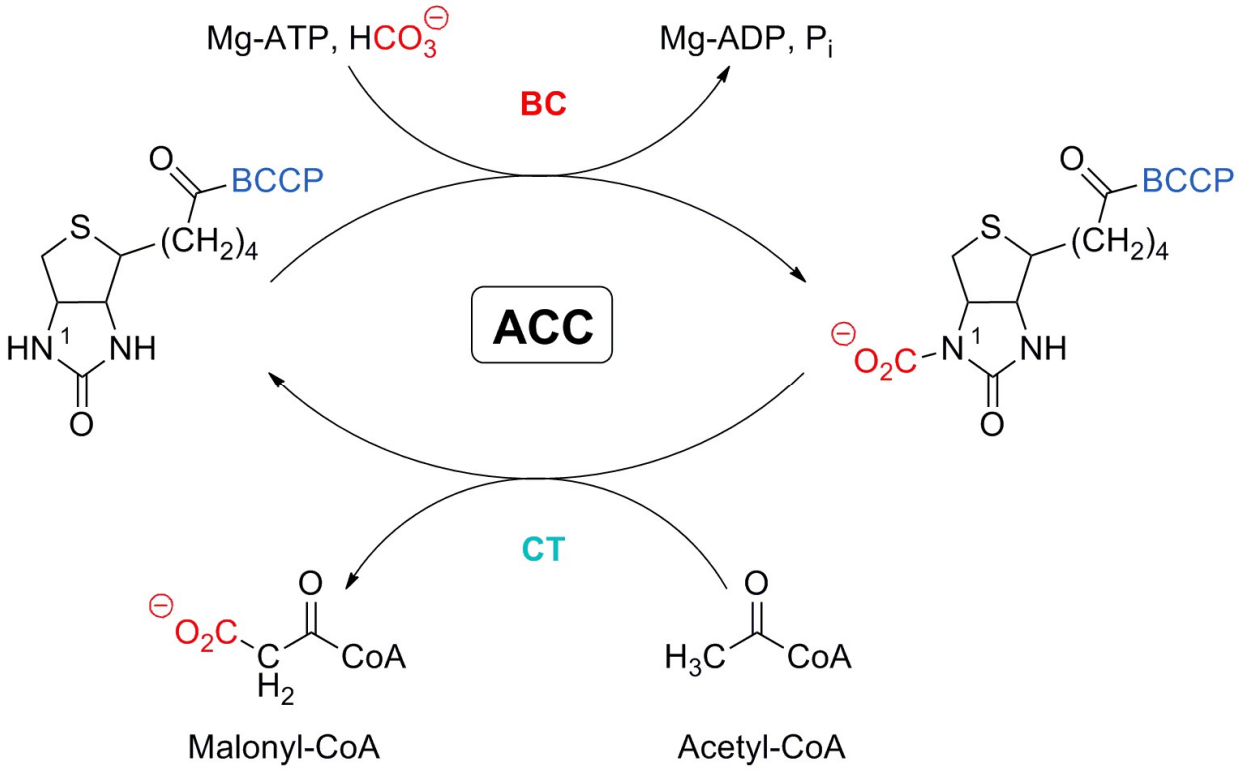

Figure 8: Catalysis cycle of Malonyl-CoA.
The conversion from acetyl-CoA to malonyl-CoA by ACC is performed in two steps and catalyzed by the biotin carboxylase (BC) and carboxyltransferase (CT) domain (71). Figure according to Tong *et al.* (79).

ACCs are found in all branches of life including archaea, bacteria, yeast, fungi, plants, animals and humans. The human ACC is a large multi-domain enzyme (> 200 kDa) carrying a BC domain, a CT domain and a biotin carboxyl-carrier protein (BCCP) domain in a single polypeptide (80-82). Mammalian ACC is composed of two tissue-specific isoforms. The isoform ACC1 (265 kDa) is present in lipogenic tissue (liver, adipose), while ACC2 (280 kDa) is located in oxidative tissues

(71, 79). Cytosolic ACC1 generates malonyl-CoA, which is necessary for *de novo* lipogenesis and is utilized as a building block with two carbon units to extend the chain length of fatty acids. This process is catalyzed by the fatty acid synthase (FAS). Long chain fatty acids are then incorporated into triglycerides and phospholipids (79, 80). Mitochondrial ACC2 generates malonyl-CoA, which regulates the mitochondrial β-oxidation by acting as a potent inhibitor of the carnitine palmitoyl-transferase I (CPT-1) (75, 83). CPT-1 mediates the conversion of long chain acyl-CoAs to acylcarnitines, which allows acylcarnitines to cross the mitochondrial membrane (79, 84-88). These processes are schematically illustrated in Figure 9.

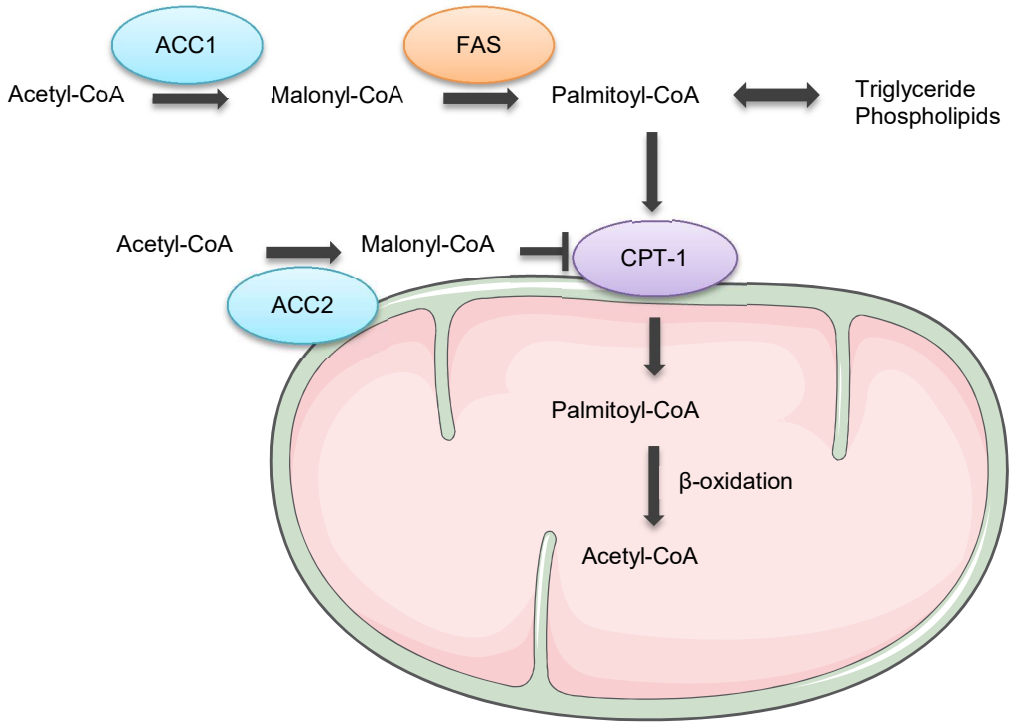

Figure 9: The role of acetyl-CoA carboxylase (ACC).
ACC1 regulates the fatty acid synthesis (FAS), while malonyl-CoA derived from ACC2 inhibits the carnitine palmitoyltransferase I (CPT-1). CPT-1 allows long chain acyl-CoAs to cross the mitochondrial membrane. Figure according to Tong *et al.* (79).

1.4.1 ACC – a promising drug target

Due to its central role in metabolism, ACC has emerged as a promising drug target to treat a variety of different diseases (71, 79). Especially, the rising prevalence of the metabolic syndrome has moved ACC into the spotlight after its discovery about 60 years ago (79, 80). Several studies

have shown beneficial effects after ACC inhibition or knockdown to control lipid synthesis in an attempt to treat diseases like obesity and diabetes (74, 89-93). For instance, a study has confirmed that ACC2-defficient mice on a high fat diet have lower rates of malonyl-CoA, reduced body fat and weight and an increment of fatty acid β-oxidation (89).

Since it has been revealed that ACC is upregulated in many different kinds of human cancers and upregulated ACC is linked to increased lipogenesis and rapid cancer cell growth, the inhibition of ACC has promised to be an interesting therapeutic strategy (94-96). In addition, T_H17 cell-mediated autoimmune disease in mice was impaired by both the pharmacological inhibition and the deletion of ACC1 (97). Interestingly, ACC inhibition by soraphen A also potently inhibited hepatitis C virus replication by interfering with membranous web formation (98).

1.4.2 ACC inhibitors

Since ACC inhibition was shown to offer interesting and promising therapeutic approaches, various ACC inhibitors have been created in pharmaceutical research. In general, there are three classes of ACC inhibitors depending on their modes of inhibition (71, 74). The first class compromises lipophilic fatty acid mimetics. Their inhibitory function is dependent on their ability to compete with acetyl-CoA in the CT reaction. Representatives of this class are for example the aryloxyphenoxypropionate and cyclohexanedione herbicides as well as TOFA (5-(tetradecyloxy)-2-furancarboxylic acid (71, 74). The chemical structure of TOFA is displayed in Figure 10. The second class are substituted bipiperidylcarboxamides, for example CP-640186, which are reversible isozyme-nonselective inhibitors of the CT reaction. This class of ACC inhibitors interact within the active center of the enzyme, which is located near the binding site for the (carboxy) biotin moiety (99). The third class is composed of polyketide natural product fungicides (e.g., soraphen A). The inhibition of the BC activity of fungal and mammalian ACCs was described above (see 1.3.2).

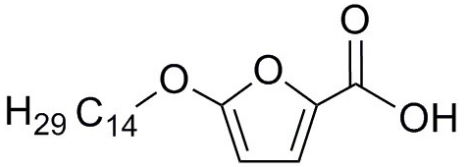

Figure 10: Chemical structure of TOFA.

1.5 Phospholipids

This study had a closer look on the phospholipid composition of endothelial cell membranes. Mammalian cell membranes consist of a lipid bilayer with defined amounts of mainly phospholipids and cholesterol. Many different lipid molecules form transient or stable structures, which serve proteins as platforms for their functions and also for their interactions with other proteins. Fatty acids can be part of complex lipids or found as free units in the membrane. In general, membrane lipids can be categorized into three classes: phospholipids, glycolipids and sterols (100). The most frequent phospholipid is phosphatidyl-choline (PC) with over 45 % of the total lipids in mammalian cell membranes. Also phosphatidyl-ethanolamine (PE), phosphatidylserine (PS), sphingomyelin (SM), cardiolipin (CL) and phospha-tidylinositol (PI) are important components of cell membranes. The most frequently found representatives of glycolipids and sterols are glycosphingolipids and cholesterol (101). Table 1 shows the lipid composition of typical mammalian cells.

Table 1: Lipid composition of common mammalian cells. Table according to Vance *et al.* (101).

	Total lipids [%]
Phosphatidylcholine	45–55
Phosphatidylethanolamine	15–25
Phosphatidylinositol	10–15
Phosphatidylserine	5–10
Phosphatidic acid	1–2
Sphingomyelin	5–10
Cardiolipin	2–5
Phosphatidylglycerol	<1
Glycosphingolipids	2–5
Cholesterol	10–20

Depending on the cell type and tissue, the lipid composition differs. Different cell organelles have distinct phospholipid membrane compositions (101).

For many years, lipids have been recognized as simple building block in a lipid layer, which separates living cells from their surroundings. But besides their function as a building block and as source of energy, lipids have been found to carry out a couple of unique biological functions: On the one hand, membrane lipids are able to control the cell's trafficking and, on the other hand,

influence the activity of membrane proteins and signals (100). Proteins, which are embedded in the lipid bilayer of eukaryotic cells, function as receptors, transporters and enzymes. Defined amounts of phospholipids are needed to maintain the function of these proteins. Changes in the lipid composition of membranes modulate the activity of membrane proteins (102).

Due to a rising interest in human health and a healthy diet, lipids in general have been set into focus of research. Since saturated and trans-fatty acids are known for their negative cardiovascular effects, a healthy lifestyle is associated with a reduced intake of these fatty acids and an increased intake of mono- and polyunsaturated fatty acids, which are known to have cardioprotective functions (100, 103). For instance, docosahexaenoic acid (DHA; 22:6) and eicosapentaenoic acid (EPA; 20:5) are reported to prevent cardiovascular diseases and cancer (104), while the omega-6 polyunsaturated fatty acid (PUFA) gamma linolenic acid (18:3) is described to have antiinflammatory properties (105). The monounsaturated fatty acid (MUFA) oleic acid (18:1) attracted attention for lowering blood pressure and decreasing the incidence of hypertension (100, 106). Furthermore, alterations of free fatty acids have been linked to diseases like coronary heart disease, hypertension, obesity, diabetes mellitus, alcoholism, schizophrenia, Alzheimer's disease, atherosclerosis and cancer (107). These findings highlight the importance of lipids for human health and the progression of severe diseases.

1.6 Aim of the study

ACC plays a fundamental role in the fatty acid metabolism. By catalyzing the carboxylation of acetyl-CoA to malonyl-CoA it regulates the first and rate limiting step in the biosynthesis of fatty acids (74-76). In the last few years, ACC has been highlighted as an attractive drug target to treat a variety of different diseases (71, 79). The inhibition of ACC offers two interesting ways to influence the fatty acid metabolism. It prevents the *de novo* lipogenesis in lipogenic tissues and stimulates the mitochondrial fatty acid β-oxidation (80). Nevertheless, the role of ACC in vascular endothelial cells has been neglected until now. In this study, we used both a gene silencing approach and the natural compound soraphen A to investigate the role of ACC in primary human endothelial cells. Even though soraphen A is lacking optimal drug-like properties *in vivo*, this well-established ACC-inhibitor represents a great chemical tool to investigate the role of the fatty acid metabolism in primary endothelial cells with a special focus on endothelial cell migration and angiogenesis. Endothelial cell migration is a very important function during processes like wound

healing and tissue regeneration as well as developmental and growth processes. Since an altered endothelial cell migration participates in the pathogenesis and progression of many severe disorders, such as ischemia reperfusion injury, diabetic angiopathy, macular degeneration, rheumatoid arthritis and cancer (108, 109), interfering with EC migration might offer new therapeutic opportunities for the treatment of migration-related diseases in the endothelium.

2 MATERIALS & METHODS

2.1 Materials

2.1.1 Soraphen A

The acetyl-CoA carboxylase inhibitor soraphen A was first isolated by Gerth *et al*. as described previously (65) and was kindly provided by the group of Prof. Dr. Rolf Müller (Helmholtz-Institute for Pharmaceutical Research Saarland, Saarland University). Soraphen A was dissolved in dimethyl sulfoxide (DMSO) to a concentration of 30 mM or 100 mM. Aliquots were stored at -80 °C. For further use, the compound was diluted in medium without exceeding a final concentration of 0.1 % (v/v) DMSO in cell culture experiments to avoid toxic side effects.

2.1.2 Fatty acids

Oleic acid and α-linolenic acid were dissolved in ethanol; linoleic acid sodium salt in ethanol supplemented with 0.1 % Tween 20; stearic acid in DMSO. Due to the low solubility of 1,2-dioleoyl-*sn*-glycero-3-phospho-*rac*-(1-glycerol) sodium salt (DOPG, PG(18:1(9*Z*)/18:1(9*Z*)), liposomes (multilaminar vesicles) of DOPG were prepared by the thin film hydration method: DOPG was diluted with dichloromethane and a rotary evaporator was utilized to generate a thin film of lipids. Beginning at a 500 mbar vacuum, the pressure was reduced by 100 mbar every 10 min at room temperature (RT) to obtain a lipid film on the inner surface of a round-bottom flask. Ending at 50 mbar for 1 h, the lipid film was rehydrated with phosphate buffered saline (PBS) by vortexing for 10 min. Finally, the liposome solution was sterilized by filtration.

2.1.3 Biochemicals, dyes, inhibitors and cell culture reagents

The following tables list all biochemicals, dyes, inhibitors and cell culture reagents, which have been used in this work.

Table 2: Biochemicals and dyes.

Reagent	Provider
1,2-Dimyristoyl-*sn*-glycero-3-phosphatidylcholine	Cayman, Ann Arbor, MI, USA
1,2-Dimyristoyl-*sn*-glycero-3-phosphatidyl-ethanolamine	Cayman, Ann Arbor, MI, USA
1,2-Dioleoyl-*sn*-glycero-3-phospho-*rac*-(1-glycerol) sodium salt (DOPG, PG(18:1(9*Z*)/18:1(9*Z*))	Sigma-Aldrich, St Louis, MO, USA
1,4-Piperazinediethanesulfonic acid (PIPES)	Sigma-Aldrich, St Louis, MO, USA
1,6-Diphenyl-1,3,5-hexatriene-4′-trimethylammonium tosylate (TMA-DPH)	Sigma-Aldrich, St Louis, MO, USA
^{13}C-malonyl-CoA	Sigma-Aldrich, St Louis, MO, USA
3-(Cyclohexylamino)-1-propanesulfonic acid (CAPS)	Sigma-Aldrich, St Louis, MO, USA
Accustain, formalin free fixative	Sigma-Aldrich, St Louis, MO, USA
Bovine serum albumin (BSA)	Sigma-Aldrich, St Louis, MO, USA
CellTiter-Blue Reagent	Promega Corp., Heidelberg, Germany
Chloroform, HPLC grade	Sigma-Aldrich, St Louis, MO, USA
Crystal violet	Sigma-Aldrich, St Louis, MO, USA
Dichloromethane	Acros Organics, New Jersey, USA
Dimethyl sulfoxide (DMSO)	Sigma-Aldrich, St Louis, MO, USA
FluorSave Reagent, mounting medium	Merck Millipore, Darmstadt, Germany
Glutaraldehyde, 25 % aqueous solution	Sigma-Aldrich, St Louis, MO, USA
Growth Factor Reduced Matrigel	Corning Inc., New York, USA
IGEPAL CA-630	Sigma-Aldrich, St Louis, MO, USA
Isopropyl alcohol	Carl Roth GmbH, Karlsruhe, Germany
Linoleic acid sodium salt	Sigma-Aldrich, St Louis, MO, USA
Luminol	Sigma-Aldrich, St Louis, MO, USA
Magnesium chloride ($MgCl_2$)	Merck Millipore, Darmstadt, Germany
Not-fat dry milk powder, blotto reagent	Carl Roth GmbH, Karlsruhe, Germany

Table 2: continue biochemicals and dyes.

Reagent	Provider
Oleic acid	Sigma-Aldrich, St Louis, MO, USA
Page Ruler Prestained Protein Ladder	PEQLAB Biotechnologie GmbH, Erlangen, Germany
p-Coumaric acid	Sigma-Aldrich, St Louis, MO, USA
Propidium iodide	Sigma-Aldrich, St Louis, MO, USA
Pyronin Y	AppliChem, Darmstadt, Germany
Roti-Histofix 4 %, phosphate-buffered formaldehyde solution 4 %	Carl Roth GmbH, Karlsruhe, Germany
Rotiphorese Gel 30 (37.5:1), polyacrylamide	Carl Roth GmbH, Karlsruhe, Germany
Sodium borohydride ($NaBH_4$)	Merck Millipore, Darmstadt, Germany
Sodium dodecyl sulfate (SDS)	Carl Roth GmbH, Karlsruhe, Germany
Spectra Multicolor High Range Protein Ladder	Thermo Fisher Scientific, Dreieich, Germany
Staurosporine	Sigma-Aldrich, St Louis, MO, USA
Stearic acid	Sigma-Aldrich, St Louis, MO, USA
SuperScript II Reverse Transcriptase (Life Technologies)	Thermo Fisher Scientific, Dreieich, Germany
SYBR Green PCR Master Mix	Life Technologies, Darmstadt, Germany
Tetramethylethylenediamine (TEMED)	Sigma-Aldrich, Taufkirchen, Germany
Triethylene glycol diamine tetraacetic acid (EGTA)	Carl Roth GmbH, Karlsruhe, Germany
Triton X-100	Merck Millipore, Darmstadt, Germany
Tween 20	Carl Roth, Karlsruhe, Germany
α-Linolenic acid	Sigma-Aldrich, St Louis, MO, USA
β-Mercaptoethanol	Carl Roth GmbH, Karlsruhe, Germany

All other common chemical substances were purchased from AppliChem, Carl Roth GmbH, Merck Millipore or Sigma-Aldrich.

Table 3: Inhibitors.

Reagent	Provider
5-(Tetradecyloxy)-2-furoic acid (TOFA)	Santa Cruz Biotechnology, Dallas, TX, USA
Complete, Mini, EDTA free	Roche, Basel, Switzerland
Phenylmethanesulfonyl fluoride (PMSF)	Sigma-Aldrich, Taufkirchen, Germany
Sodium fluoride (NaF)	Merck Millipore, Darmstadt, Germany
Sodium orthovanadate (Na_3VO_4)	Sigma-Aldrich, Taufkirchen, Germany

Table 4: Cell culture reagents.

Reagent	Provider
Amphotericin B (250 µg/ml)	PAN-Biotech, Aidenbach, Germany
Collagen G	Biochrom AG, Berlin, Germany
Collagenase A	Roche GmbH, Penzberg, Germany
Dulbecco's Modified Eagle's Medium (DMEM), low glucose	GE-Healthcare, Little Chalfont, United Kingdom
EASY Endothelial Cell Growth Medium (ECGM)	PELOBiotech GmbH, Martinsried, Germany
Fetal Bovine Serum (FBS)	Biochrom, Berlin, Germany
Medium 199/EBSS	GE-Healthcare, Little Chalfont, United Kingdom
Penicillin (10,000 U/ml)	PAN-Biotech, Aidenbach, Germany
Streptomycin (10 mg/ml)	PAN-Biotech, Aidenbach, Germany
Trypsin/EDTA	Biochrom AG, Berlin, Germany

2.1.4 Buffers, media and solutions

The following buffers, media and solutions (Table 5) were used for the cultivation of primary endothelial cells as well as other cell lines.

Table 5: Buffers used in cell culture.

Reagent	Composition	Concentration
Lysis buffer	RIPA buffer	1000 µl
	Complete, Mini, EDTA free	5 mM
	NaF	1 mM
	PMSF	1 mM
PBS (pH 7.4)	NaCl	137 mM
	KCl	2.7 mM
	KH_2PO_4	2 mM
	$Na_2HPO_4 \cdot 2\ H_2O$	10 mM
	Aqua dest.	
PBS (pH 7.4) + Collagen G	Collagen G	0.001 % (v/v)
	PBS (pH 7.4)	
PBS+ (pH 7.4)	$Na_2HPO_4 \cdot 2\ H_2O$	1.44 g/l
	NaCl	8.0 g/l
	KCl	0.2 g/l
	KH_2PO_4	0.2 g/l
	$MgCl_2 \cdot 6\ H_2O$	0.1 g/l
	$CaCl \cdot 2\ H_2O$	0.1 g/l
	Aqua dest.	
Trypsin + EDTA solution	Trypsin	0.05 % (w/v)
	EDTA	0.02 % (w/v)

Table 6: Cell culture media.

Solution	Composition	Concentration
Endothelial cell growth medium	Supplement Mix	2.5 %
(ECGM)	Amphotericin B	1 % (v/v)
	Penicillin	1 % (v/v)
	Streptomycin	1 % (v/v)
	FBS superior	10 % (v/v)
	ECGM	

Table 6: continue cell culture media.

Solution	Composition	Concentration
Dublecco's modified eagle medium (DMEM), low glucose	Penicillin	1 % (v/v)
	Streptomycin	1 % (v/v)
	FBS superior	10 % (v/v)
	DMEM	
Freezing medium	FBS superior	20 % (v/v)
	DMSO	10 % (v/v)
	suitable growth medium	
Stopping medium	FBS superior	10 % (v/v)
	Medium 199	
Starvation medium	Amphotericin B	1 % (v/v)
	Penicillin	1 % (v/v)
	Streptomycin	1 % (v/v)
	FBS superior	1 % (v/v)
	Medium 199	

Before its use, FBS was heat inactivated for 30 min at 56 °C. Aliquots were stored at -20 °C.

2.1.5 Buffers and solutions used for *in vitro* assays

The following table lists all buffers and solutions used for *in vitro* assays, immunoblotting and immunocytochemistry.

Table 7: Buffers used for *in vitro* assays.

Solution	Composition	Concentration
CAPS buffer (pH 11)	CAPS	0.01 M
	Methanol	15 % (v/v)
	Aqua dest.	

Table 7: continue buffers used for *in vitro* assays.

Solution	Composition	Concentration
Cell extraction buffer (CEB)	PIPES (pH 6.9)	80 mM
	$MgCl_2$	1 mM
	EGTA	5 mM
	Triton X-100	0.5 %
Crystal violet staining solution	Crystal violet	0.5 %
	Methanol	20 %
	H_2O	
Dissolving buffer (proliferation assay)	Sodium citrate (0.1 M)	50 %
	Ethanol	50 %
Electrophoresis buffer	10x Tris-Glycin buffer	10 % (v/v)
	SDS	0.1 % (w/v)
	Aqua dest.	
Hypotonic fluorochrome (HFS) solution	Triton X-100	0.1 % (v/v)
	Sodium citrate	0.1 % (w/v)
	Propidium iodide (PI)	50 µg/ml
	PBS (pH 7.4)	
Laemmli sample buffer, 1x	Tris-HCl (pH 6.8)	125 mM
	Glycerol	20 % (w/v)
	SDS	4 % (w/v)
	DTT	0.8 % (w/v)
	Pyronin Y	0.01 %
	Aqua dest.	
Laemmli sample buffer, 5x	Tris-HCl (pH 6.8)	312.5 mM
	Glycerol	50 % (w/v)
	SDS	5 % (w/v)
	DTT	2 % (w/v)
	Pyronin Y	0.025 %
	Aqua dest.	

Table 7: continue buffers used for *in vitro* assays.

Solution	Composition	Concentration
Stacking gel	Rotiphorese Gel 30	17 %
	Tris-HCl (pH 6.8)	125 mM
	SDS	0.1 %
	APS	0.1 %
	TEMED	0.2 %
	Aqua dest.	
Stripping buffer	Tris-HCl	625 mM
	SDS	2 %
	Aqua dest.	
Tank buffer, 1x	Tris-Glycin buffer, 10x	10 % (v/v)
	Methanol	10 % (v/v)
	Aqua dest.	
Tris-Glycin buffer, 10x	Tris	250 mM
	Glycin	1.92 M
	Aqua dest.	
Wash buffer	Tween 20	0.1 %
	PBS (pH 7.4)	
Triton X-100, 0.2 %	Triton X-100	0.2 % (v/v)
	PBS	
TBS (pH 7.4), 1x	Tris	25 mM
	NaCl	150 mM
	Aqua dest.	
Separation gel, 7.5 %	Rotiphorese Gel 30	25 % (v/v)
	Tris-HCl (pH 8.8)	150 mM
	SDS	0.1 %
	TEMED	0.1 %
	APS	0.05 %
	Aqua dest.	

Table 7: continue buffers used for *in vitro* assays.

Solution	Composition	Concentration
Enhanced Chemiluminescence (ECL) solution (pH 8.5)	Tris-Base	100 mM
	Luminol	1 % (v/v)
	p-Coumaric acid	0.4 % (v/v)
	H_2O_2	0.06 % (v/v)
	Aqua dest.	
RIPA lysis buffer (pH 7.6)	Tris	50 mM
	NaCl	150 mM
	NP-40	1 %
	Sodium deoxycholate	0.25 %
	SDS	0.1 %
	Aqua dest.	

2.1.6 Commercial kits

Following commercial kits were used in this study.

Table 8: Commercial kits used in this work.

Kit	Provider
Amaxa HUVEC Nucleofector Kit	Lonza, Basel, Switzerland
Amplex Red Cholesterol Assay Kit	Invitrogen, Carlsbad, CA, USA
CellTiter-Blue Assay	Promega, Mannheim, Germany
CytoTox 96 Non-Radioactive Cytotoxicity Assay	Promega, Mannheim, Germany
Massive Analysis of cDNA Ends (MACE) Library Prep Kit	GenXPro, Frankfurt, Germany
MiSeq Reagent Kit v3	Illumina, San Diego, CA, USA
Pierce BCA Protein Assay Kit	Thermo Fisher Scientific, Schwerte, Germany
Qiagen RNase-Free DNase Set	Qiagen, Hilden, Germany
Qiagen RNeasy Mini kit	Qiagen, Hilden, Germany
QIAquick PCR Purification Kit	Qiagen, Hilden, Germany

Table 8: continue commercial kits used in this work.

Kit	Provider
QIAshredder	Qiagen, Hilden, Germany

2.1.7 Technical equipment

The technical equipment, which has been used for the experiments, is listed the following table.

Table 9: Technical equipment.

Name	Device	Producer
Acquity Ultra-Performance Liquid Chromatography system	Ultra-performance liquid chromatography system	Waters, Milford, MA, USA
Acquity UPLC BEH C_{18} column	Columns for ultra-performance liquid chromatography	Waters, Milford, MA, USA
Acquity UPLC BEH C8 column	Columns for ultra-performance liquid chromatography	Waters, Milford, MA, USA
ARPEGE 110	Liquid nitrogen storage system	Air Liquide S.A., Paris, France
Astacus	Ultra pure water system	MembraPure GmbH, Berlin, Germany
CP 1000	Tabletop film processor	AGFA, Cologne, Germany
Criterion Blotter	Blotting unit	Bio-Rad Laboratories, Inc., Hercules, CA, USA
DM IL LED	Inverted microscope	Leica, Wetzlar, Germany
FACSVerse	Flow cytometer	BD Biosciences, Heidelberg, Germany
FE20	pH-measurement device	Mettler Toledo, Columbus, USA

Table 9: continue technical equipment.

Name	Device	Producer
FORMA 900	Freezer (-80 °C)	Thermo Fisher Scientific, Dreieich, Germany
HERACell 150i	Incubator	Thermo Fisher Scientific, Dreieich, Germany
HERAEUS MEGAFUGE 16R	Centrifuge	Thermo Fisher Scientific, Dreieich, Germany
IKA RH basic 2	Magnetic stirrer	IKA-Werke GmbH & Co. KG, Staufen, Germany
Infinite F200 Pro	Microplate multifunction reader	Tecan, Männedorf, Switzerland
Julabo ED	Water bath	JULABO GmbH, Seelbach, Germany
Laborota 4003	Rotary evaporator	Heidolph Instruments, Schwabach, Germany
Leica DMI 6000 B	Inverted fluorescence microscope	Leica, Wetzlar, Germany
MICRO STAR 17R	Microcentrifuge	VWR International GmbH, Darmstadt, Germany
Mini-PROTEAN System Glass Plates	Glass plates	Bio-Rad Laboratories, Inc., Hercules, CA, USA
Mini-PROTEAN Tetra Cell	Gel electrophoresis cell	Bio-Rad Laboratories, Inc., Hercules, CA, USA
MiniStar silverline	Tablecentrifuge	VWR International GmbH, Darmstadt, Germany
Neubauer-improved	Hemocytometer	Marienfeld-Superior, Lauda-Königshofen, Germany
Nucleofector 2b	Electroporation device	Lonza, Basel, Switzerland
P 330	Nanophotometer	Implen GmbH, Munich, Germany

Table 9: continue technical equipment.

Name	Device	Producer
PIONEER	Precision balance	Ohaus Corporation, Parsippany, US-NJ
Pipetus	Electrical pipetting aid	Hirschmann Laborgeräte GmbH & Co. KG, Eberstadt, Germany
QTRAP 5500	Mass Spectrometer	Sciex, Darmstadt, Germany
SAFE 2020	Clean bench	Thermo Fisher Scientific, Dreieich, Germany
SONOPULS HD 70	Sonificator	BANDELIN electronic GmbH & Co. KG
StepOnePlus System	Real-time PCR system	Applied Biosystems, Foster City, CA, USA
Systec X-95	Autoclav	Systec GmbH, Linden, Germany
USC300TH	Ultrasonic water bath	VWR International GmbH, Darmstadt, Germany
Varioskan Flash	Microplate multifunction reader	Thermo Fisher Scientific, Dreieich, Germany
Vortex Genie 2	Vortex mixer	Scientific Industries Inc., Bohemia, US-NY

2.2 Cell Culture

For all experiments, untreated control cells are defined as cells treated with the respective vehicle control.

2.2.1 Human umbilical vein endothelial cells

Primary human umbilical vein endothelial cells (HUVECs) were obtained from PELOBiotech (Martinsried, Germany) and used for experiments until the third passage. Primary endothelial cells

were cultured in Endothelial Cell Growth Medium (ECGM) containing 10 % heat-inactivated fetal bovine serum (FBS), 100 U/ml penicillin, 100 µg/ml streptomycin and 0.25 µg/ml amphotericin B at 37 °C in an incubator with an atmosphere containing 5 % CO_2. All cell culture flasks, multi-well plates and Petri dishes were coated for 20 min with collagen G.

2.2.2 Human dermal microvascular endothelial cells

The human dermal microvascular endothelial cell line (HMEC-1) was purchased from ATCC (Manassas, VA, USA). This cell line has been once established by transfecting human dermal microvascular endothelial cells with a plasmid containing the coding region for SV40 large T-antigen (110). HMECs show similar morphologic, phenotypic and functional characteristics of normal human microvascular endothelial cells (110, 111). HMECs were cultured as described above for HUVECs (see section 2.2.1).

2.2.3 Human liver carcinoma cell line

The human liver carcinoma cell line HepG2 was obtained from the Leibniz Institute DSMZ/German Collection of Microorganisms and Cell Cultures (Leipzig, Germany) and cultivated in DMEM (low glucose) supplemented with 10 % FBS, 100 U/ml penicillin and 100 µg/ml streptomycin. This adherent cell line has been established from a 15-year-old adolescent having a well-differentiated hepatocellular carcinoma. HepG2 contain 55 chromosome pairs and an epithelial morphology (112).

2.2.4 Passaging

Confluent HUVECs or HMECs were sub-cultured 1:3 in 75 cm² coated culture flaks or seeded into multi-well plates, Petri dishes or special slides for the respective experiment. Cells were washed with PBS (pH 7.4) twice and incubated with trypsin/EDTA at 37 °C for 1–2 min. To terminate the enzymatic reaction, stopping medium was added to the cell suspension. After centrifugation (300 g, 5 min, RT), pelleted cells were resuspended in cell medium. Usually, HUVECs were used until the third passage and were passaged 1:3 twice a week. HMECs were cultivated until passage 30 and were split 1:3 twice a week. The human liver carcinoma cell line HepG2 was passaged 1:4

every 3–4 days and cultivated in DMEM with low glucose. Cell amount and viability were determined by using a hemocytometer.

2.2.5 Freezing and thawing cells

Confluent HepG2 cells or HMEC-1 cultivated in a 75 cm² flask were trypsinized, centrifuged in stopping medium (300 g, 5 min, RT) and resuspended in ice-cold freezing medium (1 x 10^6 cells/ml). Aliquots of 1 ml were frozen in cryovials at -80 °C for 24 h and transferred into liquid nitrogen for long-term storage.
For thawing, cryovials were warmed up to 37 °C in a water bath und prewarmed growth medium was immediately added to the cell suspension. The freezing medium was removed by centrifugation and resuspending in their appropriate cell culture medium. Finally, cells were seeded in 75 cm² cell culture flasks.

2.3 Cell viability assays

2.3.1 CellTiter-Blue Cell Viability Assay

In order to exclude a possible cytotoxic effect of soraphen A or TOFA in endothelial cells, a CellTiter-Blue Assay (Promega, Mannheim, Germany) was performed. This assay uses the ability of living cells to convert resazurin (redox dye) into resorufin (fluorescent product) in the presence of NADPH (see Figure 11), which is part of the metabolism. Due to the loss of the metabolic activity in nonviable cells, these cells are not able to generate a fluorescent signal. The assay was performed according to the manufacturer's protocol. HUVECs were grown in 96-well plates and treated with soraphen A (0.3–100 µM) or TOFA (0.01–30 µM) for 24 h and 48 h, respectively. Resazurin was added to each well and after 4 h of incubation fluorescence intensity (ex: 560 nm; em: 590 nm), which directly correlates to the number of viable cells, was detected by a Tecan Infinite F200 Pro plate reader.

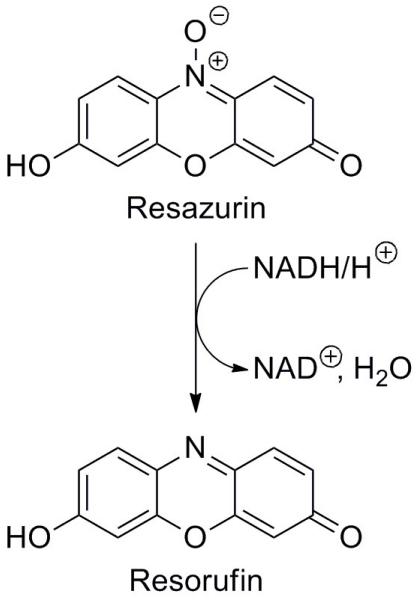

Figure 11: CellTiter-Blue Cell Viability Assay reaction.
Viable cells reduce resazurin to resorufin, which shows fluorescence at 590 nm. Figure according to O'Brien *et al.* (113).

2.3.2 Quantification of cells with sub-diploid DNA content

Quantification of apoptosis was performed as described by Nicoletti *et al.* (114, 115). The percentage of apoptotic cells is determined by counting the number of cells with sub-diploid DNA content after staining the cells with propidium iodide. This assay is based on the principle that DNA in apoptotic cells are degraded by endonucleases. Therefore, apoptotic cells contain less DNA than healthy cells. Confluent HUVECs seeded in 24-well plates were treated for 24 h or 48 h with soraphen A at different concentrations (0.3–100 µM). Staurosporine (1 µM) was used as positive control. After incubation with soraphen A, each supernatant was collected and washed twice with ice-cold PBS. Accordingly, cells were trypsinized and centrifuged (600 g, 10 min, 4 °C). Following two additional washing steps with PBS, cells were incubated overnight at 4 °C with a hypotonic fluorochrome solution (HFS) containing propidium iodide for cell membrane permeabilization and DNA labeling. Finally, the number of cells with subdiploidic DNA content was measured by flow cytometry (BD FACSVerse) and determined by the analyzing software BD FACSuite.

2.3.3 Release of lactate dehydrogenase

Cell death was determined using the CytoTox 96 Non-Radioactive Cytotoxicity Assay Kit (Promega). This assay determines the amount of the cytosolic enzyme lactate dehydrogenase (LDH), which is released upon loss of cell membrane integrity (cell lysis). Released LDH results in a conversion of the added tetrazolium salt (iodonitrotetrazolium violet; INT) into a red formazan product (see Figure 12). The amount of generated formazan is proportional to the number of lysed cells (116, 117). The assay was performed according to the manufacturer's protocol. 25,000 cells/well were plated in a 96-well plate and after two days treated with soraphen A (0.3–100 µM) for 24 h or 48 h. For maximum LDH release, Lysis Solution was used as a positive control. The amount of released LDH was measured by a Tecan Infinite F200 Pro plate reader at 490 nm.

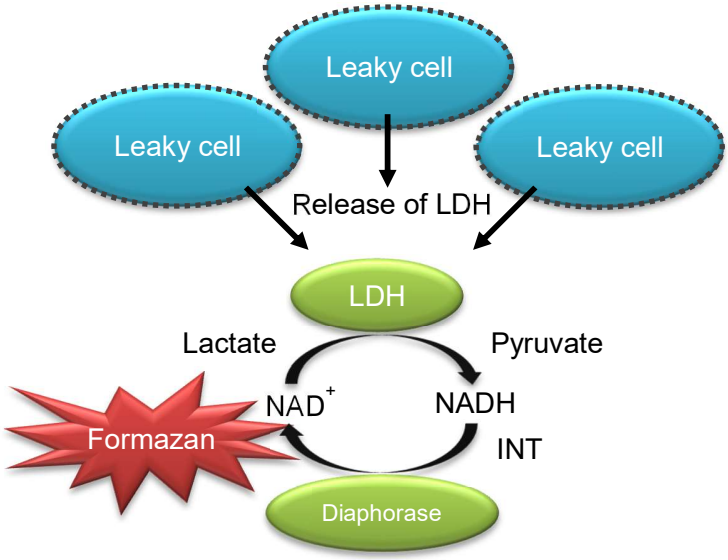

Figure 12: General chemical reaction of the CytoTox 96 Non-Radioactive Cytotoxicity Assay.
Damaged cells release lactate dehydrogenase (LDH), which is measured by supplying lactate, NAD^+ and iodonitrotetrazolium violet (INT) as substrates in the presence of diaphorase. The generated red product formazan is proportional to the number of lysed cells. Figure according to the manufacture's protocol CytoTox 96 Non-Radioactive Cytotoxicity Assay Kit (Promega) (118).

2.4 Quantification of cellular malonyl-CoA levels

This experiment was performed in collaboration with Dr. Andreas Koeberle and Helmut Pein in the laboratory of Prof. Dr. Oliver Werz (Chair of Pharmaceutical/Medicinal Chemistry, Institute of Pharmacy, Friedrich-Schiller-University, Jena, Germany).

HUVECs (1 x 10^7) were twice washed with PBS (pH 7.4), incubated with trypsin/EDTA at 37 °C for 1–2 min and centrifuged (300 g, 5 min, RT). Cells were resuspended in 70 % methanol supplemented with the internal standard ^{13}C-malonyl-CoA (1 nmol). Proteins were precipitated for 1 h at -20 °C. After a centrifugation step (20,000 g, 5 min, 4 °C), the supernatant was evaporated to complete dryness and extracted with 50 µl water. Chromatography was performed on an Acquity UPLC BEH C_{18} column (1.7 µm, 2.1 x 100 mm) using an Acquity Ultra Performance Liquid Chromatography system from Waters. Acyl-CoA ester were separated by isocratic elution (0.75 ml/min, 50 °C, 1 min) with 100 % eluent A (10 mM aqueous ammonium acetate) and afterwards with a linear gradient to 100 % eluent B (acetonitrile/10 mM aqueous ammonium acetate, 95/5, 3 min). The chromatography setup was equipped with an electrospray ionization source and coupled to a QTRAP 5500 mass spectrometer. By the use of multiple reaction monitoring in the positive ion mode after neutral loss of 2'-phospho-ADP ($[M+H-507]^+$) malonyl-CoA ($[M+H]^+$) was quantified. The ion spray voltage was used at 3000 V and the heated capillary temperature was set to 600 °C. The pressure of the curtain gas, of the sheath gas and of the auxiliary gas was set to 30, 45 or 55 psi, respectively. The declustering potential, the entrance potential and the collision energy was set to 60, 10 or 45 V, respectively.
Analyst software 1.6 (Sciex, Darmstadt, Germany) was utilized for processing the analytical data.

2.5 Analysis of phospholipid profiles

This experiment was performed in collaboration with Dr. Andreas Koeberle and Konstantin Löser in the laboratory of Prof. Dr. Oliver Werz (Chair of Pharmaceutical/Medicinal Chemistry, Institute of Pharmacy, Friedrich-Schiller-University, Jena, Germany).

The extraction and analysis of phospholipids were performed using a method that has been described previously by Koeberle *et al*. (119). In brief, the extraction of phospholipids from cells was achieved by successive addition of PBS pH 7.4, methanol, chloroform and saline (final ratio: 14:34:35:17). After evaporating the organic layer, lipids were dissolved in 100 µl methanol. As

internal standards for subsequent analysis 1,2-dimyristoyl-*sn*-glycero-3-phosphatidylcholine and 1,2-dimyristoyl-*sn*-glycero-3-phosphatidylethanolamine were added.
The chromatographic separation of phospholipids was carried out using an Acquity UPLC BEH C8 column (1.7 µm, 1 x 100 mm, Milford, MA) in combination with an Acquity Ultra-Performance LC system. Eluted lipids were detected by a QTRAP 5500 Mass Spectrometer, which was equipped with an electrospray ionization source. The fatty acid anion fragments of glycerophospholipids were determined by multiple reaction monitoring in the negative ion mode. For performing the quantification, the most intensive transition was used. Mass spectra were performed using Analyst 1.6 (Sciex, Darmstadt, Germany).

2.6 Cholesterol assay

This experiment was performed in cooperation with Anna Stark (Institute of Pharmaceutical Biology, Biocenter, Goethe University, Frankfurt, Germany).

The Amplex Red Cholesterol Assay Kit (Invitrogen, Carlsbad, CA, USA) provides a fluorometric method to measure the amount of cholesterol. The principle of this assay is based on an enzyme-coupled reaction, which detects free cholesterol and cholesterol esters. Cholesterol esterase hydrolyzes cholesteryl esters into cholesterol resulting in the production of H_2O_2. Generated H_2O_2 is then detected by 10-acetyl-3,7-dihydroxyphenoxazine (Amplex Red reagent). Amplex Red reagent reacts with H_2O_2 and horseradish peroxidase to the fluorescent resorufin (120). The assay was performed according to the manufacturer's protocol. After treatment of HUVECs with soraphen A (30 µM, 24 h), cells were detached and centrifuged. For extraction of lipids, the cell pellet was homogenized in 200 µl of the organic solvents mixture (chloroform, isopropanol, IGEPAL CA-630; 7:11:0.1). After sonication and a centrifugation step (13,000 g, 10 min), the probe was evaporated to dryness. Dried lipids were dissolved in 200 µl of the 1x reaction buffer. 50 µl of the Amplex Red reagent (2 U/ml horseradish peroxidase (HRP), 2 U/ml cholesterol oxidase, 2 U/ml cholesterol esterase) were added to 50 µl of the lipid solution. The fluorescence intensity (ex: 560 nm; em: 590 nm) was detected by a Tecan Infinite F200 Pro plate reader.

2.7 Membrane fluidity determination

This experiment was performed in cooperation with Nelli Keksel in the laboratory of Prof. Dr. Hanns Häberlein (Institute of Biochemistry and Molecular Biology, Rheinische Friedrich-Wilhelms-University of Bonn, Bonn, Germany).

Steady-state fluorescence anisotropy measurements (L-configuration) were used to determine the membrane fluidity of endothelial cells. This measurement uses a water-insoluble fluorescent probe, which incorporates itself into the cell membrane and allows to determinate the movement of its surrounding environment. The fluorescent probe trimethylammonium diphenylhexatriene (TMA-DPH) was used in this measurement. The hydrophilic region of TMA-DPH is anchored at the lipid/water interface, while the hydrophobic part is incorporated in the lipid part of the membrane (121) (see Figure 13).

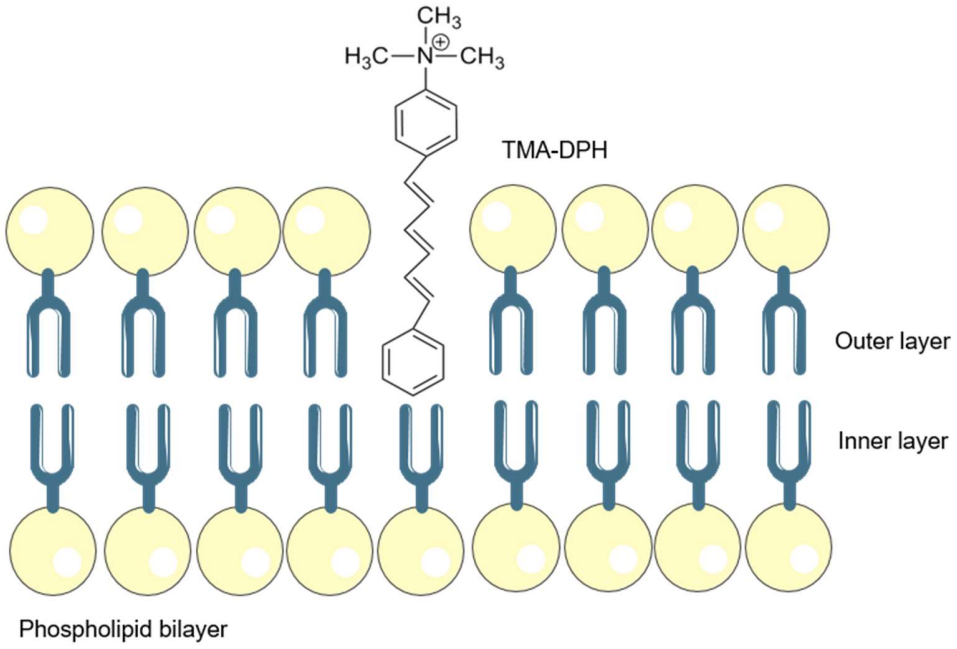

Figure 13: Chemical structure and location within the lipid bilayer of the fluorescent probe trimethylammonium diphenylhexatriene (TMA-DPH).
Figure according to Marczak *et al.*(121).

First, HUVECs were plated on glass cover slips with a size of 13.5 x 13.5 mm and treated with soraphen A (24 h, 30 µM) or were left untreated. The glass cover slip, which perfectly fits into a quartz glass cuvette, were rinsed with Hanks' balanced salt solution (HBSS) and placed vertically

into the quartz cuvette. The cuvette was transferred into a sample holder, which allows an incident light angle of 30° relative to the cell monolayer grown on glass cover slips. An angle of 30° allows the light beam to hit a larger surface area, resulting in measuring a larger number of cells. Additionally, this setup yields more stable and reliable data, since reflected polarized light is deflected away from the detector. By adjusting the height of the cuvette, the light beam was allowed to pass through the monolayer. To measure the intensity of polarized light signals parallel (II) by vertical as well as polarized light signals vertical (v/v) and perpendicular (⊥) by vertical and horizontal (v/h) settings, the emission polarizer was set vertical and the absorption polarizer was set vertical or horizontal. The wavelengths for excitation and emission were set to 360 nm (slit 5 nm) and 430 nm (slit 10 nm), respectively. For measuring the individual background (Bkg) intensities parallel and perpendicular to the initial polarized light beam, 2 ml of HBSS were added to the cuvette. Afterwards, cells were labeled with 30 µM trimethylammonium diphenylhexatriene (TMA-DPH) for 30 min at 37 °C and washed with HBSS. Within 30 min, seven individual measurements were executed at 37 °C. Each individual measured intensity was corrected by subtracting the Bkg signals v/v and v/h from the measured intensity v/v and v/h. The following mathematical formula was used to calculate the fluorescence anisotropy (r):

$$\text{anisotropy } r = \frac{I\,v/v - Gf \times I\,v/h}{I\,v/v + 2 \times Gf \times I\,v/h}$$

$$Gf = \frac{I\,h/v}{I\,h/h}$$

I v/v = measured I v/v – Bkg v/v

I v/h = measured Iv/h – Bkg v/h

The grating factor (Gf) indicates a correcting factor, which compensates the polarization bias of the detection system and was defined ahead of measuring the anisotropy. Obtained data were normalized to untreated control and were displayed as relative changes of anisotropy allowing to present alterations in membrane fluidity.

2.8 siRNA transfection

HUVECs were transfected with the Amaxa HUVEC Nucleofector Kit (Lonza, Basel, Switzerland) using ON-TARGET plus human ACACA siRNA smart pool, ON-TARGET human ACACB siRNA smart pool or siGENOME Control Pool to downregulate ACC1 or ACC2 gene expression. HUVECs (1 x 10^6) were resuspended in 100 µl Nucleofactor Solution and mixed with 300 nmol

small interfering RNA (siRNA) according to the manufacturer's protocol. This cell/siRNA solution was transfected using the electroporation device Nucleofector 2b (Lonza).

Table 10: siRNA used for gene silencing *via* electroporation.

siRNA	Description	Provider
ON-TARGET plus human ACACA siRNA smart pool	ACC1-targing siRNA	Thermo Scientific Dharmacon, Lafayette, CO, USA
ON-TARGET human ACACB siRNA smart pool	ACC2-targing siRNA	Thermo Scientific Dharmacon, Lafayette, CO, USA
siGENOME Control Pool	non-targeting siRNA	Thermo Scientific Dharmacon, Lafayette, CO, USA

2.9 Immunocytochemistry

2.9.1 F-actin staining and measurement of filopodia formation

HUVECs where either cultured to confluence on a µ-Slide 8-well (ibidi, Martinsried, Germany) and treated with soraphen A (30 µM, 24 h) or soraphen A pretreated cells (30 µM, 22 h) were detached and allowed to reattach for 2 h in low density (15,000 cells/well, µ-Slide 8 Well) in cell culture medium containing 30 µM soraphen A. HUVECs, which have been transfected with siRNA, were cultivated for 46 h. Then, cells were detached and allowed to reattach for 2 h. Afterwards, cells were washed with prewarmed PBS+ (37 °C), fixed with Roti-Histofix 4 % for 10 min at RT and permeabilized with 0.2 % Triton X-100 in PBS (max. 2 min, RT). Subsequently, cells were washed three times with PBS, unspecific binding sites were blocked with 0.2 % BSA (20 min, RT) and incubated with rhodamine-phalloidin (1:800, 1 h, RT). Cells were washed again three times with PBS and finally embedded in FluorSave mounting medium. Images were taken using a Leica DMI6000 B fluorescence microscope. The number of filopodia was counted manually. 25 cells per experiment were analyzed.

2.9.2 Microtubule staining

HUVECs were cultivated and treated like described in 2.9.1. Cells were incubated in cell extraction buffer to remove monomeric and dimeric tubulin subunits. After 30 s of extraction, cells were fixed for 10 min with 0.5 % glutaraldehyde in H_2O. After removing excess glutaraldehyde, probes were quenched with 0.1 % $NaBH_4$ in PBS for 7 min. Afterwards, cells were washed with PBS, blocked with PBS 0.2 % BSA for 10 min and stained with α-tubulin antibody (1:800, 1 h). After washing with PBS, cells were stained with Alexa Fluor 488 secondary antibody (1:400, 1 h). Nuclei were stained with Hoechst 33342 (1 µg/ml, 45 min).

Table 11: Dyes and antibodies used for immunocytochemistry.

Antibody/Dye	Dilution	Provider
Alexa Fluor 488 dye, goat-anti-rabbit IgG	1:400	Life Technologies, Darmstadt, Germany
Hoechst 33342	1 µg/ml	Sigma-Aldrich
Rhodamine-phalloidin	1:800	Life Technologies, Darmstadt, Germany
α-Tubulin	1:800	Abcam, Cambridge, UK

2.10 Migration assays

2.10.1 Undirected migration: “Wound healing”/scratch assay

A “wound healing”/scratch assay was used to determine the undirected migration of HUVECs. This assay is based on the observation that – after the creation of an artificial gap – cells migrate towards this gap until the free area is completely covered with cells to establish cell-cell contacts (122).

A confluent monolayer of HUVECs was treated for 12 h as indicated or siRNA-transfected cells were used 36 h after transfection. A wound of approximately 1 mm was inflicted to a monolayer of endothelial cells using a pipette tip. Detached cells were removed by two washing steps with serum free medium. Remaining cells were incubated in either starvation medium (Medium 199 with 1 % FBS, representing 0 % migration), culture medium (ECGM with 10 % FBS, representing 100 % migration) or culture medium containing the respective compound. The assay was stopped

after 12 h, when untreated HUVECs nearly closed the inflicted gap. Cells were washed with PBS+ and fixed with prewarmed Roti-Histofix 4 % (10 min, RT). Fixed probes were analyzed microscopically using a Leica DMIL LED microscope (Leica Microsystems). The cell free area was analyzed using ImageJ (version 1.49k). Relative migration was calculated based on the starvation control.

2.10.2 Directed migration: Boyden chamber assay

The Boyden chamber assay was used to analyze the chemotactic migration of endothelial cells (see Figure 14). HUVECs were seeded onto collagen G-coated Millicell Hanging Cell Culture Inserts (polyethylene terephthalate) with a pore size of 8 µm (Merck, Darmstadt, Germany). After reaching confluency, cells were treated with soraphen A (30 µM, 24 h) and were allowed to migrate towards a 20 % FBS gradient for 6 h. Cells were fixed with Accustain (10 min, RT) and stained with crystal violet staining solution (0.5 % crystal violet in 20 % methanol, 10 min, RT). Non-migratory cells from the upper compartment of the cell culture inserts and excess staining solution were removed using a cotton swab. Crystal violet was solubilized by addition of a dissolving buffer (50 % ethanol (v/v), 0.1 M sodium citrate in H_2O) under constant agitation at RT for 10 min. The optical density, which directly correlates to the number of migrated cells, was measured at 540 nm by a Tecan Infinite F200 Pro plate reader.

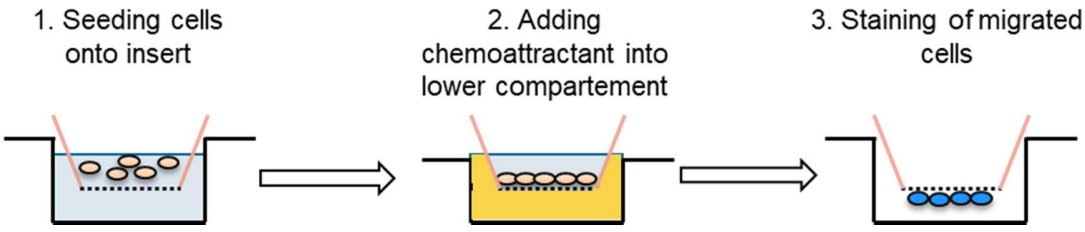

Figure 14: Principle of the Boyden chamber assay.
Cells are loaded onto the insert. After reaching confluency, the chemoattractant is added to the lower compartment. Cells were allowed to migrate for 6 h and finally stained by crystal violet solution.

2.10.3 Chemotaxis migration assay

HUVECs were seeded onto µ-slides chemotaxis chambers coated with collagen IV (ibidi, Martinsried, Germany) at a concentration of 3 x 10^6 cells/ml (1,8 x 10^4 cells/well) according to the manufactures' protocol (see Figure 15). After cell attachment, HUVECs were carefully washed twice with PBS to remove non-adherent cells und culture medium. Washed cells were incubated in a FBS gradient (0 % to 20 %) combined with 30 µM soraphen A. Cell migration was observed using a Leica DMI 6000 B for 20 h. Images where taken every 10 min.

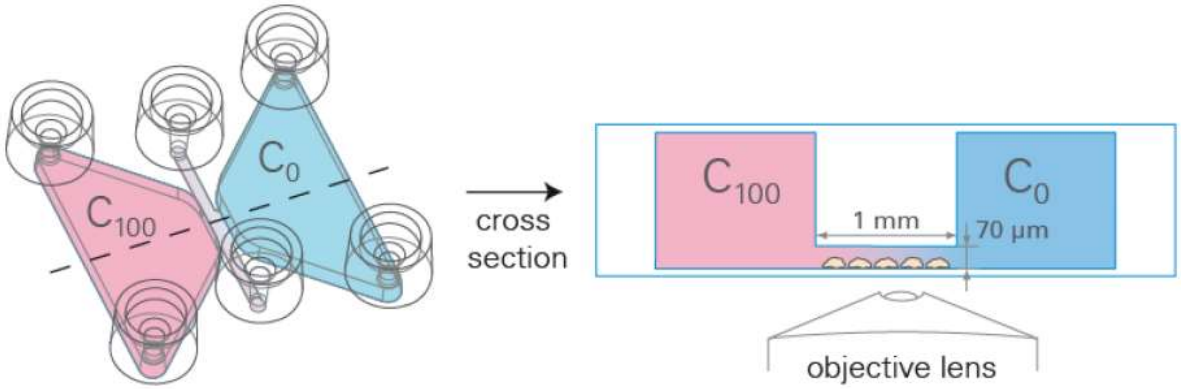

Figure 15: Schematic illustration of a µ-Slide Chemotaxis.
Cells are seed onto a gap between two reservoirs containing either chemoattractant (C_{100}) or no chemoattractant (C_0). Figure is reprinted with permission of ibidi (123).

The ImageJ plugins "Manual Tracking" and "Chemotaxis Analysis" were used to track cell movement and calculate the following parameters: forward migration index towards Y-axis direction (FMI:Y), directness, accumulated distance, Euclidean distance and the velocity of the endothelial cells.

2.11 Proliferation

Adherent cells undergoing cell death lose their ability to attach to surfaces of culture plates. This characteristic is used to determine cell death and differences in proliferation rates. Therefore, HUVECs (1.5 x 10^3 cells/well, 96-well plate) were grown for 24 h. Subsequently, HUVECs were treated with soraphen A (0.3–100 µM) for 72 h. Untreated control cells were fixed and stained with crystal violet solution (10 min, RT) after 24 h. After 72 h of incubation with soraphen A, treated

cells were fixed and stained with crystal violet solution for 10 min at RT. Excess crystal violet dye was removed by several washing steps with distilled water. Cell monolayers were finally dried in the air. Crystal violet, which binds to proteins and DNA, was solubilized by addition of dissolving buffer under constant agitation at RT for 10 min. The optical density of each well was measured at 540 nm using the plate reader Tecan Infinite F200 Pro. The proliferation rate was determined by comparing the intensity of 72 h treated cells to untreated control cells. The IC_{50} was calculated by using the statistics software GraphPad Prism 5 (GraphPad Software, Inc., San Diego, CA, USA).

2.12 Tube formation assay

A tube formation assay was performed to analyze the ability of HUVECs to form tube-like structures. The µ-Slide Angiogenesis (ibidi) was coated with 10 µl ice-cold Growth Factor Reduced Matrigel for at least 45 min at 37 °C. Pretreated HUVECs (1 x 10^3 cells/well) were seeded out in 50 µl cell culture medium containing soraphen A or vehicle control. After 7 h of incubation at 37 °C, the formation of tube-like structures was analyzed using a Leica DMI 6000 B. The quantitative parameters number of junctions, number of segments and branches and the total branching length were determined by the ImageJ plugin “Angiogenesis Analyzer”.

2.13 Quantitative polymerase chain reaction

For the quantification of mRNA *via* the quantitative polymerase chain reaction (qPCR), HUVECs were treated as indicated or transfected with siRNA as described in 2.8. In accordance to the manufacturer’s protocol, total RNA was isolated with an RNeasy Mini Kit (Qiagen, Hilden, Germany) including on-column DNase digestion (RNase-Free DNase Set, Qiagen). Using SuperScript II Reverse Transcriptase, 1 µg of RNA was reversely transcribed. The qPCR was performed by utilizing the StepOnePlus System with SYBR Green PCR Master Mix (Life Technologies). The mRNA values were normalized to the GAPDH house keeping gene based on the $2^{-\Delta\Delta CT}$ method (124).

Table 12: Primer sequences used for qPCR

Target mRNA	Forward primer	Reverse primer
ACC1	5'-TCC ACT TGG CTG AGC GAT TG-3'	5'-CAA GTC AGC AAA CTG CAC GG-3'
ACC2	5'-TCT CGT GAG TCT ACC CGG AA-3'	5'-AGC TTC TTG TGT TCC CGT CC-3'
GAPDH	5'-CCA CAT CGC TCA GAC ACC AT-3'	5'-TGA AGG GGT CAT TGA TGG CAA-3'

2.14 Transcriptome analysis

The library preparation for transcriptome analysis was performed *via* Massive Analysis of cDNA Ends (MACE) Library Prep Kit (GenXPro, Frankfurt, Germany). Subsequently, the transcriptome sequencing was performed by a MiSeq Reagent Kit v3 (Illumina, San Diego, CA, USA). This next-generation method provides a single sequencing from the 3'-end of each individual complementary DNA (cDNA). In short, 5 µg mRNA of each sample were transcribed into cDNA by the usage of biotinylated primers. These primers tag each cDNA with barcodes adapters. Then, the QIAquick PCR Purification Kit (Qiagen, Hilden, Germany) was used to purify the cDNA with silica columns. After pooling and shearing cDNA into ≤ 200 bp fragments *via* sonication, the biotinylated cDNA was captured with streptavidin-coated paramagnetic beads. Immediately afterwards, end repair, adapter ligation and PCR amplification with 12 cycles were performed. Finally, according to the manufacture's protocol "Preparing Libraries for Sequencing on the MiSeq" (Illumina), 16 pM cDNA were used for Illumina sequencing.

The quotient of the average raw count of each gene within the library and the geometric mean of all counts in all samples were calculated and displayed as normalized mRNA expression. The median's quotient was calculated per library. Each raw count was divided by the library-specific median value, according to Anders *et al*. (125).

2.15 Western Blot

2.15.1 Sample preparation

HUVECs or HepG2 were seeded onto 6-well plates and treated as indicated or transfected with siRNA. For lysis cells were washed with ice-cold PBS and frozen in RIPA lysis buffer at -80 °C. After thawing on ice, cells were scraped off, sonicated and centrifuged (16,000 g, 15 min, 4 °C). The supernatant was collected, mixed with 5x Laemmli sample buffer and heated at 95 °C for 5 min. An aliquot of the supernatant was taken to determine the protein concentration by using a Pierce Assay. Finally, cells were stored at -20 °C for further use.

2.15.2 Protein quantification

In order to determine and adapt the protein concentration of each cell lysate, a Pierce Assay was performed. The assay is based on a protein binding dye-metal complex (bicinchoninic acid). After binding, the reddish dye-metal complex turns to green, which results in an absorbance shift (126). According to the manufacturer's instructions, the Pierce BCA Protein Assay Kit (Thermo Fisher Scientific, Schwerte, Germany) was used. Aliquots of the lysate supernatant were incubated with Pierce solution at 37 °C for 30 min. The absorbance was measured by using Tecan Infinite F200 Pro plate reader at 560 nm. Dilutions (0, 50, 100, 150, 200, 300, 400 and 500 µg/ml) of a 2 mg/ml BSA stock solution were used for calibration. A linear regression was used to determine the protein concentration of each protein sample.

2.15.3 Sodium dodecyl sulfate polyacrylamide gel electrophoresis

According to Laemmli (127), a sodium dodecyl sulfate polyacrylamide gel electrophoresis (SDS-PAGE) was used to separate proteins dependent on their molecular weight. Each sample was diluted with Laemmli sample buffer (1x) to obtain equal amounts of proteins and loaded onto polyacrylamide gels, which consist of one stacking and one separating gel. The concentration of acrylamide (7.5 %) in the separating gel was adjusted depending on the respective molecular weight. The SDS-PAGE was performed using the Bio-Rad System (Mini-PROTEAN Tetra System) at 80 V until the proteins left the stacking gel. When the proteins reached the separating gel, 120 V

was used for separation. The prestained protein ladders Spectra Multicolor High Range Protein Ladder was used to identify the molecular weights.

2.15.4 Tank electroblotting

The separated proteins from SDS-PAGE were transferred onto a polyvinylidene difluoride (PVDF) membrane (Immobilon-P; Merck Millipore) *via* tank electroblotting. This technique was first patented by William J. Littlehales (128). After activating the PVDF membrane in methanol for 1 min, the blotting sandwich consisting of cathode fiber pad, two filter papers, separating gel, PVDF membrane, two filter papers and finally the fiber pad anode, was prepared. Depending on the isoelectric point and molecular weight of the target protein, the CAPS tank electroblotting buffer was chosen. The blotting sandwich were placed in a blotting tank (Bio-Rad Laboratories, Inc., Hercules, CA, USA) filled with the respective precooled buffer. The protein transfer was performed overnight (4 °C, 30 V).

2.15.5 Protein detection and visualization

After protein transfer, the membrane was blocked for 1 h in either BSA (5 %) solution or non-fat dry milk powder solution (Blotto, 5 %) to minimize the binding of antibodies to unspecific protein-binding sites. To immunologically detect the protein of interest, the membrane was incubated with the respective primary antibody while gently shaking overnight at 4 °C (see Table 13). To wash unbound and residual antibody away, the membrane was washed five times (5 min each) with TBS buffer containing 0.05 % Tween 20 (TBS-T) under constant agitation. Afterwards, the membrane was incubated in the compatible secondary antibody for 1 h (see Table 14) and washed again like described before. Finally, the membrane was incubated for 1 min with enhanced chemiluminescence (ECL) solution and was protected from light. Hereby, in the presence of H_2O_2 and horseradish peroxidase (HRP), luminol catalyzes the oxidation resulting in chemi-luminescence. The luminescence was detected by the exposure of X-ray films (Super RX; Fuji, Düsseldorf, Germany) to the membrane. The X-ray film processor CP 1000 was used to develop exposed X-ray films. Densitometric analysis of scanned Western blot films were performed with ImageJ software version 1.49k.

Table 13: Primary antibodies used for Western blot analysis

Antibody	Dilution	Supplier
Anti-acetyl-CoA Carboxylase 1 catalogue no. 4190	1:1000	Cell Signaling Technology/NEB Danvers, Massachusetts, USA
Anti-ACCβ (F-9) catalogue no. sc-3773313	1:500	Santa Cruz Biotechnology, Dallas, TX, USA

Table 14: Horseradish peroxidase-conjugated secondary antibodies

Antibody	Dilution	Supplier
Goat anti-rabbit catalogue no. sc-2004	1:10,000	Santa Cruz Biotechnology, Dallas, TX, USA
Goat anti-mouse catalogue no. sc-2005	1:10,000	Santa Cruz Biotechnology, Dallas, TX, USA
Mouse monoclonal anti-β-actin antibody catalogue no. A3854	1:100,000	Sigma-Aldrich, St Louis, MO, USA

2.15.6 Membrane stripping

Stripping buffer (25 ml) with freshly added β-mercaptoethanol (200 µl) was used to remove bound antibodies from the PVDF membrane. This allows to detect different proteins with a similar molecular weight on a single membrane. Therefore, the membrane was incubated with this solution for 20 min at 50 °C and afterwards washed several times. Subsequent steps were performed as described before (see 2.15.5).

2.16 Statistical analysis

Each experiment was performed for at least three times. The precise number of independently conducted experiments (n) is stated in the respective figure legend. In case of using primary cells, each n represents a single HUVEC donor. Bar graph data are expressed as mean values ± standard error of the mean (S.E.M.). The statistical analyses were performed with the GraphPad Prism 5.0 software (San Diego, CA, USA). For significance analysis, unpaired *t*-test or one-way

ANOVA with Tukey's *post hoc* test were used. Statistically significant differences were considered at $P \leq 0.05$.

3 RESULTS

3.1 The ACC inhibitors soraphen A and TOFA do not affect the viability of human endothelial cells

To characterize the role of ACC in primary human endothelial cells, both a gene silencing approach and pharmacological inhibitors were used. Besides the macrocyclic polyketidic natural compound and well-established ACC inhibitor soraphen A, also the lipophilic fatty acid mimetic TOFA was used to inhibit the enzymatic activity of ACC1 and ACC2. First, to investigate a possible cytotoxic effect of ACC inhibition on endothelial cell viability, the metabolic activity, apoptosis rate and the release of lactate dehydrogenase were analyzed up to 48 h of treatment.

3.1.1 The metabolic activity of HUVECs is not impaired by soraphen A or TOFA

The metabolic activity was measured by the ability of viable cells to reduce the non-fluorescent dye resazurin into the fluorescent dye resorufin (see 2.3.1). Both ACC inhibitors did not lower the reduction of resazurin in HUVECs up to concentrations of 30 µM after 24 h and 48 h indicating that soraphen A and TOFA do not affect the viability of endothelial cells (Figure 16). High concentrations of soraphen A (100 µM), however, significantly reduced the endothelial cell viability by ~ 16 % after 24 h. Consequently, for all following experiments, soraphen A and TOFA were only used at concentrations ≤ 30 µM.

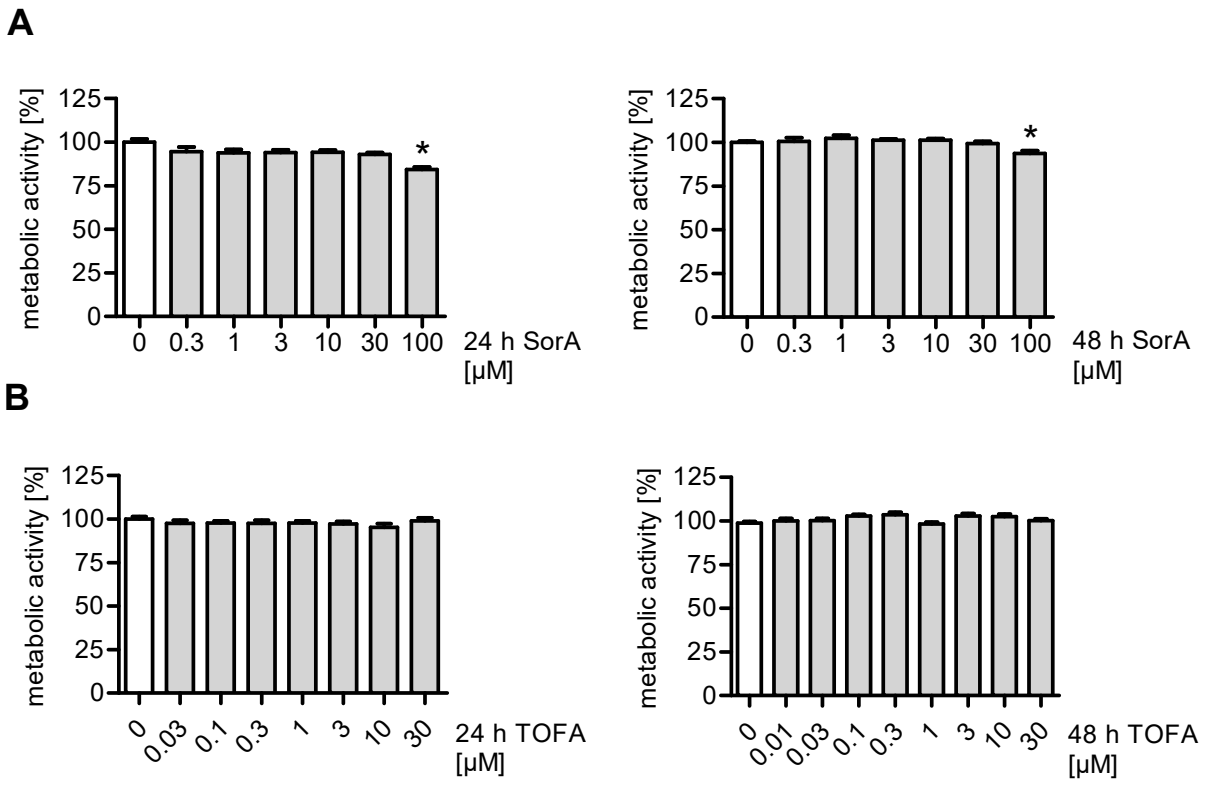

Figure 16: Soraphen A and TOFA do not impair the metabolic activity of HUVECs up to concentrations of 30 µM. HUVECs were treated with increasing concentrations of soraphen A (A) or TOFA (B) for 24 h or 48 h. The metabolic activity was measured by the CellTiter-Blue assay. Data are expressed as mean ± S.E.M. (n = 3), (**P* ≤ 0.05 *vs*. control).

3.1.2 Soraphen A does not induce apoptosis in endothelial cells

According to Nicoletti *et al*. (114), the number of subdiploid DNA content was measured in HUVECs treated with increasing concentrations of soraphen A. Propidium iodide, which intercalates into nucleic acids, was used to stain the chromatin. As shown in Figure 17, treatment with soraphen A until concentrations of 100 µM did not evoke any increase in the number of apoptotic cells compared to untreated control cells after 24 h or 48 h. A treatment with 100 µM soraphen A for 48 h only slightly increased the apoptosis rate of endothelial cells to a level of approximately 13 % compared to the control level (7 %). Staurosporine (STS; 1 µM) was used as a positive control.

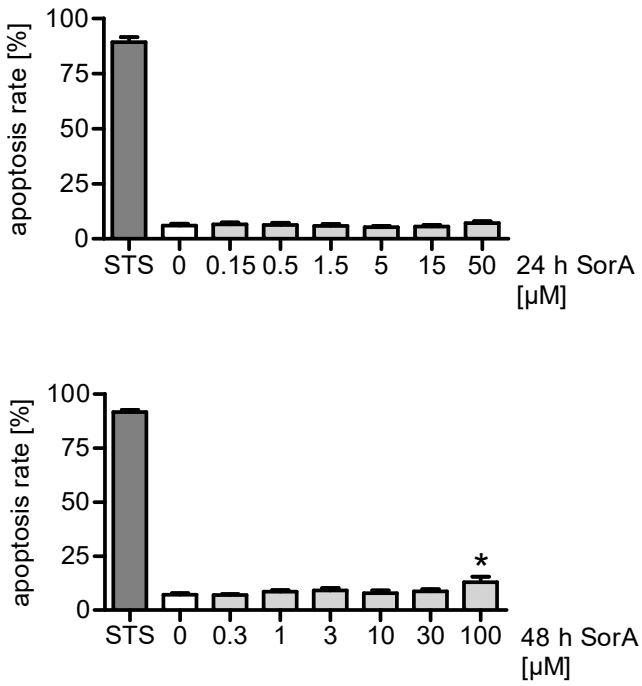

Figure 17: Soraphen A does not induce apoptosis in human endothelial cells after 24 h or 48 h of treatment. HUVECs were treated with increasing concentrations of soraphen A for 24 h or 48 h. Staurosporine (STS; 1 µM) served as positive control. The subdiploid DNA content was measured by flow cytometry. Data are expressed as mean ± S.E.M. (n = 3), (**P* ≤ 0.05 *vs*. control).

The quantification of the apoptosis rate confirmed that soraphen A – up to a concentration of 30 µM – did not induce apoptosis in HUVECs.

3.1.3 Soraphen A does not induce cell death

The CytoTox 96 Non-Radioactive Cytotoxicity Assay Kit was used to determine cell death upon soraphen A treatment by measuring the amount of lactate dehydrogenase (LDH) released from dying cells. Soraphen A treatment (0.3–100 µM) did not induce the number of endothelial cells with compromised membrane integrity after 24 h or 48 h (Figure 18). For maximum LDH release, Lysis Solution (LYS) was used as positive control.

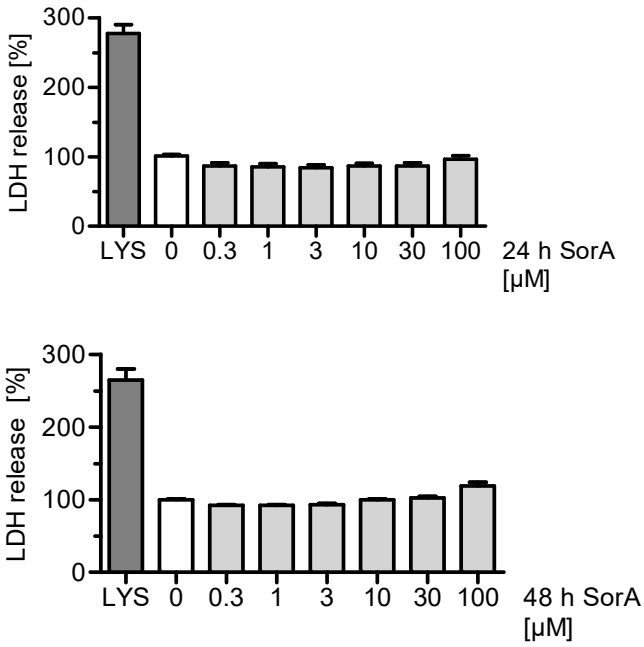

Figure 18: The release of lactate dehydrogenase (LDH) from endothelial cells is not influenced by soraphen A treatment.
HUVECs were treated with soraphen A (0.3–100 µM) for 24 h or 48 h. The LDH release of dying cells was used to determine the cell integrity. Lysis solution (LYS) was used as positive control. Data are expressed as mean ± S.E.M. (n = 3), (*$P \leq 0.05$ *vs.* control).

In summary, these results (Figure 16–18) show that neither soraphen A nor TOFA treatment impair the viability of endothelial cells up to a concentration of 30 µM (24 h). The non-toxic concentrations of soraphen A were used in all experimental settings of this study.

3.2 Endothelial cell proliferation is inhibited by soraphen A

HUVECs were treated with different concentrations of soraphen A (0.3–100 µM) for 72 h. Cells were stained with crystal violet to determine the influence of soraphen A on the endothelial cell proliferation. Soraphen A inhibited the proliferation of HUVECs with a half maximal inhibitory concentration (IC_{50}) of 34 µM (Figure 19). The x-axis shows the applied concentrations of soraphen A logarithmically (log_{10}).

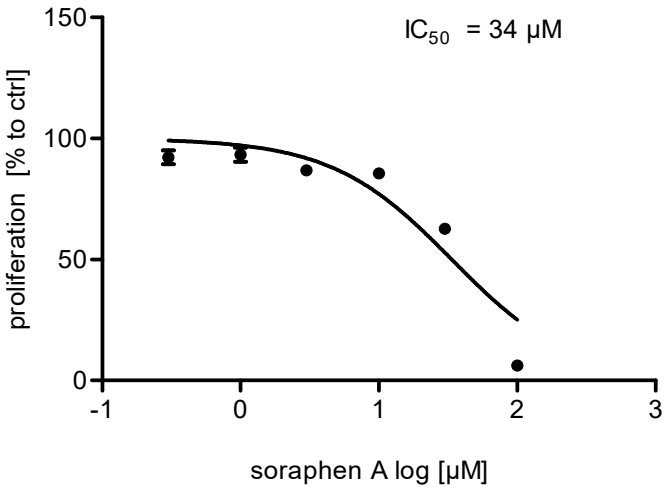

Figure 19: Soraphen A inhibits endothelial cell (HUVEC) proliferation.
HUVECs were treated with increasing concentrations of soraphen A (0.3–100 µM) for 72 h. The applied concentrations of soraphen A are displayed logarithmically (log_{10}) on the x-axis. Cell proliferation was analyzed by staining cells with crystal violet. The absorbance was measured at 540 nm. The half maximal inhibitory concentration (IC_{50}) of soraphen A was calculated as 34 µM (n = 4).

3.3 ACC1 is the predominant isoform in endothelial cells

In the literature, a functional redundancy between the isoform ACC1 and ACC2 has not been clarified unequivocally (129-131). Hence, the role of ACC in endothelial cells was characterized by investigating which isoform of ACC dominates in untreated, quiescent endothelial cells. The basal mRNA levels of ACC1 and ACC2 were determined both by quantitative PCR and by transcriptome analysis. The mRNA levels of both isoforms in HUVECs were compared to the mRNA levels in the human microvascular endothelial cell line HMEC-1 and in the human liver cancer cell line HepG2 (positive control). The protein levels of both isoforms were analyzed by immunoblotting.

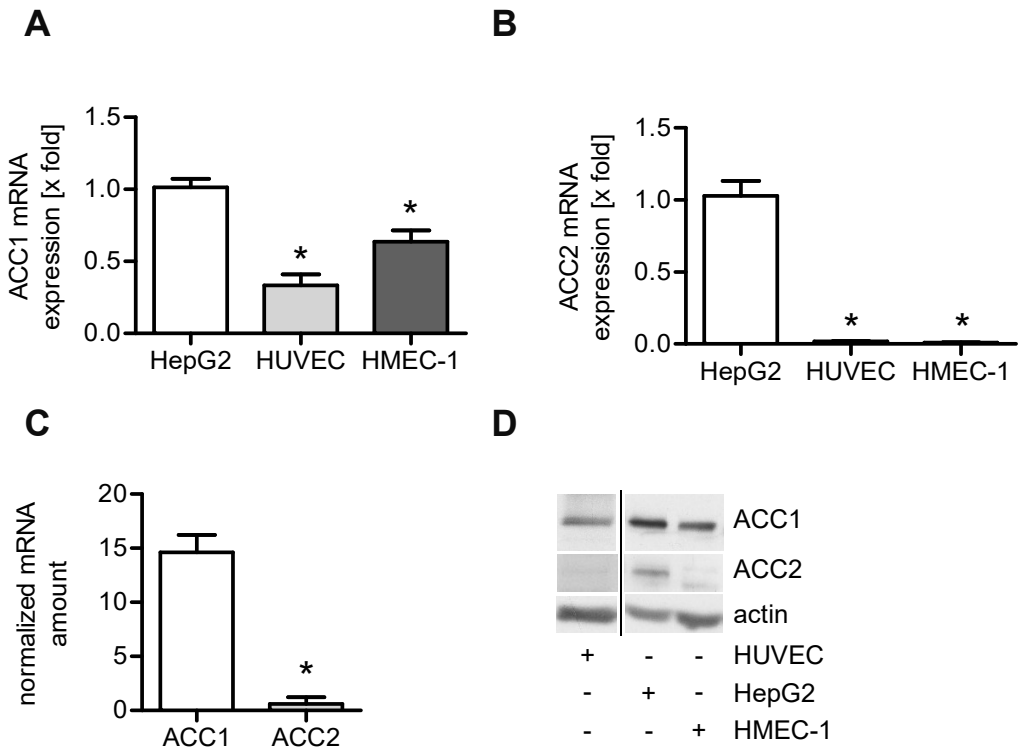

Figure 20: ACC1 is the predominant isoform in endothelial cells.
The mRNA expression of ACC1 (A) and ACC2 (B) in HUVECs and in the human microvascular endothelial cell line HMEC-1 was compared to the liver cancer cell line HepG2 (positive control) by qPCR analysis. Data are expressed as mean ± S.E.M. (n = 3), (**P* ≤ 0.05 *vs.* HepG2). (C) RNA expression of ACC1 and ACC2 in HUVECs were determined by transcriptome analysis. Data are expressed as mean ± S.E.M. (n = 3), (**P* ≤ 0.05 *vs.* ACC1). (D) ACC1, ACC2 and β-actin protein levels were measured in HUVECs, HMEC-1 and HepG2 cells (positive control). One representative Western blot out of three independently performed experiments is depicted.

As shown in Figure 20, ACC1 mRNA expression found in HUVECs was about one third, the ACC1 expression in HMECs was about two third of the expression found in HepG2 cells. On the contrary, the expression of ACC2 mRNA in HUVECs and HMEC-1 were less than 2 % of the expression levels in HepG2 cells. Accordingly, the transcriptome analysis showed that the normalized ACC2 mRNA expression (see 2.14) is only 10 % of the normalized ACC1 mRNA expression. The results of the Western blot analysis confirmed these findings.

In summary, these findings clearly demonstrate that ACC1 is the predominant isoform in endothelial cells.

3.4 Malonyl-CoA levels are strongly reduced by soraphen A treatment

Several studies have demonstrated that soraphen A is as a potent inhibitor of ACC (59, 72). Since ACC inhibition should result in reduced malonyl-CoA levels, we measured the action of soraphen A on malonyl-CoA levels to verify the functionality of soraphen A in HUVECs.

Ultra-performance liquid chromatography-coupled electrospray ionization tandem mass spectrometry (UPLC-MS/MS) was performed to measure the amount of malonyl-CoA upon soraphen A treatment (30 µM, 24 h). Soraphen A treatment strongly reduced the malonyl-CoA levels by almost 90 % (Figure 21). This demonstrates the strong inhibitory action of soraphen A on endothelial ACC without showing any cytotoxic effect (see Figure 16–18).

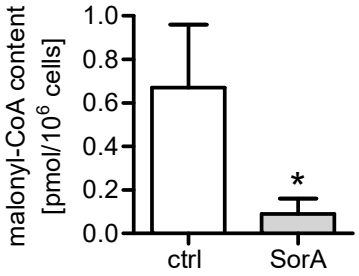

Figure 21: Soraphen A strongly reduces the malonyl-CoA content in HUVECs.
HUVECs were either left untreated (ctrl) or were treated with soraphen A (30 µM, 24 h). The level of malonyl-CoA was measured by UPLC-MS/MS. Data are expressed as mean ± S.E.M. (n = 3), (*$P \leq 0.05$ *vs.* ctrl).

3.5 ACC inhibition affects endothelial membrane composition

Since the conversation of acetyl-CoA into malonyl-CoA is a key step in the biosynthesis of fatty acids and since most of the fatty acids, which are generated *via de novo* synthesis, are incorporated into membrane phospholipids (132-134), we hypothesized that soraphen A might influence the phospholipid membrane composition. Therefore, the impact of ACC inhibition on the phospholipid profile of HUVECs was analyzed.

3.5.1 Soraphen A leads to a shift in the membrane lipid composition of HUVECs

The phospholipid profile of HUVECs treated with soraphen A (30 µM, 4 h or 24 h) was determined by UPLC-MS/MS. Untreated cells were defined as 100 %. Short time treatment of soraphen A (30 µM, 4 h) had neither a significant impact on the cellular phospholipid composition nor on the grade of fatty acid saturation of endothelial cells (see Figure 22).

In contrast to the short time treatment, long-term soraphen A treatment (30 µM, 24 h) markedly altered the membrane phospholipid composition. Endothelial ACC inhibition significantly reduced the amount of phosphatidylglycerol (PG) by 54 % and exhibited a minor tendency to lower the levels of the major membrane lipids phosphatidylcholine (PC) and phosphatidylethanolamine (PE) after 24 h (see Figure 22 A). Furthermore, long-term soraphen A treatment significantly reduced the cellular ratio of PI and PC containing saturated fatty acids (SFA; Figure 22 B) relative to PI with monounsaturated fatty acids (MUFA; Figure 22 C) and PC with polyunsaturated fatty acids (PUFA; Figure 22 D).

Aside from altering the grade of saturation, ACC inhibition also altered the length of fatty acid chains: Figure 23 A shows that soraphen A significantly decreased the subgroup of PC phospholipids with short fatty acids (C-14), whereas the subgroup of PC with C-20 fatty acids was significantly augmented. In contrast, as shown in Figure 23 B, the portion of PG with long chain fatty acids PG(18:1/18:1) decreased compared to PG with shorter fatty acid chains PG(16:0/18:1).

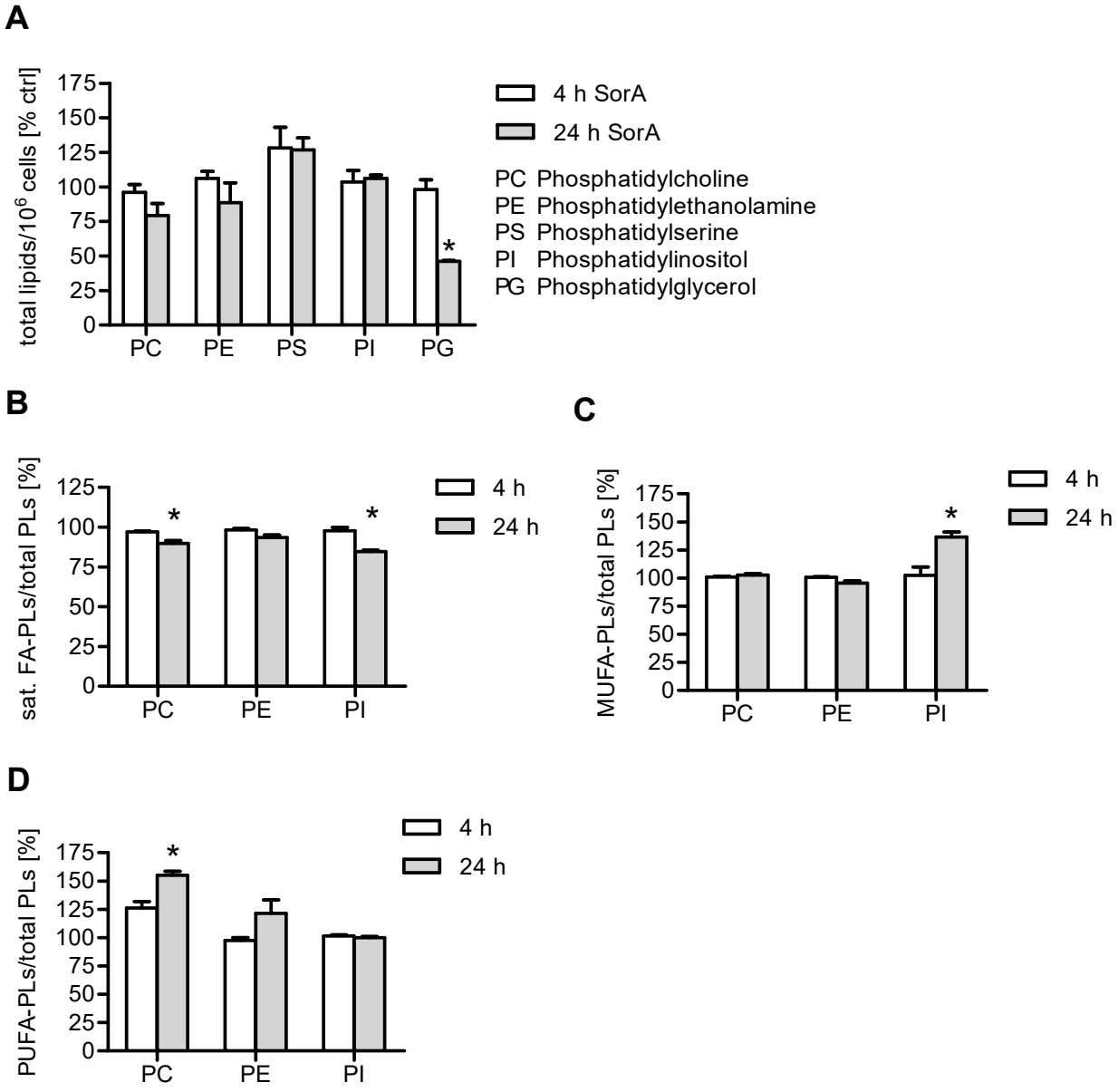

Figure 22: ACC inhibition changes the membrane composition of endothelial cells.
(A-D) HUVECs were either left untreated or were treated with soraphen A (30 µM) for 4 h or 24 h. The membrane lipid composition and the grade of membrane lipid desaturation was measured by UPLC-MS/MS. Sat. FA-PLs, saturated fatty acid-containing phospholipids; MUFA-PLs, MUFA-containing phospholipids; and PUFA-PLs, phospholipids containing PUFAs with more than two double bonds were measured. Untreated cells (control) are represented as 100 %. Data are expressed as mean ± S.E.M. (n = 3, n = 2 for PI), (*$P \leq 0.05$ *vs.* control).

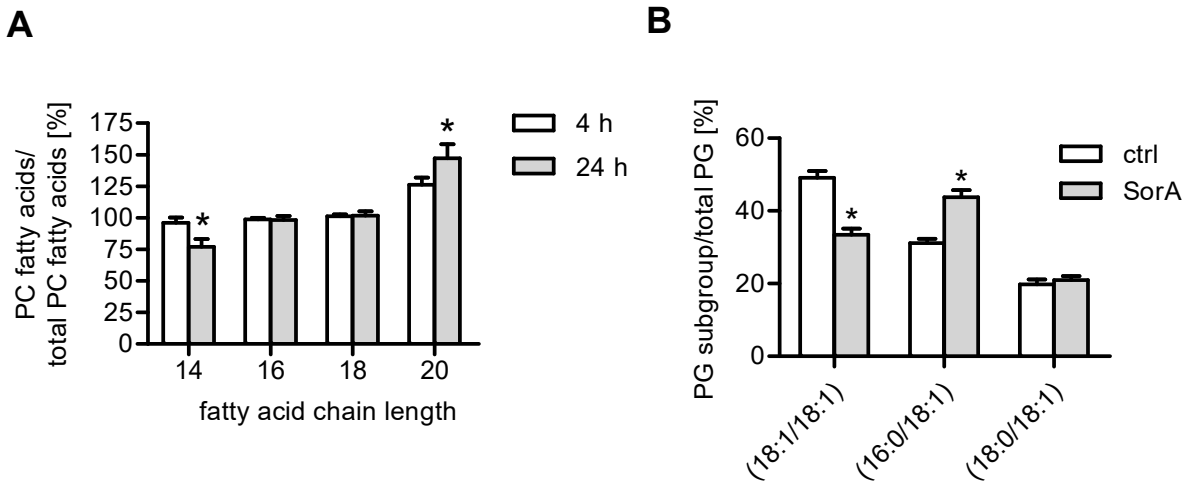

Figure 23: ACC inhibition by soraphen A alters the length of fatty acid chains.
HUVECs were either left untreated (ctrl) or were treated with soraphen A (30 µM) for 4 h (A) or 24 h (A-B). The length of fatty acid chains was measured within the phospholipid subgroup PC (phosphatidylcholine) and PG (phosphatidylglycerol) by UPLC-MS/MS. Untreated cells (control) are represented as 100 % (A). Data are expressed as mean ± S.E.M. (n = 3), (*$P \leq 0.05$ *vs*. control).

Since the amount of cholesterol is an important component of mammalian cell membranes (135), we also examined cholesterol levels besides phospholipids. The cellular cholesterol concentrations were not altered by ACC inhibition *via* soraphen A (Figure 24).

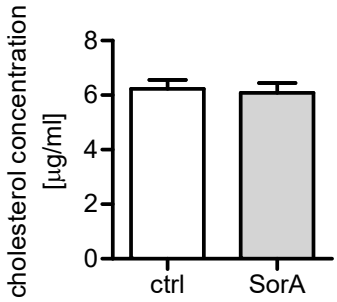

Figure 24: Soraphen A does not alter the cellular cholesterol concentrations.
HUVECs were either left untreated (ctrl) or were treated with soraphen A (30 µM, 24 h). The Amplex Red Cholesterol Assay was used to determine the amount of cellular cholesterol. Data are expressed as mean ± S.E.M. (n = 3), (*$P \leq 0.05$ *vs*. ctrl).

In summary, ACC inhibition augments the grade of fatty acid unsaturation, while cellular cholesterol concentrations remains unaffected. Additionally, soraphen A also increases the portion

of phospholipids with longer fatty acids chains within the phospholipid subgroup PC and leads to a reduction of the fatty acid chain lengths within the subgroup PG.

3.5.2 ACC inhibition results in a decreased membrane fluidity

Since the composition of membranes (chain length, degree of saturation), is known to affect membrane fluidity, we suggested that ACC inhibition by soraphen A might influence this parameter in endothelial cells. Therefore, the membrane fluidity of HUVECs was evaluated by fluorescence anisotropy measurements. These measurements are based on the principle that the fluorescent dye trimethylammonium diphenylhexatriene (TMA-DPH) anchors itself at the membrane/water interface of cells. This enables the measurement of rotational changes in the direct proximity of a phospholipid head group. The inhibition of ACC by soraphen A (30 µM, 24 h) led to a significant increase in anisotropy values, indicating a decreased membrane fluidity (Figure 25).

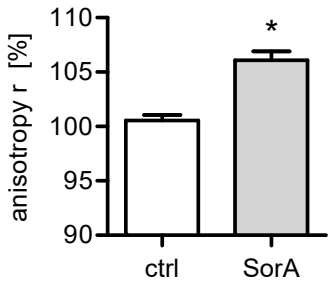

Figure 25: Soraphen A increases membrane rigidity.
HUVECs were treated with soraphen A (30 µM, 24 h) or left untreated. The fluorescence anisotropy (r) was measured by labeling cells with the fluorescent dye TMA-DPH. Data are expressed as mean ± S.E.M. (n = 3), (*$P \leq 0.05$ *vs*. control).

In conclusion, soraphen A leads to a reduction of malonyl-CoA levels, which results in a rearrangement of the phospholipid composition and to an increased membrane rigidity in endothelial cells. Overall, the levels of total PG and saturated acids are depleted, while the amount of MUFAs and PUFAs is increased and the fatty acid chain length is altered.

3.6 ACC inhibition alters the actin cytoskeleton in spreading/ migrating endothelial cells

Because of the anchorage of F-actin fibers to the cell membrane, changes in the membrane fluidity can result in rearrangements of the actin cytoskeleton (136). Hence, the impact of soraphen A on the actin cytoskeleton was investigated. In addition, the tubulin cytoskeleton was also analyzed.

3.6.1 Soraphen does not affect the actin cytoskeleton in quiescent cells

Confluent HUVECs were stained with rhodamine-phalloidin or an anti-α-tubulin antibody upon soraphen A treatment (30 µM, 24 h). Confluent, quiescent cells treated with soraphen A did neither show alterations in the morphology of the actin nor the tubulin cytoskeleton (Figure 26 A). Also the tubulin cytoskeleton of spreading/moving endothelial cells remained unaffected (Figure 26 B).

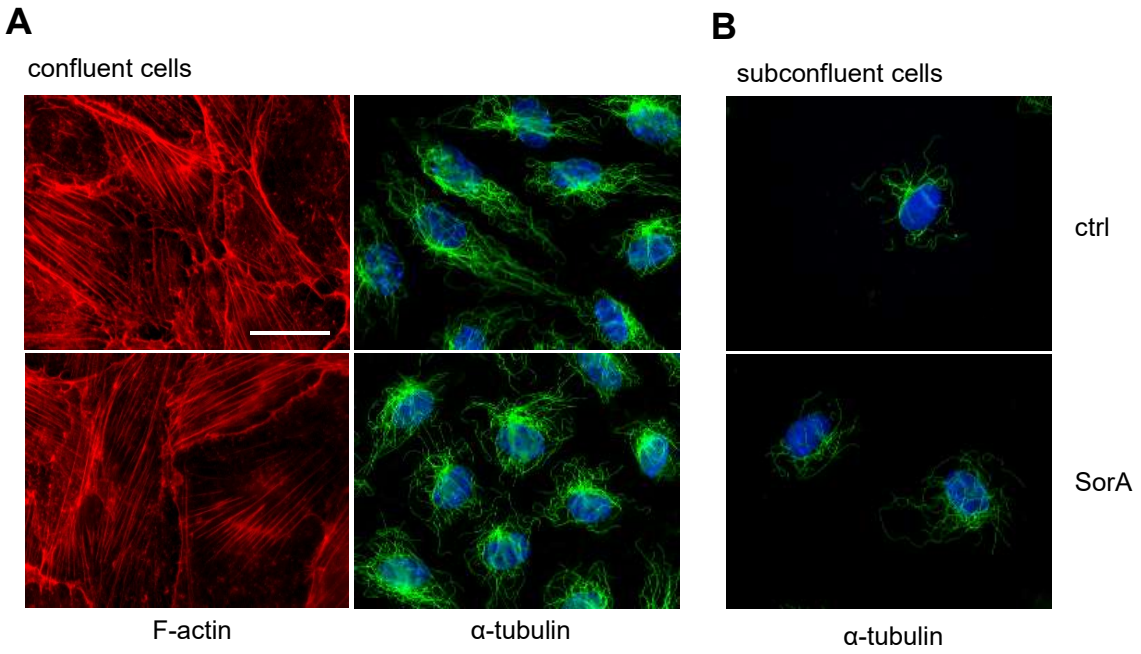

Figure 26: ACC inhibition does not affect the cytoskeleton of quiescent endothelial cells.
HUVECs grown to confluency (A) or in low density (B) were treated with soraphen A (30 µM, 24 h) or left untreated. F-actin (red), α-tubulin (green) and nuclei (blue) were visualized by immunochemical staining and fluorescence microscopy. Magnification: 64x. Scale bar represents 25 µm. One representative image out of three independently performed experiments is shown.

3.6.2 ACC inhibition decreases the number of filopodia in spreading/migrating endothelial cells

Although the treatment with soraphen A had no influence on the actin cytoskeleton of confluent, quiescent endothelial cells, most importantly, spreading/moving cells treated with soraphen A (30 µM, 24 h) exhibited significant alterations of the F-actin distribution. The quantity of filopodia in spreading HUVECs was strongly decreased by 60 % after soraphen A treatment (Figure 27 A). This effect was also observed in ACC1-silenced endothelial cells (Figure 27 B). Efficient gene silencing of ACC1 was verified by determining the mRNA and protein levels of ACC1 (Figure 28).

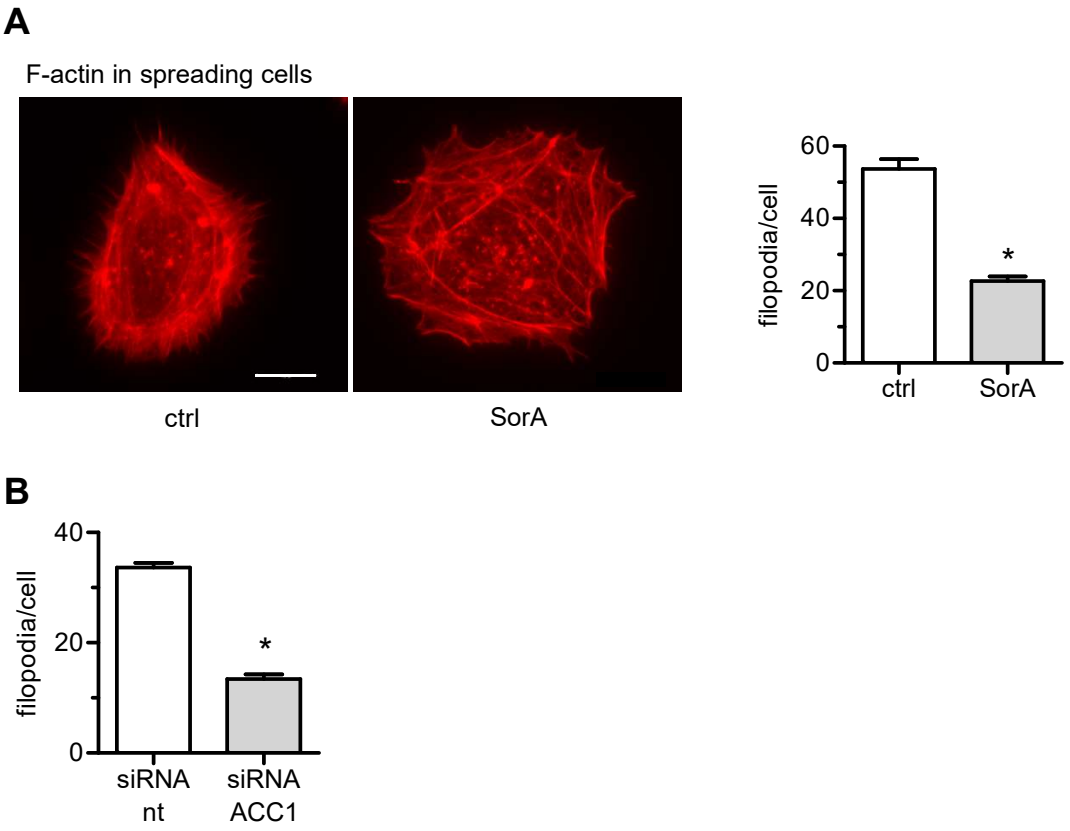

Figure 27: The number of filopodia is reduced in spreading/migrating endothelial cells upon ACC inhibition. (A) HUVECs were pretreated with soraphen A (30 µM, 24 h) or left untreated. Cells were detached and were allowed to reattach, spread and migrate in low density for 2 h. (B) HUVECs were transfected with non-targeting (nt) or ACC1-targeting siRNA. Cells were detached 46 h after transfection and allowed to reattach, spread and migrate in low density for 2 h. (A-B) F-actin (red) was visualized by immunochemical staining and fluorescence microscopy. Magnification: 64x. Scale bar represents 10 µm. One representative image out of three independently performed experiments is shown. The quantity of filopodia was determined by counting (25 cells per experiment). Data are expressed as mean ± S.E.M. (n = 3), (*$P \leq 0.05$ *vs*. ctrl or siRNA nt).

Filopodia have important sensory and exploratory functions, especially in cell motility. These projections have a finger-like structure containing bundled, crosslinked actin filaments (26, 27).

In summary, these findings report that ACC inhibition does not impair the cytoskeleton of quiescent cells, however, the number of filopodia, representing a crucial F-actin structure in migrating cells, is significantly reduced.

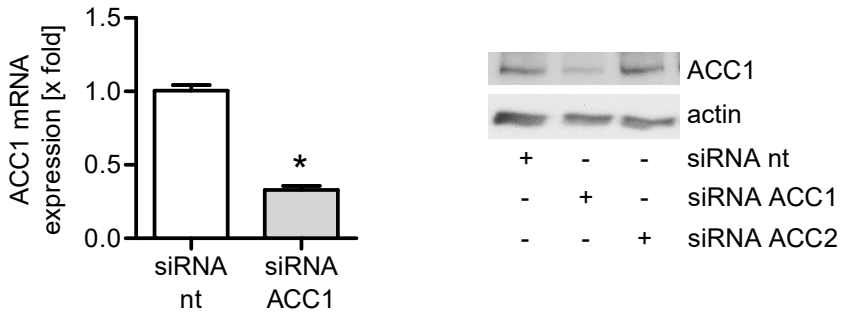

Figure 28: Successful knockdown of ACC1 in endothelial cells.
HUVECs were transfected with non-targeting (nt), ACC1-targeting siRNA or ACC2-targeting siRNA. The ACC1 mRNA expression were determined by qPCR, ACC1 and β-actin protein levels were determined by Western blot analysis 48 h after transfection. Data are expressed as mean ± S.E.M. (n = 3), (*$P \leq 0.05$ *vs.* siRNA nt). One representative image out of three independently performed experiments is shown.

3.7 ACC inhibition impairs undirected endothelial cell migration

Filopodia are known to mediate the migration of endothelial cells (19). Since ACC inhibition results in a loss of filopodia in this study, the influence of ACC inhibition on the migration was analyzed. Therefore, a scratch assay was performed in HUVECs. As shown in Figure 29, soraphen A blocked the undirected migration in a concentration-dependent manner. TOFA, another well-established ACC inhibitor, was used to exclude a compound-specific effect. Besides soraphen A, also TOFA inhibited the endothelial cell migration. To confirm the importance of ACC in regulating the endothelial cell migration, the undirected migration was determined upon silencing with either ACC1 or ACC2 siRNA.

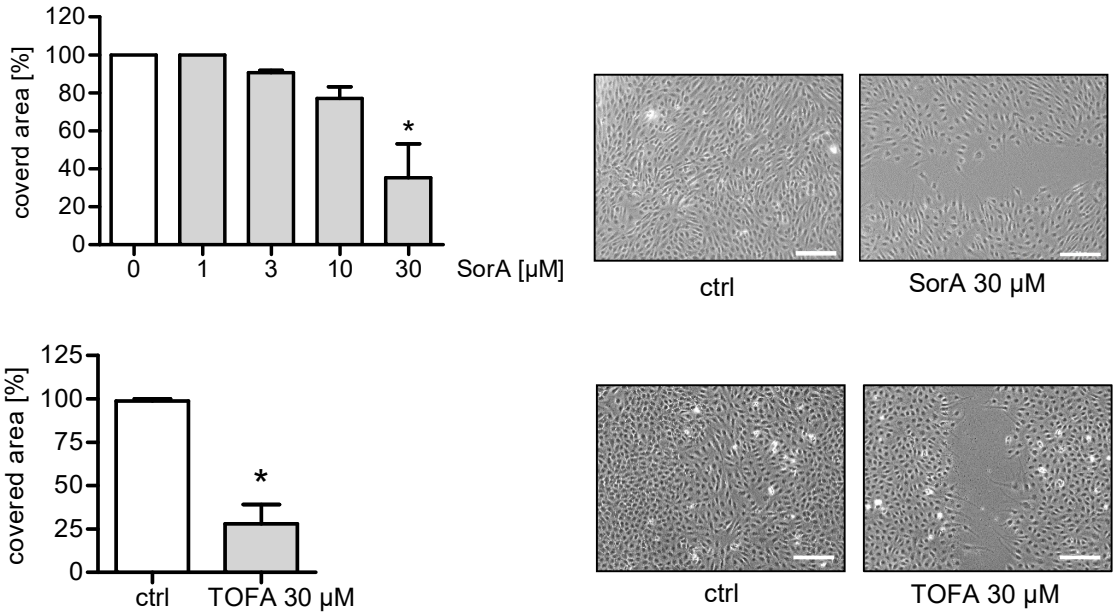

Figure 29: Soraphen A attenuates undirected endothelial cell migration.
HUVECs were left untreated or were treated with different concentrations of soraphen A or TOFA for 24 h and a scratch assay was performed. Cells were allowed to migrate for 12 h. The covered area was determined. Data are expressed as mean ± S.E.M. (n = 3), (*$P \leq 0.05$ *vs*. ctrl). One representative image out of 3 independently performed experiments is shown. Magnification: 10x. Scale bar represents 200 µm.

The knockdown of ACC1 strongly attenuated the migration of HUVECs (Figure 30 A). The additional treatment with soraphen A had no further effect on HUVECs treated with ACC1 siRNA. As expected, ACC2 silencing had no impact on the migration due to its low expression in endothelial cells (Figure 30 B). The successful silencing of ACC2 was verified on the mRNA level (see Figure 30 C).

The protein levels of ACC1 were analyzed in ACC2-silenced HUVECs to exclude that ACC2 knockdown influences the protein levels of ACC1. Figure 28 shows that ACC2 inhibition does not lead to counterregulatory effects.

These data confirm that ACC1 is the predominant isoform in HUVECs and that it is crucially involved in the undirected migration of endothelial cells.

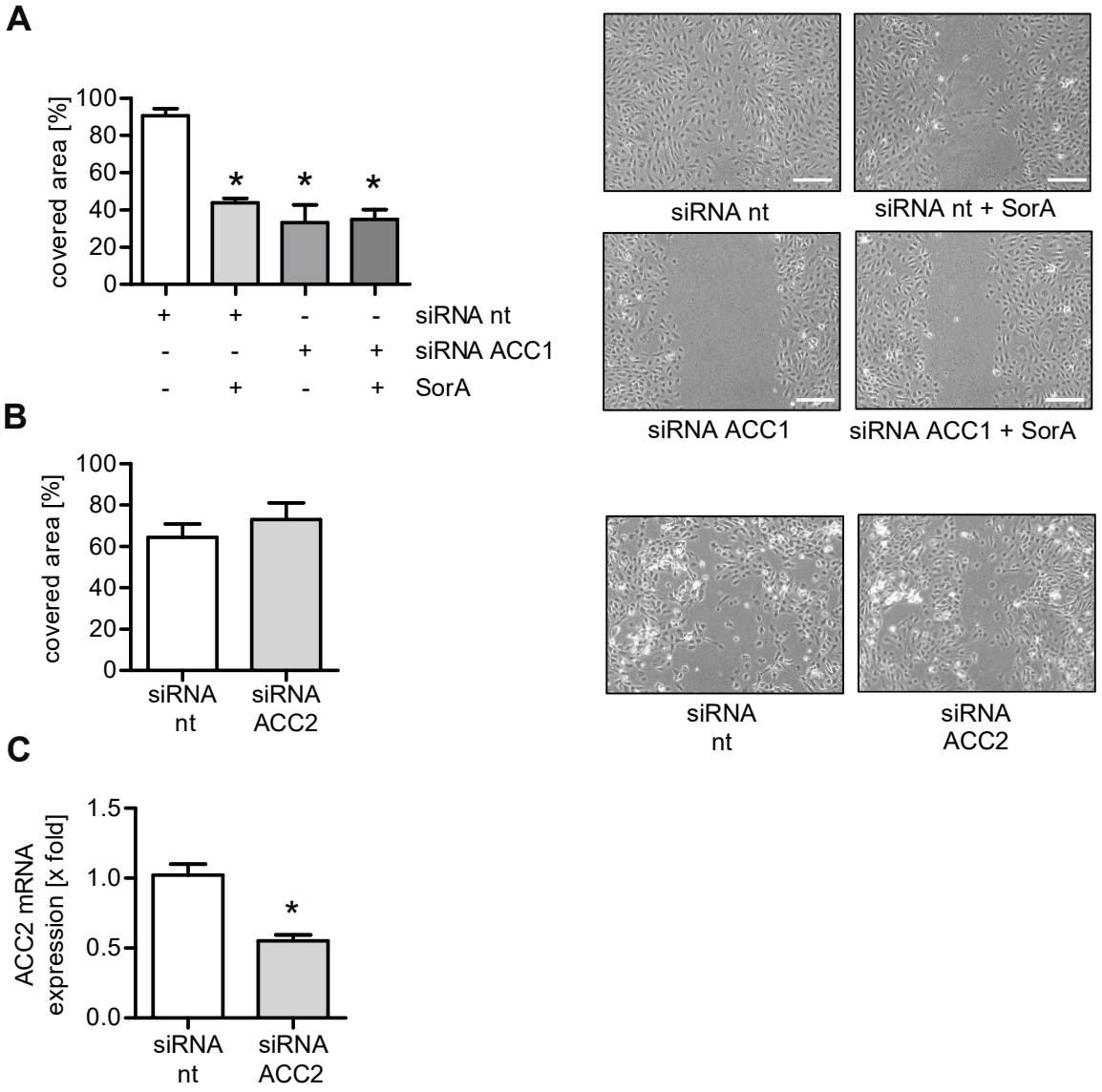

Figure 30: ACC1-silenced cells show a deceased migratory capacity.
(A) HUVECs were transfected with non-targeting (nt) or ACC1-targeting siRNA. Additionally, cells were treated with soraphen A (30 µM, 24 h). (B) HUVECs were transfected with non-targeting (nt) or ACC2-targeting siRNA. (A-B) A scratch assay was performed 36 h after transfection. Cells were allowed to migrate for 12 h. The covered area was determined. Data are expressed as mean ± S.E.M. (n = 3), (**P* ≤ 0.05 *vs.* siRNA nt). One representative image out of 3 independently performed experiments is shown. Magnification: 10x. Scale bar represents 200 µm. (C) HUVECs were transfected with non-targeting (nt) or ACC2-targeting siRNA. ACC2 mRNA levels were analyzed by qPCR 48 h after transfection. Data are expressed as mean ± S.E.M. (n = 3), (**P* ≤ 0.05 *vs.* ctrl or siRNA nt).

3.7.1 ACC1 inhibition blocks directed endothelial cell migration

Besides undirected migration, the impact of ACC1 inhibition was also investigated on the process of chemotactic migration. The directed migration was determined *via* Boyden chamber assays and by live-cell imaging. In the Boyden chamber assay, both soraphen A and ACC1 siRNA led to a complete shutdown of endothelial cell migration in the direction of a chemoattractant gradient (20 % FBS) (Figure 31 A-B).

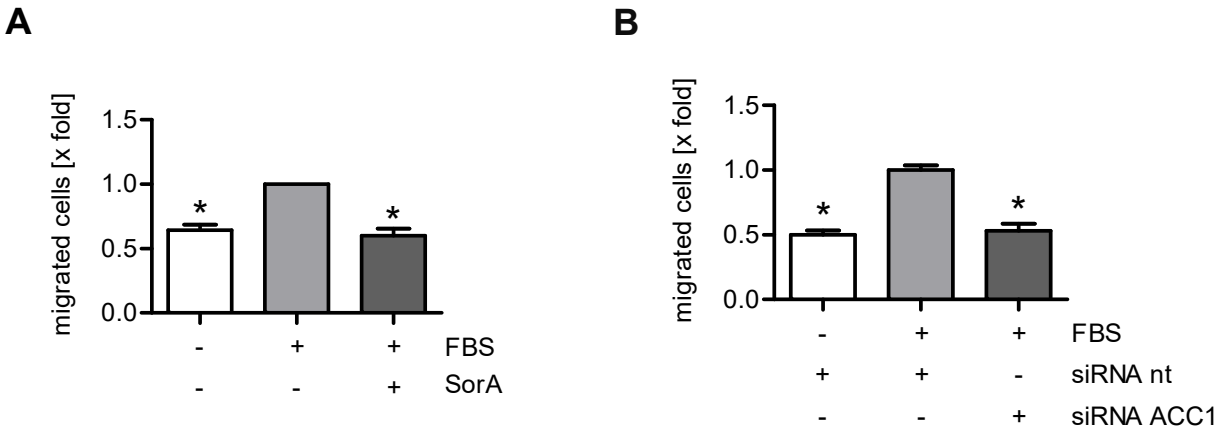

Figure 31: ACC inhibition reduces chemotactic migration in endothelial cells.
(A) HUVECs were either left untreated or were treated with soraphen A (30 µM, 24 h). (B) HUVECs were transfected with non-targeting (nt) or ACC1-targeting siRNA. (A-B) The Boyden chamber assay was started either 12 h after pretreatment or 42 h after transfection. Cells were allowed to migrate towards a chemoattractant gradient (20 % FBS) for 6 h. Migrated cells were quantified by crystal violet staining. Data are expressed as mean ± S.E.M. (n = 4 for A, n = 3 for B). (*$P \leq 0.05$ *vs.* ctrl or siRNA nt).

Additionally, the action of soraphen A and ACC1-targeting siRNA on the chemotactic migration was measured by live-cell imaging. After tracking the movement of single cells, the movement process was characterized by determining the following parameters: The forward migration index (FMI:Y) describes the cell movement towards the chemoattractant. The quantitative parameter directness is calculated by forming the quotient of the Euclidian distance and the accumulated distance. The directness represents the tendency of a cell to move in a straight line. The accumulated distance is calculated as the sum of the traveled distance, while the Euclidian distance describes length of the straight line between the cell's start and end point (137).

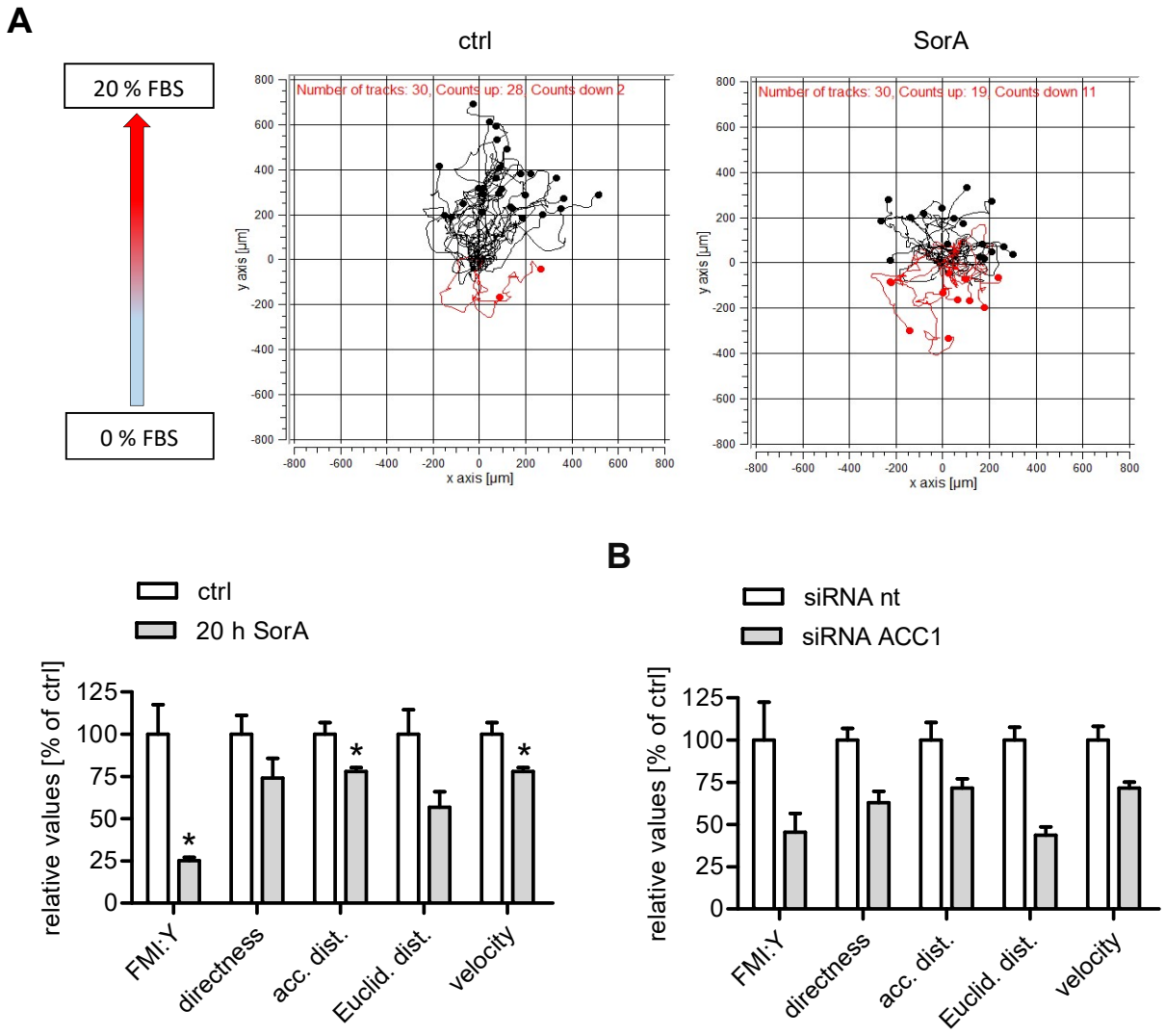

Figure 32: ACC inhibition decreases the migration towards a chemotactic stimulus.
(A) HUVECs were either left untreated or were treated with soraphen A (30 µM, 20 h). (B) HUVECs were transfected with non-targeting (nt) or ACC1-targeting siRNA. Cells were seeded into chemotaxis chambers 28 h after transfection. (A-B) Chemotactic migration towards a 20 % FBS gradient was monitored for 20 h. The parameters forward migration index (FMI:Y), directness, accumulated distance (acc. dist.), Euclidean distance (Euclid. dist.) and the velocity of cells were calculated. Data are expressed as mean ± S.E.M. (n = 3), (*$P \leq 0.05$ *vs.* ctrl or siRNA nt).

Soraphen A significantly decreased the parameters FMI:Y, accumulated distance and velocity. The parameters directness and Euclidean distance were also attenuated by ACC inhibition *via* soraphen A, even though statistically not significant. Similar effects were found in ACC1-silenced HUVECs (see Figure 32 B): ACC1-targeting siRNA markedly reduced the parameters FMI:Y, directness, accumulated distance, Euclidian distance and velocity.

In summary, both soraphen A and ACC1-targeting siRNA markedly reduced the migratory capacity of endothelial cells towards a chemotactic stimulus.

3.8 Tube formation assay

Endothelial cell proliferation and migration are two functional key aspects of angiogenesis. Since soraphen A has an immense impact on the proliferation and migration of primary endothelial cells, we investigated the role of ACC in forming tube-like structures. Therefore, cells were treated with soraphen A (30 µM, 24 h) and seeded on Matrigel for additional 24 h. The following quantitative parameters were determined: number of junctions, number of segments and branches as well as the total branching length.

Surprisingly, soraphen A-treated endothelial cells did not show any significant alteration in their capacity to form tube-like structures on Matrigel. As shown in Figure 33 the quantitative parameters were not affected by ACC inhibition.

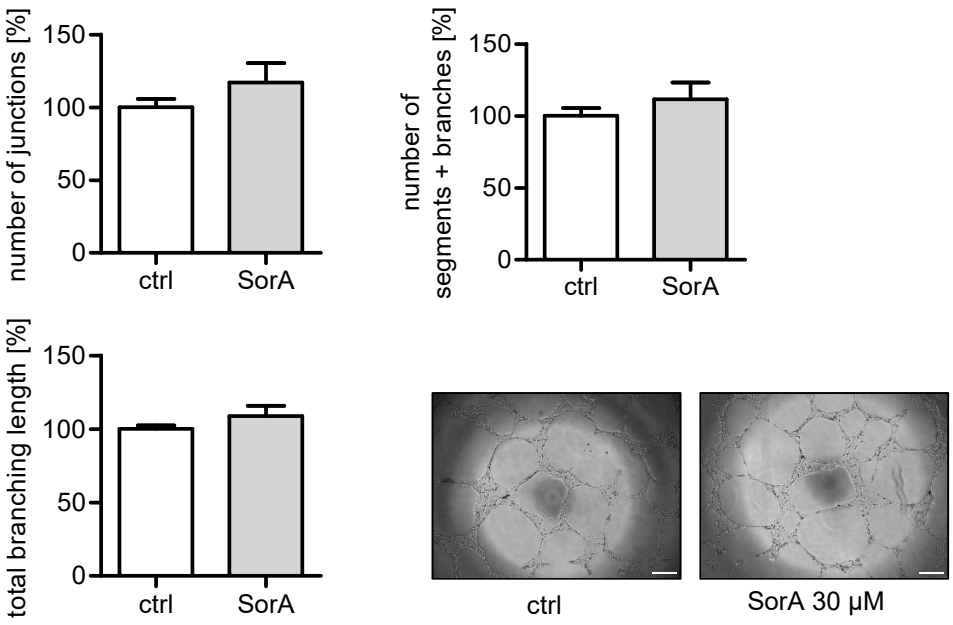

Figure 33: Soraphen A does not impair the formation of tube-like structures.
HUVECs were treated with soraphen A (30 µM, 24 h) and seeded on Matrigel for 24 h. The parameters number of junctions, number of segments and branches as well as the total branching length were determined. Data are expressed as mean ± S.E.M. (n = 3), (*$P \leq 0.05$ *vs*. ctrl). One representative image out of 3 independently performed experiments is shown. Magnification: 5x. Scale bar represents 250 µm.

3.9 Addition of polyunsaturated fatty acids mimics the antimigratory action of soraphen A

The analysis of the phospholipid profile revealed that soraphen A led to an upregulation of MUFA and PUFA species in distinct phospholipid subgroups (Figure 22 C-D). To confirm their importance for the migratory capacity of endothelial cells, their influence was determined by treating HUVECs with representative MUFA or PUFA species in a scratch assay: The MUFA oleic acid (18:1; 10 µM and 100 µM, 24 h) did not exert any influence on the migratory capacity, whereas the PUFAs linoleic (18:2) and linolenic acid (18:3; 100 µM, 24 h) mimicked the antimigratory effect of ACC inhibition (see Figure 34 A). By measuring the amount of PC(16:0/18:3), the successful incorporation of linolenic acid (18:3) into the phospholipid membrane was shown in Figure 34 B.

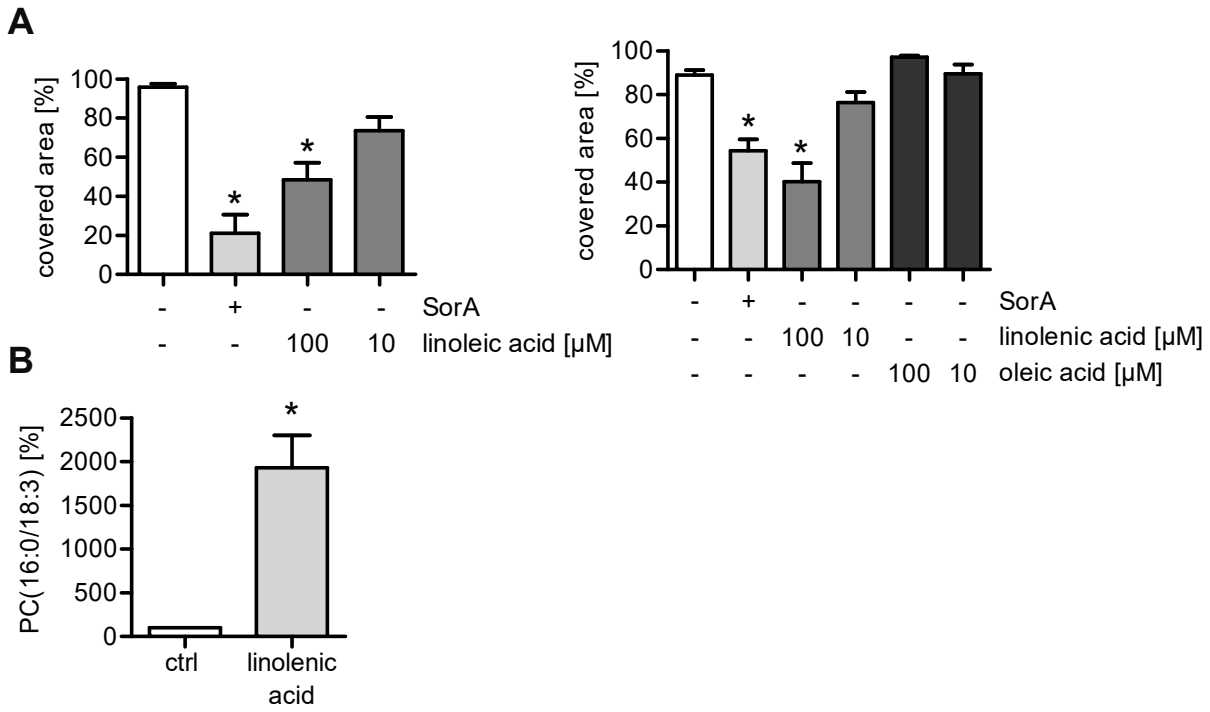

Figure 34: PUFAs mimic the antimigratory effect of ACC inhibition.
(A) HUVECs were left untreated or treated with soraphen A (30 µM, 12 h) and different concentrations of linolenic acid, linoleic acid, oleic acid or dioleoylphosphatidylglycerol (DOPG). Cells were allowed to migrate for 12 h in a assay. The covered area was determined. Data are expressed as mean ± S.E.M. (n = 5 for A left, n = 3 for A right), (*$P \leq 0.05$ *vs.* control). (B) The amount of PC(16:0/18:3) in HUVECs treated with linolenic acid (100 µM, 24 h) was measured by UPLC-MS/MS. Data are expressed as mean ± S.E.M. (n = 3), (*$P \leq 0.05$ *vs.* ctrl).

Taken together, these results prove the crucial involvement of PUFAs in the antimigratory effect of ACC inhibition.

3.10 Phosphatidylglycerol rescues the antimigratory effect of soraphen A

As shown before, the results of the lipidomics analysis revealed that ACC inhibition *via* soraphen A reduced the amount of saturated fatty acids (Figure 22 B) and strongly attenuated the portion of PG (Figure 22 A). Thus, we evaluated the capacity of stearic acid (18:0) and PG to prevent the antimigratory effect of soraphen A in endothelial cells.

The treatment of endothelial cells with stearic acid (1 µM, 24 h) did not alter the undirected migration in a scratch/migration assay (Figure 35 A). PG was supplied in the form of 1,2-dioleoyl-*sn*-glycero-3-phosphoglycerol (DOPG). Multilaminar vesicles (liposomes) of DOPG were generated in order to increase the low solubility of DOPG. The successful incorporation of DOPG into the endothelial phospholipid cell membrane was verified by measuring the total amount of PG *via* UPLC-MS/MS (Figure 35 B). To verify the specific incorporation of PG into the cell membrane, we measured the amount of other phospholipids and exemplarily chose PC. As expected, the amount of PC was not significantly affected (Figure 35 B).

As shown before (Figure 22 A), soraphen A strongly depleted the amount of the phospholipid subgroup PG. The reduction of PG after soraphen A treatment was restored by the addition of DOPG (Figure 35 B).

After verifying the successful incorporation, we analyzed the effect of DOPG on the antimigratory action of soraphen A. Therefore, HUVECs or HMEC-1 were treated with soraphen A (30 µM, 24 h) and different concentrations of DOPG (100 µM and 10 µM, 24 h). DOPG completely rescued the action of soraphen A to inhibit the process of undirected endothelial cell migration (Figure 35 C).

These findings clearly show that the antimigratory effect of ACC inhibition is causally linked to the reduction of PG in the phospholipid membrane of endothelial cells.

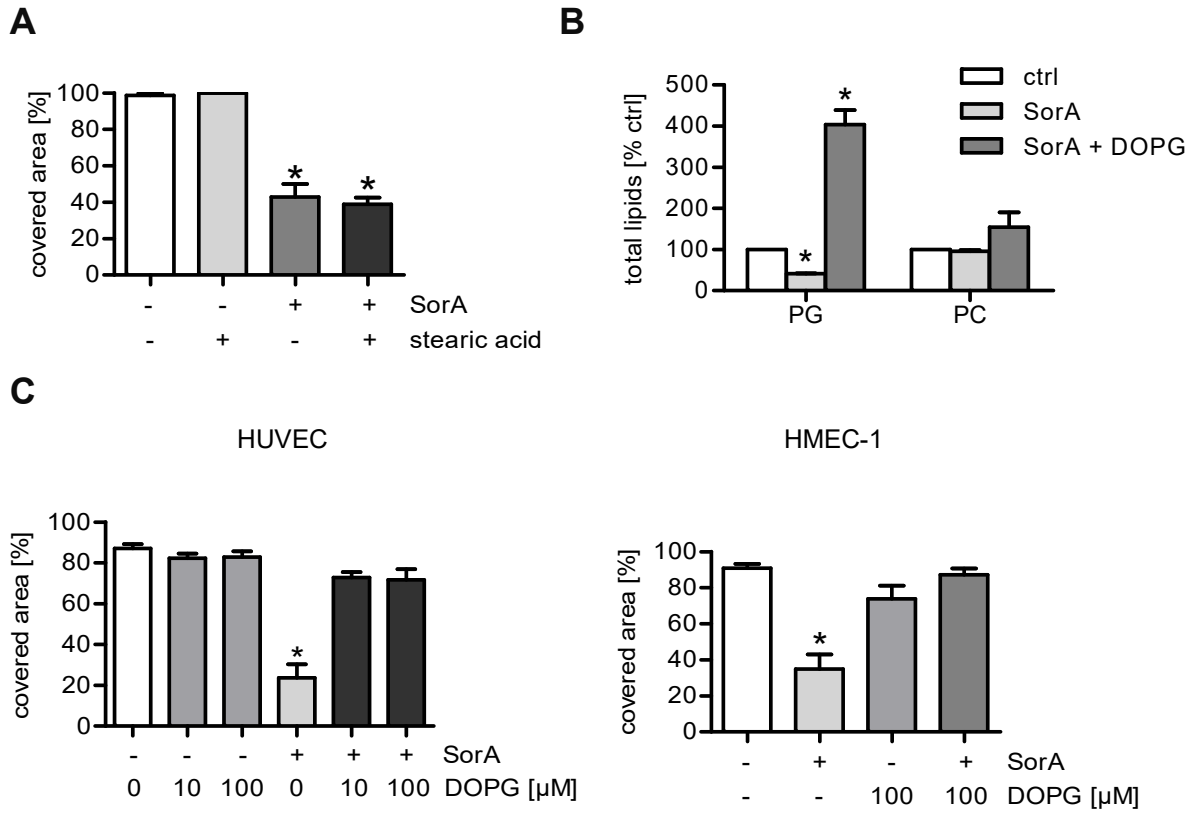

Figure 35: DOPG completely rescues the antimigratory effect of soraphen A.
(A) HUVECs were either left untreated or were treated with soraphen A (30 µM, 24 h) and stearic acid (1 µM, 24 h). (B) UPLC-MS/MS were used to determine the amount of the membrane lipids phosphatidylglycerol (PG) and phosphatidylcholine (PC). Data are expressed as mean ± S.E.M. (n = 3), (**P* ≤ 0.05 *vs*. ctrl). (C) HUVECs or HMECs were either left untreated or were treated with soraphen A (30 µM, 24 h) or 1,2-dioleoyl-*sn*-glycero-3-phosphoglycerol (DOPG, 100 µM, 24 h). (A, C) Migratory capacity were analyzed in a cell migration assay for 12 h. The covered area was determined. Data are expressed as mean ± S.E.M. (n = 3, n = 5 for C left,), (**P* ≤ 0.05 *vs*. control).

4 DISCUSSION

This work aimed to investigate the role of ACC and the fatty acid metabolism in regulating endothelial cell functions. The fatty acid metabolism has emerged as a promising target system for the treatment of various metabolic diseases like insulin resistance, hepatic steatosis, dyslipidemia, obesity, metabolic syndrome and nonalcoholic fatty liver disease. Changes in the fatty acid metabolism are also recognized as hallmarks of cancer cell proliferation (138, 139). In comparison to cancer cells, healthy cells can provide energy from circulating lipids. In contrast, the energy supply of cancer cells is mainly based on *de novo* synthesized fatty acids. This elevated synthesis of fatty acids results in an increased dependence on lipogenesis (140).

4.1 Targeting the fatty acid metabolism in endothelial cells

Besides the fatty acid metabolism of cancer cells, also the fatty acid metabolism of endothelial cells has been set into the focus. Even though the endothelium is constantly exposed to fatty acids in the blood flow, the fatty acid metabolism has been reported to maintain and regulate various important cell functions and has emerged as a promising drug target.

For example, Wei *et al.* suggested that the *de novo* lipogenesis maintains the endothelial vascular homeostasis *via* endothelial nitric oxide synthase activity (eNOS) (141). Defects in eNOS are known to cause endothelial dysfunctions, which lead to diabetes and vascular diseases such as atherosclerosis (16, 142). The authors reported that the *de novo* lipogenesis, a process which is controlled by the fatty acid synthase (FAS), regulates important endothelial cell functions by maintaining the eNOS integrity. In FAS-deficient mice (FASTie mice), the content of eNOS at the membrane and its activity were reduced. FASTie mice also revealed proinflammatory characteristics, such as rising vascular permeability, increased amounts of inflammatory markers, and elevated leukocyte migration. FAS-deficient HUVECs showed a diminished migratory capacity in a scratch assay and FASTie mice exhibited impaired angiogenesis in a chronic hindlimb ischemia model. Furthermore, the knockdown of FAS in HUVECs reduced the amount of palmitoylated eNOS, while insulin-induced FAS increased the amount of palmitoylated eNOS in a biotin switch assay. This study revealed a novel relationship between FAS and eNOS, which might participate in the progression of vascular complications in diabetes and other metabolic disorders (141).

Further physiological and pathophysiological endothelial functions have been observed to be regulated by the fatty acid metabolism. For instance, Browne *et al.* reported that pharmacological inhibition of FAS with orlistat, an antiobesity drug, reduces fatty acid syntheses and the proliferation of endothelial cells (143). By inhibiting human neovascularization in an *ex vivo* assay, orlistat emerged as a promising antiangiogenic drug. The authors attribute the reported effects to reduced exposure of VEGFR2 on surfaces of endothelial cells after treatment with orlistat (143). Seguin *et al*. confirmed the antiangiogenic effects of orlistat treatment and FAS knockdown (144). In endothelial cells, FAS inhibition resulted in reduced viability, proliferation and the formation of capillary-like structures (144).

Also β-oxidation has been reported to be critical for various endothelial cell functions. Patella *et al.* showed a link between carnitine palmitoyltransferase 1 (CPT-1), which is an important part of the β-oxidation, and the regulation of endothelial permeability *in vitro* (145). CPT-1 is responsible for the formation of acyl carnitines, which allows long chain acyl-CoAs to cross the mitochondrial membrane (79). The inhibition of CPT-1 resulted in reduced ATP levels and oxygen consumption. Furthermore, endothelial cells with inhibited CPT-1 showed hyperpermeability *in vitro* and leakage of blood vessels *in vivo*. Besides its role in regulating important endothelial functions and blood vessel stability, β-oxidation has found to be a promising target to control vascular permeability (145). Interestingly, several studies showed that the energy homeostasis in endothelial cells is not based on the fatty acid oxidation. Less than 5 % of the total amount of ATP are produced by β-oxidation (146, 147).

A recent study also reported a relationship between the fatty acid oxidation and vessel sprouting in endothelial cells (146). The loss of CPT-1a caused defects in vessel sprouting by inhibiting endothelial proliferation, without influencing migration (146). This study will be explained in detail in section 4.6.

These reports illustrate that the fatty acid metabolism is involved in many important endothelial functions and might be an interesting target system to interfere with these cell functions.

4.2 ACC as promising drug target

Due to its central role in the fatty acid metabolism, ACC offers an attractive pharmacological target for interfering with the fatty acid metabolism. Hereby, two functional key aspects can be regulated: ACC inhibition stimulates the fatty acid oxidation in oxidative tissues and simultaneously inhibits the *de novo* lipogenesis in lipogenic tissue (71, 148). ACC catalyzes the ATP-dependent carboxylation step of acetyl-CoA into malonyl-CoA. This carboxylation is the first and rate limiting step in the synthesis of fatty acids. Malonyl-CoA generated *via* ACC functions as a substrate in the fatty acid biosynthesis and controls the mitochondrial uptake of fatty acids by inhibiting CPT-1. In response to dietary alterations or changed nutritional requirements malonyl-CoA acts as a metabolic signal for controlling the fatty acid production and for controlling the switch between carbohydrate and fatty acid utilization (71, 74).

The activity and pharmacological importance of ACC has been highlighted in numerous different mouse knockout models (149). Wakil *et al.* reported the first ACC2 knockout ($ACC2^{-/-}$) mouse model and found that these $ACC2^{-/-}$ mice have significantly reduced malonyl-CoA levels in their heart tissue and skeletal muscle (89, 150-152). This results in increased fatty acid oxidation in both tissues. Compared to wild type mice, $ACC2^{-/-}$ mice also showed enhanced insulin and lipid profiles while being on a high fat/high calorie diet. A further mouse model generated by a different method also showed reduced malonyl-CoA levels in heart and muscle tissues, increased muscle and whole body fatty acid oxidation (153). In contrast to these findings, $ACC2^{-/-}$ mice generated by the group of Lowell showed only modest decreased malonyl-CoA levels in heart tissue without showing any other metabolic changes (154). These variations might be due to different methods to generate knockout mice and might be contributed to inactive ACC2 proteins, which have a dominant negative effect on ACC1 in Wakil's mice (149).

The generation of ACC1 knockout mice failed due to embryonic lethality (150). Nevertheless, the groups of Wakil and Kusunoki achieved to generate two liver specific ACC1 knockout mouse ($LACC1^{-/-}$) models (129, 155). Liver samples of Wakil's $LACC1^{-/-}$ mice showed decreased malonyl-CoA levels, reduced ACC activity and fatty acid synthesis (155). In contrast to this, the group of Kusunoki found elevated levels of both ACC2 mRNA and protein expression in $LACC1^{-/-}$ mice. This suggests that ACC2 was increased to compensate the knockout of ACC1 (129). In accordance to different ACC2 knockout mice, these differences also lack a proper

explanation for the different phenotypes seen in the two reported ACC1 knockout mice models. Studies trying to generate ACC1$^{-/-}$/ACC2$^{-/-}$ double knockout mice models are not available (149).

Besides the data obtained in knockout mice models, also some human data highlighted ACC as an attractive therapeutic target. For example, during a 3-month low-intensity endurance training program, healthy volunteers had reduced levels of ACC2 mRNA and elevated fatty acid oxidation (156). Furthermore, obese type 2 diabetic patients were reported to have elevated malonyl-CoA levels in muscle tissue and increased ACC2 activity, which led to impaired fatty acid oxidation and increased lipogenesis (157). Treatment with the antidiabetic drug hiazolidinedione reversed these defects (157). In addition to these studies, the antidiabetic drug metformin was reported to exert its efficacy *in vivo* by stimulating the adenosine monophosphate-activated protein kinase (AMPK), which is known to inhibit the ACC2 activity (158).

These promising studies led to the development of many different ACC inhibitors. Prominent ACC inhibitors are listed in the following Figure 36 and are described in the subsequent sections.

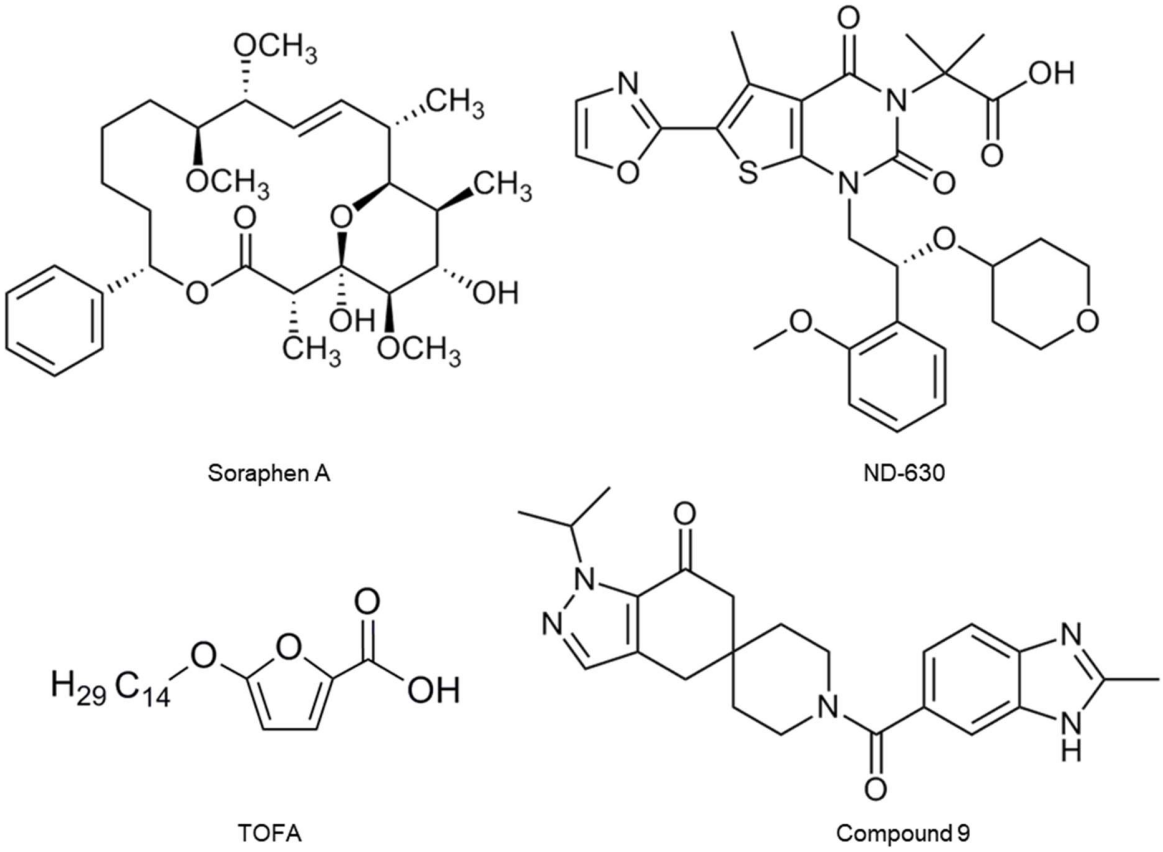

Figure 36: Chemical structure of common ACC inhibitors.

Jump *et al.* reported that a pharmacological inhibition of ACC lowers the *de novo* lipogenesis and also attenuates the microsomal fatty acid elongation (159). They found that soraphen A (with an IC_{50} of approximately 5 nM) led to reduced amounts of palmitate (16:0) and linoleate (18:2, n-6) in HepG2 and LNCaP cells. Furthermore, ACC inhibition reduced the formation of very long chain saturated, mono- and polyunsaturated fatty acids. This shows that, besides fatty acid oxidation and *de novo* lipogenesis, ACC is also crucially involved in the formation of long chain saturated, mono- and polyunsaturated fatty acids (159).

Several recent studies confirm ACC as an attractive therapeutic drug target for treating metabolic diseases, obesity or even cancer. For example, the study of Harriman *et al.* underlined the benefit of ACC inhibition in the treatment of metabolic disorders (93). They discovered and characterized the ACC inhibitor ND-630 (see Figure 36). This potent allosteric protein-protein interaction inhibitor prevents the dimerization of both ACC1 and ACC2 and inhibits their enzymatic activity. In a diet-induced obesity model in rats, ND-630 reduced hepatic steatosis and weight gain as well as led to improved insulin sensitivity and favorably modulated dyslipidemia. This data suggests, that ACC inhibition might be useful for the treatment of various metabolic disorders such as the fatty liver disease, metabolic syndrome and type 2 diabetes mellitus (93).

Furthermore, Luo *et al.* demonstrated the importance of ACC inhibition in the field of cancer therapy by using the epidermal growth factor receptor (EGFR) inhibitor cetuximab (160). This antitumor drug was reported to downregulate the Warburg effect by inhibiting a subunit of the hypoxia-inducible factor-1 (HIF-1) as a downstream signal of EGFR inhibition (160, 161). As a key transcription factor, HIF-1 regulates glycolysis, glucose uptake and lactate production (162). The Warburg effect, also called “aerobic glycolysis”, describes the observation that cancer cells primarily use glycolysis to produce lactate as a main source of energy, even in the presence of oxygen. Usually, normal cells produce energy *via* oxidative phosphorylation. Thus, targeting the Warburg effect has emerged as a promising strategy to treat cancer (163). The study of Luo *et al.* pointed out that cetuximab increased the total amount of ACC. Under low glucose conditions, ACC was supposed to maintain the cell survival *via* increasing lipogenesis. Cetuximab in combination with TOFA (see Figure 36) achieved notable growth inhibition of cetuximab-resistant head and neck squamous carcinoma cells (HNSCC) (164). This study demonstrates that ACC inhibition might improve therapies targeting the Warburg effect in cancer cells.

Additionally, a recent study reported that the ACC inhibitor ND-646 successfully blocked the tumor growth of non-small-cell lung cancer (NSCLC) in xenograft and genetically engineered *in vivo* mouse models (165). The structure of ND-646 is similar to ND-630 with the exception that the hydroxyl group is replaced by a primary amine group. The publication of Svensson *et al.* highlighted that the deletion of ACC1 led to a complete loss of the fatty acid synthesis resulting in a reduced proliferation, viability and a diminished tumorigenic potential. Inhibition *via* the orally bioavailable inhibitor ND-646 blocked lung tumor growth in KRAS p53 and KRAS Lkb1 mouse models of NSCLC. These findings underline the potential of ACC inhibition for the treatment of cancer (165).

Also Beckers *et al.* showed the importance of ACC inhibition in the field of cancer therapy (166). In LNCaP and PC-3M prostate cancer cells, soraphen A attenuated fatty acid synthesis and increased fatty acid oxidation. This resulted in a reduced phospholipid content, blocked proliferation and death of cancer cells. Interestingly, the growth arrest and cytotoxicity caused by soraphen A was abolished by the addition of palmitic acid. This study demonstrates the dependency of cancers cells on ACC activity to supply the cell with fatty acids and verifies ACC inhibitors as promising antitumor agents (166).

Moreover, ACC1 inhibition proved to attenuate T_H17 cell-mediated inflammatory diseases. Soraphen A stimulated antiinflammatory T_{reg} cells and depleted proinflammatory T_H17 cells (97). In contrast to T_{reg} cells, the development of T_H17 cells was reported to depend on the ACC1-mediated *de novo* fatty acid synthesis. Although T_{reg} cells use the *de novo* fatty acid synthesis to produce phospholipids, T_{reg} cells were able to incorporate exogenous fatty acids into the cell membrane. These results report a fundamental difference between T_H17 and T_{reg} cells regarding their dependency on the *de novo* fatty acid synthesis. This difference might be used as a novel treatment of T_H17 cell-mediated inflammatory diseases (97).

In addition, some clinical trials in human subjects report success in the treatment of metabolic diseases with ACC inhibitors. For example, a clinical trial of Pfizer reported to decrease the fatty acid metabolism and stimulate the fatty acid oxidation after single oral doses of an ACC inhibitor (167). The inhibitor, called compound 9 (see Figure 36), was used to treat human type 2 diabetes mellitus. This study demonstrates that using this ACC inhibitor might be of advantage for the treatment of human metabolic diseases (167).

A recently published double-blind and randomized crossover study reported beneficial effects of ACC inhibition (92). In this study, single doses (20, 50 or 200 mg) of the ACC inhibitor NDI-010976, also called ND-630, were orally administered to overweight and obese but otherwise healthy male patients. Single doses of NDI-010976 (≤ 200 mg) were well tolerated and were shown to reduce the *de novo* lipogenesis compared to placebo. NDI-010976 was discovered and characterized by Harriman *et al.* as described before (93). These findings suggest that NDI-010976 treatment might be beneficial for the treatment of impaired fatty acid metabolism and nonalcoholic steatohepatitis (92). The nonalcoholic steatohepatitis is the most frequently occurring hepatic disease in the Western world and has been associated with dysregulated fatty acid metabolism, elevated *de novo* lipogenesis and reduced fatty acid oxidation (74, 168).

Despite the knowledge about the importance of ACC in general, the impact of ACC on the endothelial physiology and pathophysiology has not been examined so far. We provide a first link between ACC/fatty acid metabolism and migration of endothelial cells. We showed that ACC1 is the predominant isoform in macrovascular HUVECs and microvascular HMECs. Soraphen A treatment depleted malonyl-CoA levels, shifted the membranes' phospholipid composition and reduced membrane fluidity. The reduced migratory capacity evoked by ACC inhibition was connected to the reduced amount of filopodia in migrating cells. Soraphen A mediated its antimigratory effect *via* increased concentrations of PUFAs and decreased levels of phosphatidylglycerol.

4.3 The role of ACC isoforms

In this work, ACC1 was found as the predominant isoform in endothelial cells (see Figure 20 A-D). We clearly verified that ACC1 is the major isoform on mRNA and protein level and showed that ACC1 is crucially involved in the migration of endothelial cells. Our experiments revealed that, due to its low expression, ACC2 is not involved in the regulation of endothelial migration (see Figure 30 B). Interestingly, the literature shows divergent results regarding the functionality of cytosolic ACC1 und mitochondrial ACC2. Under physiologic conditions, cytosolic ACC1 generates malonyl-CoA for *de novo* lipogenesis and elongation of fatty acids (75, 169), while mitochondrial ACC2 generates malonyl-CoA, which controls the mitochondrial β-oxidation. Contrary to this, Harada *et al*. report that liver-specific ACC1 null mice show induced ACC2 mRNA and elevated protein levels to compensate the loss of ACC1 (129). The authors showed that malonyl-CoA

generated *via* ACC2 can become a substrate for the *de novo* lipogenesis in the absence of ACC1 and they suggest no strict functional distinction of hepatic ACC isoforms under certain circumstances.

However, in this present work, neither upregulated ACC2 protein levels nor the ability of this enzyme to rescue the functional loss of ACC1 was detected (see Figure 28). It was even found that ACC2 is not involved in crucial endothelial cell functions like migration and that the amount of ACC2 is negligible compared to the expression of ACC1. The different outcomes regarding the functionality of ACC isoforms might be due to differences in cell types: liver cells rely more on lipogenesis compared to endothelial cells and endothelial cells have a minor expression of ACC2.

Supporting data has been published by Abu-Elheiga *et al.* According to their data, they confirm that the isoforms ACC1 and ACC2 have different roles in the fatty acid metabolism (89, 150). They showed that mutant mice lacking ACC1 are embryonically lethal, while ACC2 null mice are viable. The authors suggest that malonyl-CoA generated *via* ACC1 is essential for the development of mouse embryos and that ACC1 and ACC2 function independently leading to different physiological roles in the fatty acid metabolism (89, 150).

The already mentioned study of Svensson *et al.* reported that deletion of ACC1 inhibited proliferation, while ACC2 deletion had no impact (165). The authors attribute this finding to the minor expression of ACC2 in the used cancer cell line. Also Luo *et al.* demonstrated that mainly ACC1 helps cancer cells to survive cetuximab treatment (164).

4.4 Antiproliferative action of soraphen A

In this study, soraphen A was identified as an antiproliferative compound in endothelial cells (see Figure 19). Soraphen A concentration-dependently inhibited the proliferation of HUVECs without showing any toxic effects up to a concentration of 30 µM (see Figure 16–18). In accordance to our findings, several publications described an antiproliferative effect of soraphen A in different cancer cell lines, for example in LNCaP and PC-3M prostate cancer cells (166) or in the human liposarcoma cell line LiSa2 (170). Additionally, Stoiber *et al.* also reported antiproliferative effects of ACC inhibitors in the breast cancer cell line SKBR3 and the hepatocellular carcinoma cell line Huh7 (171).

In contrast to our results, many studies found antiproliferative effects in cancer cell lines already at nanomolar concentrations of soraphen A. This phenomenon might be explained by the cells' differences in metabolic states and dependence on lipogenic pathways. Various publications report that endothelial cells use glucose as predominant source of energy (147, 172) and, thus, might have higher tolerance towards influences in the ACC/fatty acid metabolism.

Furthermore, Olsen *et al.* found a causal link between the antiproliferative effect of soraphen A and the long chain fatty acid synthesis by preventing the antiproliferative effect through the addition of palmitate (170). In our study, a direct, causal link between the antiproliferative effect of soraphen A and the rearrangement of fatty acids remains to be confirmed and can only be hypothesized at this moment.

4.5 Migration and filopodia

Besides proliferation, also endothelial cell migration is an essential part of angiogenesis. A constant remodeling of the actin cytoskeleton into stress fibers, lamellipodia and filopodia provides the basis for a successful cell migration. Our experiments revealed that ACC inhibition led to a reduced migratory capacity and to a depleted filopodia formation. We hypothesize that the impaired filopodia formation might be the mechanistic principle, which causes this antimigratory effect. Filopodia are known to sense their environment and have important functions in regulating endothelial cell migration and wound healing (26-29). These bundled, parallel actin filaments set the direction of cell migration by probing their microenvironment (28). Integrins, located at the tip of filopodia, promote cell adhesion and guide migration (173).

As shown by our experiments, soraphen A reduced the formation of filopodia and decreased the undirected and directed migration capacity of endothelial cells. The ability to guide the direction while migrating is also represented by the parameter FMI:Y. In our experiments, the FMI:Y was strongly decreased, whereas the effect of ACC inhibition on the velocity of endothelial cell migration was less pronounced (see Figure 32). Due to the reduced amount of filopodia, the cells lose their sensing capacity and hence FMI:Y is decreased.

Scott *et al*. confirmed the crucial involvement of the fatty acid metabolism and ACC in regulating the F-actin distribution. Chemical inhibition of ACC *via* TOFA led to a decreased formation of

invadopodia in a Src-transformed fibroblast cell line (133). Invadopodia are dynamic actin-based protrusions of the plasma membrane found in invasive cancer cells. They facilitate matrix degradation and coordinate the invasion of cancer cells through the extracellular matrix (174-176). The addition of exogenous 16:0 and 18:1 fatty acids restored the impaired formation of invadopodia and decreased the activity of ACC1. In accordance with our result, the study by Scott *et al.* identified ACC1 as the major isoform in regulating the F-actin distribution. The authors attribute the functional connection between ACC1 and the altered F-actin distribution to changes in lipid raft domains. It has been reported that *de novo* synthesized fatty acids are enriched in lipid raft-like domains (134). These findings suggest that the fatty acid synthesis is important for the formation of invadopodia by regulating and maintaining the structure of lipid rafts (133).

Yamaguchi *et al*. reported that the composition of lipid rafts and especially the content of PI regulate the formation and functionality of invadopodia (177, 178). Invadopodia are enriched with the phospholipid phosphatidylinositol 4,5-bisphosphate [PI(4,5)P_2]. The functional inhibition of PI(4,5)P_2 blocked invadopodia formation in human breast cancer cells (178). Further experiments would be interesting to verify weather PI is also crucially involved in the formation of endothelial filopodia.

In accordance to our findings, a recently published study by Stoiber *et al.* demonstrated that ACC inhibition *via* soraphen A impaired the formation of filopodia in the breast cancer cell line MDA-MB-231 (171). Furthermore, soraphen A treatment attenuated the migratory capacity and reduced the maximal deformation of the membrane. The authors supposed that the reduced mechanical deformation alters the formation of filopodia, since mechanical deformations of plasma membranes are known to be necessary for the formation of membrane protrusions (171, 179). This hypothesis might also explain the reduced filopodia formation in endothelial cells. In this work, the soraphen A-induced increase in cell membrane stiffness could cause the altered filopodia formation. Nevertheless, further experiments are needed to verify this hypothesis.

Most of our results regarding cell migration were performed in endothelial cells treated with ACC inhibitors (soraphen A or TOFA) and some findings were verified in cells treated with ACC1 siRNA. Noticeably, ACC1 silencing had only minor effects on the endothelial migration in a 2D chemotaxis assay compared to soraphen A. The reason for this effect remains to be clarified. One explanation might be that the cells were exposed to high stress due to the process of electroporation. This would also explain why endothelial cells treated with non-targeting siRNA exhibited reduced

velocity and migration distance values compared to untreated control cells. Furthermore, 2D chemotaxis seemed to be a very stressful setup for endothelial cells. In this experiment cells are grown in low density without establishing cell-cell contacts. Due to the stressful electroporation process and 2D chemotaxis setup, the differences in ACC inhibition were not as distinct as with soraphen A-treated cells.
It should be noted that a link between ACC/fatty acid metabolism and the reduction of filopodia in endothelial cells was not established and a causal link still has to be confirmed in further experiments. However, most importantly, in our study, we found a direct link between ACC/fatty acid metabolism and the antimigratory effect of soraphen A. This point will be discussed in the following sections.

4.6 The role of ACC in angiogenesis

Since we determined an immense impact of soraphen A on the proliferation and migration of endothelial cells, we also presumed ACC inhibition to alter angiogenesis. Angiogenesis occurs, among other processes, during wound healing and is regulated by different aspects, including the proliferation and migration of endothelial cells (30).

Although we detected a decreased proliferation and migration, we surprisingly did not detect any impact of ACC inhibition on the formation of tube-like structures in endothelial cells. This unexpected result is not fully explainable with the data obtained in this study, at this moment we can only speculate: Unknown factors in the Matrigel, might preserve the antiproliferative and antimigratory effect of ACC inhibition and, thus, result in an uninfluenced tube formation. Most importantly, tube formation might be independent from changes in the phospholipid composition or membrane fluidity of endothelial cells. In accordance to our data with soraphen A, preliminary data obtained in HUVECs treated with TOFA or ACC1 siRNA did not show any impact on the formation of tube-like structures (data not shown). This suggests, that the formation of tube-like structures might be independent of ACC activity.

A very interesting phenomenon was reported by Schoors *et al.* They showed that angiogenesis might be independent from key processes like migration (146). They analyzed the metabolism of endothelial cells during vessel sprouting and demonstrated that endothelial cell sprouting *in vivo* is mainly based on fatty acid oxidation. The role of fatty acid oxidation for vessel sprouting was

more central than reported in their previously studies. They have recently shown that 85 % of ATP used for the process of vessel sprouting were generated by glycolysis, while fatty acid oxidation provided only 5 % of the total amount of ATP (147). In their present study, deletion of CPT-1, a crucial regulator of fatty acid oxidation, attenuated vessel sprouting and proliferation *in vitro* and *in vivo* without impairing endothelial cell migration. Interestingly, the reduction of fatty acid oxidation did not impair ATP levels, but attenuated the *de novo* synthesis of nucleotides for DNA replication. Isotope labeling revealed that fatty acid carbons fueled the citric acid cycle and were incorporated into precursors of nucleotides and nucleoside triphosphates and into DNA strands. This finding was unexpected since many cancer cell lines only use glucose and glutamine to fuel the citric acid cycle (180). *In vivo*, CPT-1 inhibition blocked pathological ocular angiogenesis in mice. This study presents a novel strategy for inhibiting angiogenesis and shows that specific metabolic pathways regulate specific functions during vessel sprouting in endothelial cells (146). Since ACC inhibition by soraphen A inhibits *de novo* lipogenesis in lipogenic tissue and, of note, concurrently activated fatty acid oxidation, the unaffected tube formation in our work might consequently be explained by these differences. Nevertheless, further investigations are needed to explain this unexpected result.

4.7 Phospholipid composition alters membrane fluidity in endothelial cells

Besides a reduced migratory capacity, ACC inhibition resulted in a shift in the phospholipid composition and in a decreased membrane fluidity. Since malonyl-CoA is crucial for the biosynthesis of fatty acids and since the majority of *de novo* synthesized fatty acids are incorporated into membrane phospholipids (132-134), ACC is proven to be an important regulator of membrane fluidity.

Changes in membrane fluidity are hypothesized to have extensive impairments on the physiology and pathology of cells. Proteins located in cell membranes sense environmental changes by detecting chemical and physical stimuli. Signals detected by these proteins trigger distinct pathways of signal-transduction and gene-expression inside the cells. Thus, altered membrane properties can influence the activation of these pathways or regulate the activity of membrane-bound enzymes and proteins, such as translocators of small molecules, receptor-associated protein kinases, ion channels or sensor proteins (181-185). Several studies postulated that fluid

shear stress increases membrane fluidity in endothelial cells, which results in an activation of heterotrimeric G proteins (186, 187). Consequently, alterations in membrane fluidity can indirectly affect gene expression and signaling pathways. This might be the mechanistic explanation for the link between altered membrane lipid composition and the effects found in our study. Receptors or pathways, which are activated or inactivated by an altered membrane lipid composition *via* soraphen A in endothelial cells, are still unknown and have to be investigated in further analyses.

We showed that a shift in the phospholipid composition induced by ACC inhibition leads to a decreased membrane fluidity (see Figure 25). The membrane fluidity is depended on a broad spectrum of factors. Important mediators are the fatty acid composition (degree of desaturation, fatty acid chain length) and the amount of cholesterol in the lipid membrane. Lipids with longer acyl chains are less fluid due to their lower sensitivity towards alterations in kinetic energy. This is explained by their higher molecular size, which results in a higher surface area and, consequently, leads to intensified van der Waals forces within surrounding acyl chains (188). Unsaturated lipids carrying carbon-carbon double bonds are expected to be more fluid than saturated lipids with single bonds. “Kinks” resulting from bond angle changes of carbon-carbon double bonds (120° instead of 109.5°) prevent unsaturated acids from packing as dense as saturates ones.

In this study, soraphen A led to an increased membrane stiffness. In accordance to the knowledge about the regulation of membrane fluidity, soraphen A increased the length of fatty acid chains within the major membrane phospholipid subgroup PC (see Figure 23 A). In contrast, soraphen A increased the ratio of unsaturated fatty acids (Figure 22) and reduced the content of fatty acids with shorter acyl chains within the minor membrane phospholipid subgroup PG (Figure 23 B). Although these divergent results might seem paradoxical at first sight, these findings can be explained by the following hypothesis: Since the phospholipid subgroup PC is much more predominant in membranes than PG, the rising fatty acid chain length in PC overcompensates the decrease in PG as well as the increase in desaturation. This results in a dominating effect of ACC1 inhibition in altering the membrane fluidity.

Another important parameter regulating membrane fluidity is the amount of cholesterol. Pitchard *et al.* pointed out that an increasing amount of cholesterol leads to a decreased membrane fluidity in human endothelial cells (189). Therefore, we investigated the concentration of cholesterol and found that soraphen A did not alter this crucial regulator of membrane fluidity (see Figure 24).

Our results are consistent with the findings of Braig *et al.* (190). They observed that soraphen A treatment of the mammary cancer cell line MDA-MB-231 augmented the acyl chain length and the amount of desaturated phospholipids. This also led to decreased membrane fluidity and cell migration. However, they did not detect any changes in the total amount of phospholipid subgroups after ACC inhibition. The divergent results might be due to the use of different cell lines, concentrations and incubation times of the ACC inhibitor.
Comparable data regarding the phospholipid composition are provided by Scott *et al.* (133). Similar to our results, they detected a shift in the membrane lipid composition after ACC inhibition in 3T3-Src cells. In accordance to soraphen A treatment in endothelial cells, ACC inhibition resulted in reduced levels of the phospholipid subgroup PC and even lead to a shift from saturated and monounsaturated fatty acids towards polyunsaturated fatty acids (133).
The limitation of our study lies within the fact that only the acyl chain length distribution of the phospholipid subgroup PG and PC has been measured. Although PC represents the main component in terms of quantity, it would, nevertheless, be interesting to determine the total length of all phospholipids in the cell membrane. This result may strengthen our hypothesis about the importance of the chain length of fatty acids for the regulation of the membrane fluidity in endothelial cells.

4.8 The role of phospholipids in mediating the migration of endothelial cells

A fundamental finding of this study was the crucial involvement of PG and PUFAs as central regulators of the endothelial migratory capacity (see Figure 34 and 35). The data showed that ACC inhibition resulted in a shift of the membrane lipid composition. Most notably, the portion of the phospholipid subgroup PG was strongly reduced, whereas the amount of PUFAs in the phospholipid membrane was augmented. We observed that PG supplied as DOPG fully restored and even overcompensated soraphen A-evoked reduction of PG levels in HUVECs and HEMCs (see Figure 35 B).

Interestingly, we found a causal link between PG/PUFAs and endothelial cell migration. The addition of PUFAs mimicked the antimigratory effect of soraphen A (see Figure 34). In contrast, saturated fatty acids had no influence on the migratory capacity of HUVECs, whereas the addition of PUFAs fully rescued the antimigratory action of soraphen A. These findings point out that the

amount of PG in the phospholipid cell membrane is linked to endothelial cell migration. A connection between PG in regulating endothelial cell migration was unknown in the literature so far.

The already mentioned study of Stoiber *et al*. found significantly reduced amounts of PC, PE and PI and a shift towards polyunsaturated and long chain fatty acids after soraphen A treatment (171). They also found a reduced migratory capacity, but they did not casually link this effect to a distinct phospholipid (171).

Nevertheless, one limitation of our study is the statement about saturated fatty acids. We revealed that saturated fatty acids did not influence the ACC-mediated antimigratory effect of soraphen A (see Figure 35 A). In contrast to other fatty acids (linolenic acid or DOPG), we did not verify the successful incorporation of the used saturated fatty acid (stearic acid) into the phospholipid cell membrane. It might be possible that saturated fatty acids did not alter the migration in endothelial cells due to an insufficient incorporation into the phospholipid membrane. To exclude this possible issue, a further lipid analysis would be worthwhile.

Another issue is the low concentration of the saturated fatty acid, which has been used in the scratch/migration assay. Due to its chemical properties, stearic acid proved to be nearly insoluble in aqueous media. In our experiment, we only used up to 10 % of the concentration compared to other fatty acids used for rescuing the antimigratory effect of soraphen A. It could be argued to increase the solubility by using a solubilizer. Because of the high sensitivity of primary endothelial cells, the tolerated detergent concentrations are very low and were not considered as useful.

Therefore, it might be considerable to repeat this experiment after verifying a successful incorporation into the cell’s phospholipid membrane.

4.9 Summary

The enzyme ACC plays a fundamental role in the fatty acid metabolism. It regulates the first and rate limiting step in the biosynthesis of fatty acids by catalyzing the carboxylation of acetyl-CoA to malonyl-CoA and exists as two different isoforms, ACC1 and ACC2. In the last few years, ACC has been reported as an attractive drug target for treating different diseases, such as insulin

resistance, hepatic steatosis, dyslipidemia, obesity, metabolic syndrome and nonalcoholic fatty liver disease. An altered fatty acid metabolism is also associated with cancer cell proliferation. In general, the inhibition of ACC provides two possibilities to regulate the fatty acid metabolism: It blocks the *de novo* lipogenesis in lipogenic tissues and stimulates the mitochondrial fatty acid β-oxidation. Surprisingly, the role of ACC in human vascular endothelial cells has been neglected so far. This work aimed to investigate the role of the ACC/fatty acid metabolism in regulating important endothelial cell functions like proliferation, migration and tube formation.

To investigate the function of ACC, the ACC-inhibitor soraphen A as well as an siRNA-based approach were used. This study revealed that ACC1 is the predominant isoform both in HUVECs and in HMECs. Inhibition of ACC *via* soraphen A resulted in decreased levels of malonyl-CoA and shifted the lipid composition of endothelial cell membranes. Consequently, membrane fluidity, filopodia formation and the migratory capacity were attenuated. Increasing amounts of longer acyl chains within the phospholipid subgroup PC were suggested to overcompensate the shift towards shorter acyl chains within PG, which resulted in a dominating effect on regulating the membrane fluidity.

Most importantly, we provided a link between changes in the phospholipid composition and altered endothelial cell migration. The antimigratory effect of soraphen A was linked to a reduced amount of PG and to an increased amount of PUFAs within the phospholipid cell membrane. This link was unknown in the literature so far. Interestingly, a reduced filopodia formation was observed upon ACC inhibition *via* soraphen A, which presumably caused the impaired migratory capacity. The main findings are summarized in Figure 37.

This work revealed a relationship between ACC/fatty acid metabolism, membrane lipid composition and endothelial cell migration. The natural compound soraphen A emerged as a valuable chemical tool to analyze the role of ACC/fatty acid metabolism in regulating important endothelial cell functions. Furthermore, regulating endothelial cell migration *via* ACC inhibition promises beneficial therapeutic perspectives for the treatment of cell migration-related disorders, such as ischemia reperfusion injury, diabetic angiopathy, macular degeneration, rheumatoid arthritis, wound healing defects and cancer.

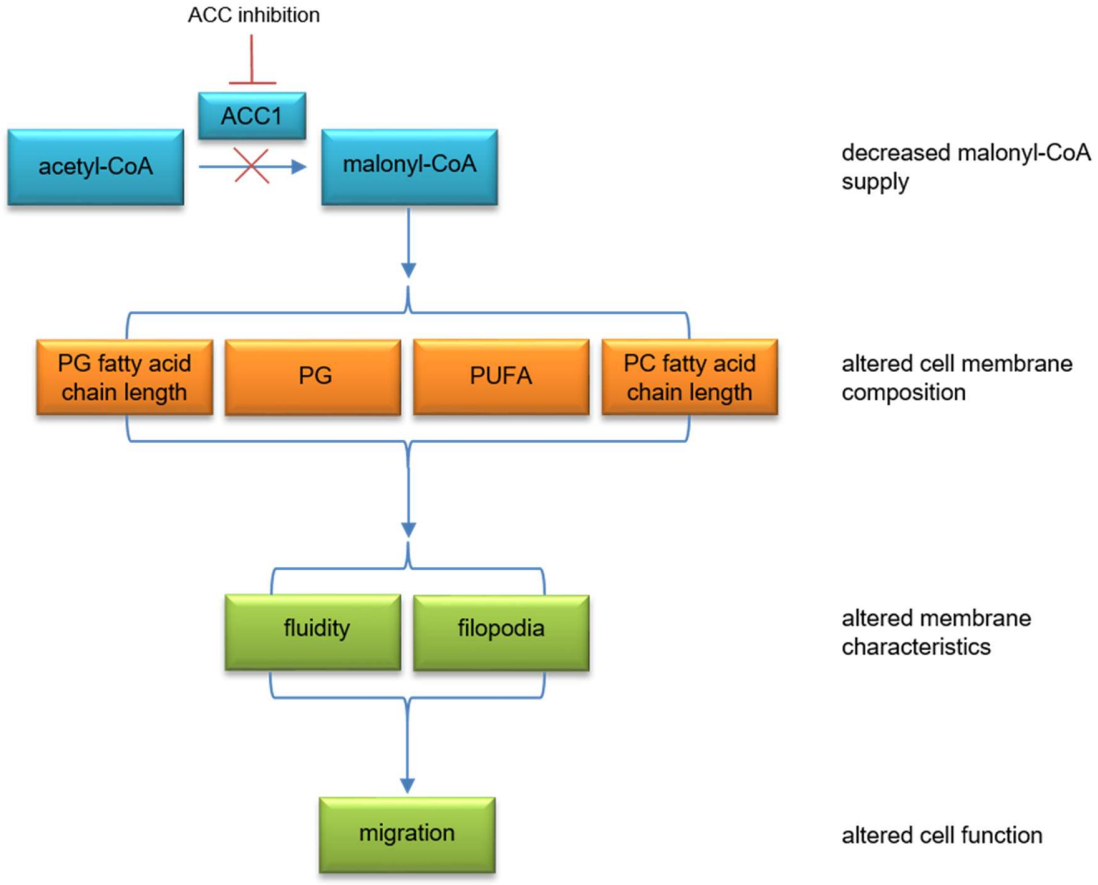

Figure 37: The action of ACC inhibition on endothelial cells.
This figure summarizes the main findings about acetyl-CoA carboxylase (ACC) inhibition and its influence on endothelial cells. ACC1 inhibition results in decreased level of malonyl-CoA. Consequently, this leads to a shift in the membrane lipid composition, namely in a reduced amount of the fatty acid chain length within the phospholipid subgroup phosphatidylglycerol (PG) and an increased fatty acid chain length within phosphatidylcholine (PC). The latter is hypothesized to be dominant in decreasing the membrane fluidity. ACC inhibition also strongly decreased levels of PG and increased levels of PUFAs. PG was found to be causal for the antimigratory effect of ACC1 inhibition.

4.10 Conclusion and outlook

The results of this study increase the knowledge about endothelial cells and how they regulate important cell functions like proliferation and migration. This knowledge can provide a basis to further investigate physiological and pathological properties of human endothelial cells. This work especially pointed out that the influence of the membrane composition on the angiogenesis-associated migration is worthwhile to be examined and that the knowledge about endothelial cells in general still needs to be expanded. The results revealed that the fatty acid metabolism in

endothelial cells regulates much more important cell functions than assumed. We highlighted that interfering with the ACC/fatty acid metabolism might be an interesting therapeutic approach for the treatment of migration-related diseases. We also showed that the addition of external fatty acids mimics the effect of ACC inhibition or – depending on the fatty acid – can even revoke the effects mediated by ACC inhibition. The antimigratory effects of ACC inhibition were causally linked to altered membrane properties and could be restored by adding external fatty acids. This offers new strategies to treat diseases that are associated with disturbances in the endothelial migration process by modulating the membrane composition of these cells.

Furthermore, soraphen A proved to be a great tool to investigate the fatty acid metabolism with a distinct focus on ACC. To understand the role of the ACC/fatty acid metabolism in endothelial cells and its systemic impact on the whole human body, further experiments are needed to address this point. Different endothelial cell lines might be useful to study this topic as well as *in vivo* experiments.

It would also be interesting to answer the questions, which emerged during the course of this study. For example, this work analyzed the lipid composition of endothelial cell membranes in general. It would be of advantage to investigate the lipid composition of single cell organelles and filopodia. Several studies have shown that different cell organelles have different phospholipid membrane compositions (101). It is conceivable that an altered mitochondria membrane composition could have an impact on the membrane-bound carnitine acyltransferase system, which shuttles long chain acyl-CoAs into mitochondria. Since it is known that membrane protrusions have also a distinct membrane lipid composition, it would be interesting to analyze their lipid composition. These findings might allow to provide answers to the question of why ACC inhibition reduces the formation of filopodia in endothelial cells.

As already mentioned, additional analyses would also be useful to verify our statement about the saturated fatty acid stearic acid and its unimportance for the regulation of endothelial migration. In this study, we did not prove the successful incorporation of stearic acid into the phospholipid membrane. Thus, the role of stearic acid for the observed functional effects of ACC inhibition is still not fully clarified. A further lipid analysis could answer this question.

Furthermore, this study only investigated the acyl chain length distribution of the phospholipid subgroup PG and PC. It would be interesting to determine the total length of all phospholipids in

the cell membrane. An overview about the total chain length would help to understand the role of the ACC/fatty acid metabolism in mediating the membrane fluidity.

In this work, we found a link between changes in the phospholipid composition and endothelial cell migration. This study did not focus on a causal link between changes in the phospholipid composition and impaired filopodia formation. Therefore, according to rescue experiments with DOPG, new experiments with soraphen A- and DOPG-treated endothelial cells could establish a causal link between phospholipids and altered F-actin distribution in migrating cells.

Moreover, it would be of great interest to clarify the signaling pathways influenced by soraphen A treatment. Changes in the membrane lipid composition are known to change the activity of membrane-bound proteins such as receptors, transporters and enzymes. Presumably, ACC inhibition alters numerous signaling pathways by changing the membrane lipid compositing resulting in decreased proliferation and migration.

In summary, due to its central role as modulator of the physiology of membranes, ACC can be suggested as a new and promising target system for the treatment of diseases associated with a dysregulation of endothelial cell migration.

5 ZUSAMMENFASSUNG

In den vergangenen Jahren hat man erkannt, dass das Endothel nicht nur eine einfache Barriere zwischen Blut und Gewebe darstellt, sondern vielmehr ein hochspezialisiertes und metabolisch aktives Organ ist. Das Endothel ist an der Regulation von diversen Funktionen im menschlichen Körper beteiligt. So steuert es die Aufrechterhaltung der Homöostase und ist an physiologischen sowie pathologischen Prozessen wie zum Beispiel der Inflammation, der Gefäßwandmodellierung oder an der Entstehung von Thrombosen beteiligt.

Das Endothel besteht aus einer Schicht von Endothelzellen, die vom Herzen bis zur kleinsten Kapillare das Innerste jedes Blutgefäßes auskleidet. Als Barriere kontrolliert das Endothel den Durchfluss von Flüssigkeiten, gelösten Substanzen, Makromolekülen sowie die Extravasation von Zellen aus dem Blut in das umliegende Gewebe. Neben dieser Barrierefunktion erweist sich das Endothel als komplexes Organ mit parakrinen und autokrinen Aufgaben innerhalb des kardiovaskulären Systems. Auch für die Regulation des Blutflusses und des Gefäßwiderstandes spielt das vaskuläre Endothel eine entscheidende Rolle.

Aufgrund ihrer Lokalisation sind Endothelzellen besonders sensitiv gegenüber kleinsten Änderungen in der Zusammensetzung des Blutes oder Störungen des Blutkreislaufes. Dadurch ist das Endothel maßgeblich an der Entstehung und der Progression von Krankheiten wie der peripheren arteriosklerotischen Gefäßerkrankung, Schlaganfall und Herzerkrankungen, Insulinresistenz, chronischer Niereninsuffizienz, Diabetes, Tumorgenese und Metastasierung, venöser Thrombosen sowie manchen Virusinfektionen beteiligt. Fehlfunktionen des Endothels werden deswegen als mitverursachende Faktoren für viele Erkrankungen angesehen. Folglich liegt es nahe, dieses wichtige Organ näher zu untersuchen, dessen komplexe Funktionsweise teilweise noch nicht vollständig aufgeklärt ist.

Um endotheliale Funktionen weiter zu charakterisieren, haben wir ein in der Wissenschaft weit verbreitetes Modelsystem für das menschliche Endothel benutzt: Die Kultivierung von humanen Endothelzellen aus der Nabelschnurvene (HUVECs).

Eine der wichtigsten Aufgaben von Endothelzellen ist ihre Fähigkeit zur Migration. Dieser fundamentale Prozess ist bei der Embryogenese, bei der Entstehung von Gewebe und Organen sowie bei der Wundheilung, Geweberegeneration und bei der Aufrechterhaltung der Homöostase involviert. Bei diesen Prozessen spielt vor allem die Bildung neuer Blutgefäße (Angiogenese) eine Rolle, an der die endotheliale Migration maßgeblich beteiligt ist. Da Fehlfunktionen der

endothelialen Migration an der Entstehung von schwerwiegenden Krankheiten wie zum Beispiel Reperfusionsschäden, Makuladegeneration, rheumatoide Arthritis, Wundheilungsstörungen und Krebs beteiligt ist, verspricht ein Eingriff in regulatorische Prozesse der endothelialen Migration vielversprechende Therapieansätze.

Die Migration von Endothelzellen ist ein Zusammenspiel dreier Bewegungsmuster: Die Haptotaxis, die Mechanotaxis und die Chemotaxis. Letztere wurde in dieser Arbeit genauer untersucht. Als Chemotaxis bezeichnet man die direktionale Migration in Richtung eines löslichen, chemischen Reizes. Zur Fortbewegung von Zellen sowie zur Erkennung von löslichen Stimuli sind sogenannte Filopodien essentiell. Diese fingerartigen Strukturen bestehen aus gebündelten Aktinfilamenten und besitzen wesentliche sensorische und exploratorische Funktionen während der endothelialen Migration.

Als pharmakologisches Werkzeug wurde in dieser Arbeit der Naturstoff Soraphen A benutzt. Dieses makrozyklische Polyketid, das ursprünglich wegen seiner fungiziden Wirkung Bekanntheit erlangte, wurde erstmals 1986 als Stoffwechselprodukt des Myxobakteriums *Sorangium cellulosum* isoliert. Dieser gut charakterisierte Naturstoff wird in der Wissenschaft benutzt, um die Funktion des Enzyms Acetyl-CoA-Carboxylase (ACC) zu inhibieren. Soraphen A hemmt durch die spezifische Bindung an eine Domäne (Biotincarboxylase) beide Isoformen (ACC1 und ACC2) des Enzyms. Durch die Bindung an die Biotincarboxylase-Domäne wird die für die ACC-Aktivität benötigte Oligomerisierung dieser Domäne verhindert.

Die ACC katalysiert die Carboxylierung von Acetyl-CoA zu Malonyl-CoA. Diese Reaktion ist der limitierende und geschwindigkeitsbestimmende Schritt in der Biosynthese von Fettsäuren in allen Organismen. Malonyl-CoA ist das essentielle Substrat für die Lipogenese sowie zur Verlängerung von Fettsäureketten und dient als Inhibitor der β-Oxidation. In Säugerzellen existieren zwei Isoformen: Die im Zytosol lokalisierte Isoform ACC1 generiert Malonyl-CoA für die Fettsäuresynthese, während das in den Mitochondrien vorkommende Enzym ACC2 Malonyl-CoA generiert, das als Inhibitor des Carnitin-Acyltransferase-Systems fungiert. Dieses System transferiert Fettsäuren zur Bildung von Acetyl-CoA in das Innere von Mitochondrien.

Die Acetyl-CoA-Carboxylase gilt als wichtiger Regulator des Lipidmetabolismus. Seit einigen Jahren wird die ACC als interessantes und vielversprechendes Wirkstoff-Target zur Behandlung von verschiedenen Krankheiten angesehen. Insbesondere aufgrund der steigenden Inzidenz des

metabolischen Syndroms zeigt die Wissenschaft ein erneutes Interesse an der vor rund 60 Jahren entdeckten ACC. Die Inhibierung der ACC verspricht durch die Kontrolle der Lipidsynthese Stoffwechselerkrankungen wie Adipositas oder Diabetes erfolgreich behandeln zu können. Darüber hinaus berichten diverse Studien, dass die ACC bei verschiedenen Krebserkrankungen eine gesteigerte Aktivität aufweist. Da dieses Phänomen mit einer gesteigerten Lipogenese und einem vermehrten Tumorwachstum assoziiert wird, stellt die Inhibierung der ACC eine vielversprechende Behandlungsstrategie von Tumoren dar. Neben einer möglichen Therapie von Krebs, Adipositas und Diabetes zeigt die pharmakologische Inhibierung von ACC auch spannende Ansätze zur Behandlung von gewissen Entzündungskrankheiten.

Trotz des großen Interesses an der ACC als pharmakologisch nutzbares Target-System, wurde der ACC im Endothel bisweilen kaum Beachtung geschenkt. Dabei ermöglicht die ACC-Inhibierung den Eingriff in zwei Mechanismen des Fettsäuremetabolismus: Einerseits wird der Abbau von Fettsäuren stimuliert, während anderseits die Fettsäuresynthese heruntergefahren wird. Der größte Anteil der Fettsäuren, die bei der Fettsäuresynthese entstehen, wird in die Lipidmembran eingebaut. Aus diesem Grund hatte die vorliegende Arbeit das Ziel, die Rolle der ACC für die Lipidmembranzusammensetzung und für die Migration, eine wesentliche Funktion von Endothelzellen, genauer zu beleuchten.

Dabei stellte sich heraus, dass die Isoform ACC1, verglichen mit ACC2, in humanen mikrovaskulären (HMEC-1) und umbilikalen venösen Endothelzellen (HUVEC) mengenmäßig stark überwiegt. Dies konnte auf mRNA-Ebene mittels einer Transkriptomanalyse und mittels quantitativer PCR festgestellt sowie auf Proteinebene mittels Western Blot nachgewiesen werden.

Um die erfolgreiche pharmakologische Inhibierung der ACC nachzuweisen, wurde der Gehalt an Malonyl-CoA nach Behandlung der Zellen mit Soraphen A gemessen. Dabei zeigte sich, dass die Menge an Malonyl-CoA in HUVECs drastisch reduziert wurde. Dies deutet auf eine erfolgreiche funktionelle Hemmung hin.

Da Malonyl-CoA maßgeblich an der Synthese von Fettsäuren beteiligt ist und der größte Anteil der neu synthetisierten Fettsäuren in die Phospholipidmembran eingebaut wird, haben wir vermutet, dass eine Behandlung mit Soraphen A auch einen Einfluss auf die Lipidmembranzusammensetzung haben könnte. Aus diesem Grund wurde mittels einer Lipidom-Analyse (Lipidomics)

die Zusammensetzung der Membran untersucht. Hierbei stellte sich heraus, dass eine Langzeitbehandlung mit Soraphen A zu einer veränderten Lipidmembranzusammensetzung im Endothel führte. Soraphen A verringerte dabei signifikant den Anteil von Phosphatidylglycerol (PG) innerhalb der Membran. Des Weiteren verringerte Soraphen A den Anteil von Phosphatidylinositol (PI) und Phosphatidylcholin (PC) mit gesättigten Fettsäuren und begünstigte den Anstieg von PI mit einfach ungesättigten Fettsäuren sowie von PC mit mehrfach ungesättigten Fettsäuren. Neben dem Grad der Sättigung hatte Soraphen A auch einen Einfluss auf die Kettenlängen von Fettsäuren. Soraphen A erhöhte den Anteil von PC mit langkettigen Fettsäuren (C-20) und verringerte den Anteil von PC mit kurzkettigen Fettsäuren (C-14). Über dies hinaus wurde der Anteil von PG(18:1/18:1) verringert und der Anteil von PG(16:0/18:1) erhöht. Neben dem Einfluss von Soraphen A auf die Zusammensetzung der Phospholipide wurde auch die Menge an zellulärem Cholesterol gemessen. Die Cholesterollevel blieben nach ACC-Inhibierung allerdings unverändert.

Da die Lipidzusammensetzung unter anderem die Fluidität von Membranen reguliert, vermuteten wir, dass die Behandlung mit Soraphen A zu einer Beeinflussung der Membranfluidität führen könnte. In der Literatur wird ein vergrößerter Anteil von ungesättigten Fettsäuren mit einer erhöhten Membranfluidität assoziiert, da diese Fettsäuren aufgrund ihres räumlichen Anspruchs im Gegensatz zu gesättigten Fettsäuren nicht so dicht nebeneinander gepackt werden können. Gegenläufig dazu wird ein erhöhter Anteil an langkettigen Fettsäuren aufgrund stärkerer Van-der-Waals-Wechselwirkungen mit einer verminderten Membranfluidität in Verbindung gebracht.

In unseren Untersuchungen verringerte Soraphen A die Membranfluidität. Im Einklang mit der Literatur führte die Inhibierung von ACC zu einem erhöhten Anteil von PC mit langkettigen Fettsäuren. Gleichzeitig stiegen jedoch der Anteil von ungesättigten Fettsäuren und der Anteil von PG mit kurzkettigen Fettsäuren. Da PC im Gegensatz zu PG in der Membran mengenmäßig stärker vertreten ist, vermuten wir, dass die Erhöhung des Anteils langkettiger Fettsäuren innerhalb der PC der dominierende Effekt von Soraphen A auf die Membranfluidität ist und den Effekt der Steigerung des Anteils ungesättigter Fettsäuren überkompensiert.

In verschiedenen Migrations-Assays (Scratch Assay, Boyden Chamer Assay, 2D Chemotaxis) konnte beobachtet werden, dass nach ACC-Inhibierung sowohl die ungerichtete als auch die gerichtete Endothelzell-Migration in Richtung einer chemotaktisch aktiven Substanz inhibiert

wurde. Aufgrund der geringen Expression von ACC2 hatte nur die Inhibierung von ACC1 einen Einfluss auf die Migration.

Interessanterweise führte die Inhibierung von ACC nicht nur zu einer verminderten Migration von Endothelzellen, sondern auch zu einer Veränderung des Aktinzytosekeletts, denn die Anzahl von Filopodien in migrierenden Zellen wurde stark verringert. Das Tubulinzytoskelett von Endothelzellen blieb indes unverändert. Wir vermuten einen Zusammenhang zwischen der verminderten Migration durch ACC-Inhibierung und der verringerten Anzahl von Filopodien, da diese „Scheinfüßchen“ maßgeblich an der Fortbewegung von Zellen beteiligt sind.

Eine der wichtigsten Erkenntnisse dieser Arbeit ist, dass PG und mehrfach ungesättigte Fettsäuren (polyunsaturated fatty acids, PUFAs) wichtige Regulatoren der Membranfluidität und der Migration von Endothelzellen sind. So konnte die Zugabe von PUFAs die Wirkung von Soraphen A auf die Migration in Endothelzellen nachahmen.

Hingegen konnte die Zugabe von PG den antimigratorischen Effekt der ACC-Inhibierung vollständig aufheben. Eine Supplementierung von gesättigten Fettsäuren hatte jedoch keinen Einfluss auf die Migration. Lipidanalysen bestätigten, dass sowohl PG in Form von Dioleoylphosphatidylglycerol (DOPG) als auch Linolensäure als Vertreter der PUFAs nach Supplementierung im Medium erfolgreich in die Zellmembranen von Endothelzellen eingebaut werden. Die Zugabe von DOPG konnte darüber hinaus sogar den von Soraphen A verursachten Rückgang von PG in der Membran vollständig aufheben. Diese Ergebnisse verdeutlichen, dass der antimigratorische Effekt von Soraphen A eng mit dem Anteil von PG in der endothelialen Membran verknüpft ist. Dass PG die Zellmigration modulieren kann, war in der Literatur bis *dato* unbekannt.

Diese Arbeit enthüllt zum ersten Mal überhaupt einen Zusammenhang zwischen Migration und einer veränderten Lipidmembranzusammensetzung in Endothelzellen und zeigt, dass Soraphen A ein nützliches chemisches Werkzeug darstellt, um die Rolle des Lipidmetabolismus im Endothel genauer zu untersuchen. Durch die Inhibierung der ACC ergeben sich neue, interessante Behandlungsmöglichkeiten für Krankheiten, die mit einer Veränderung der endothelialen Migration assoziiert werden.

6 REFERENCES

1. Hunt, B. J., and Jurd, K. M. (1998) Endothelial cell activation. A central pathophysiological process. *BMJ* **316**, 1328-1329
2. Michiels, C. (2003) Endothelial cell functions. *J Cell Physiol* **196**, 430-443
3. Hahn, C., and Schwartz, M. A. (2009) Mechanotransduction in vascular physiology and atherogenesis. *Nat Rev Mol Cell Biol* **10**, 53-62
4. Rajendran, P., Rengarajan, T., Thangavel, J., Nishigaki, Y., Sakthisekaran, D., Sethi, G., and Nishigaki, I. (2013) The vascular endothelium and human diseases. *Int J Biol Sci* **9**, 1057-1069
5. Vane, J. R., Anggard, E. E., and Botting, R. M. (1990) Regulatory functions of the vascular endothelium. *N Engl J Med* **323**, 27-36
6. Sumpio, B. E., Riley, J. T., and Dardik, A. (2002) Cells in focus: endothelial cell. *Int J Biochem Cell Biol* **34**, 1508-1512
7. Pearson, J. D. (2000) Normal endothelial cell function. *Lupus* **9**, 183-188
8. Cines, D. B., Pollak, E. S., Buck, C. A., Loscalzo, J., Zimmerman, G. A., McEver, R. P., Pober, J. S., Wick, T. M., Konkle, B. A., Schwartz, B. S., Barnathan, E. S., McCrae, K. R., Hug, B. A., Schmidt, A. M., and Stern, D. M. (1998) Endothelial cells in physiology and in the pathophysiology of vascular disorders. *Blood* **91**, 3527-3561
9. Durand, M. J., and Gutterman, D. D. (2013) Diversity in mechanisms of endothelium-dependent vasodilation in health and disease. *Microcirculation* **20**, 239-247
10. Stern, D. M., Esposito, C., Gerlach, H., Gerlach, M., Ryan, J., Handley, D., and Nawroth, P. (1991) Endothelium and regulation of coagulation. *Diabetes Care* **14**, 160-166
11. Evora, P. R., Baldo, C. F., Celotto, A. C., and Capellini, V. K. (2009) Endothelium dysfunction classification: why is it still an open discussion? *Int J Cardiol* **137**, 175-176
12. Vita, J. A., and Hamburg, N. M. (2010) Does endothelial dysfunction contribute to the clinical status of patients with peripheral arterial disease? *Can J Cardiol* **26 Suppl A**, 45A-50A
13. Cosentino, F., Sill, J. C., and Katusic, Z. S. (1993) Endothelial L-arginine pathway and relaxations to vasopressin in canine basilar artery. *Am J Physiol* **264**, H413-418
14. Cosentino, F., Rubattu, S., Savoia, C., Venturelli, V., Pagannonne, E., and Volpe, M. (2001) Endothelial dysfunction and stroke. *J Cardiovasc Pharmacol* **38 Suppl 2**, S75-78
15. Behrendt, D., and Ganz, P. (2002) Endothelial function. From vascular biology to clinical applications. *Am J Cardiol* **90**, 40L-48L
16. Calles-Escandon, J., and Cipolla, M. (2001) Diabetes and endothelial dysfunction: a clinical perspective. *Endocr Rev* **22**, 36-52
17. Basu, A., and Chaturvedi, U. C. (2008) Vascular endothelium: the battlefield of dengue viruses. *FEMS Immunol Med Microbiol* **53**, 287-299
18. Jaffe, E. A., Nachman, R. L., Becker, C. G., and Minick, C. R. (1973) Culture of human endothelial cells derived from umbilical veins. Identification by morphologic and immunologic criteria. *J Clin Invest* **52**, 2745-2756
19. Lamalice, L., Le Boeuf, F., and Huot, J. (2007) Endothelial cell migration during angiogenesis. *Circ Res* **100**, 782-794
20. Michaelis, U. R. (2014) Mechanisms of endothelial cell migration. *Cell Mol Life Sci* **71**, 4131-4148
21. Li, S., Huang, N. F., and Hsu, S. (2005) Mechanotransduction in endothelial cell migration. *J Cell Biochem* **96**, 1110-1126
22. Davis, G. E., and Senger, D. R. (2005) Endothelial extracellular matrix: biosynthesis, remodeling, and functions during vascular morphogenesis and neovessel stabilization. *Circ Res* **97**, 1093-1107
23. Senger, D. R., Perruzzi, C. A., Streit, M., Koteliansky, V. E., de Fougerolles, A. R., and Detmar, M. (2002) The alpha(1)beta(1) and alpha(2)beta(1) integrins provide critical

support for vascular endothelial growth factor signaling, endothelial cell migration, and tumor angiogenesis. *Am J Pathol* **160**, 195-204
24. Srinivasan, R., Zabuawala, T., Huang, H., Zhang, J., Gulati, P., Fernandez, S., Karlo, J. C., Landreth, G. E., Leone, G., and Ostrowski, M. C. (2009) Erk1 and Erk2 regulate endothelial cell proliferation and migration during mouse embryonic angiogenesis. *PLoS One* **4**, e8283
25. Small, J. V., and Resch, G. P. (2005) The comings and goings of actin: coupling protrusion and retraction in cell motility. *Curr Opin Cell Biol* **17**, 517-523
26. Mattila, P. K., and Lappalainen, P. (2008) Filopodia: molecular architecture and cellular functions. *Nat. Rev. Mol. Cell Biol.* **9**, 446-454
27. Faix, J., and Rottner, K. (2006) The making of filopodia. *Curr. Opin. Cell. Biol.* **18**, 18-25
28. Mattila, P. K., and Lappalainen, P. (2008) Filopodia: molecular architecture and cellular functions. *Nat Rev Mol Cell Biol* **9**, 446-454
29. Faix, J., and Rottner, K. (2006) The making of filopodia. *Curr Opin Cell Biol* **18**, 18-25
30. Potente, M., Gerhardt, H., and Carmeliet, P. (2011) Basic and therapeutic aspects of angiogenesis. *Cell* **146**, 873-887
31. Hanahan, D., and Folkman, J. (1996) Patterns and emerging mechanisms of the angiogenic switch during tumorigenesis. *Cell* **86**, 353-364
32. Risau, W. (1995) Differentiation of endothelium. *FASEB J* **9**, 926-933
33. Karkkainen, M. J., Makinen, T., and Alitalo, K. (2002) Lymphatic endothelium: a new frontier of metastasis research. *Nat Cell Biol* **4**, E2-5
34. Risau, W., and Flamme, I. (1995) Vasculogenesis. *Annu Rev Cell Dev Biol* **11**, 73-91
35. Risau, W. (1997) Mechanisms of angiogenesis. *Nature* **386**, 671-674
36. Folkman, J., and Klagsbrun, M. (1987) Angiogenic factors. *Science* **235**, 442-447
37. Bouck, N., Stellmach, V., and Hsu, S. C. (1996) How tumors become angiogenic. *Adv Cancer Res* **69**, 135-174
38. Hanahan, D., and Weinberg, R. A. (2000) The hallmarks of cancer. *Cell* **100**, 57-70
39. Tan, Y., Cruz-Guilloty, F., Medina-Mendez, C. A., Cutrufello, N. J., Martinez, R. E., Urbieta, M., Wilson, D., Li, Y., and Perez, V. L. (2012) Immunological disruption of antiangiogenic signals by recruited allospecific T cells leads to corneal allograft rejection. *J Immunol* **188**, 5962-5969
40. Clements, J. L., and Dana, R. (2011) Inflammatory corneal neovascularization: etiopathogenesis. *Semin Ophthalmol* **26**, 235-245
41. Ellenberg, D., Azar, D. T., Hallak, J. A., Tobaigy, F., Han, K. Y., Jain, S., Zhou, Z., and Chang, J. H. (2010) Novel aspects of corneal angiogenic and lymphangiogenic privilege. *Prog Retin Eye Res* **29**, 208-248
42. Dallinga, M. G., Boas, S. E. M., Klaassen, I., Merks, R. H. M., van Noorden, C. J. F., and Schlingemann, R. O. (2001) Tip Cells in Angiogenesis. in *eLS*, John Wiley & Sons, Ltd. pp
43. De Smet, F., Segura, I., De Bock, K., Hohensinner, P. J., and Carmeliet, P. (2009) Mechanisms of vessel branching: filopodia on endothelial tip cells lead the way. *Arterioscler Thromb Vasc Biol* **29**, 639-649
44. Gerhardt, H., Golding, M., Fruttiger, M., Ruhrberg, C., Lundkvist, A., Abramsson, A., Jeltsch, M., Mitchell, C., Alitalo, K., Shima, D., and Betsholtz, C. (2003) VEGF guides angiogenic sprouting utilizing endothelial tip cell filopodia. *J Cell Biol* **161**, 1163-1177
45. Suchting, S., Freitas, C., le Noble, F., Benedito, R., Breant, C., Duarte, A., and Eichmann, A. (2007) The Notch ligand Delta-like 4 negatively regulates endothelial tip cell formation and vessel branching. *Proc Natl Acad Sci U S A* **104**, 3225-3230
46. Gerhardt, H., Ruhrberg, C., Abramsson, A., Fujisawa, H., Shima, D., and Betsholtz, C. (2004) Neuropilin-1 is required for endothelial tip cell guidance in the developing central nervous system. *Dev Dyn* **231**, 503-509

47. Ruhrberg, C., Gerhardt, H., Golding, M., Watson, R., Ioannidou, S., Fujisawa, H., Betsholtz, C., and Shima, D. T. (2002) Spatially restricted patterning cues provided by heparin-binding VEGF-A control blood vessel branching morphogenesis. *Genes Dev* **16**, 2684-2698
48. Tammela, T., Zarkada, G., Nurmi, H., Jakobsson, L., Heinolainen, K., Tvorogov, D., Zheng, W., Franco, C. A., Murtomaki, A., Aranda, E., Miura, N., Yla-Herttuala, S., Fruttiger, M., Makinen, T., Eichmann, A., Pollard, J. W., Gerhardt, H., and Alitalo, K. (2011) VEGFR-3 controls tip to stalk conversion at vessel fusion sites by reinforcing Notch signalling. *Nat Cell Biol* **13**, 1202-1213
49. Blanco, R., and Gerhardt, H. (2013) VEGF and Notch in tip and stalk cell selection. *Cold Spring Harb Perspect Med* **3**, a006569
50. Dvorak, H. F., Brown, L. F., Detmar, M., and Dvorak, A. M. (1995) Vascular permeability factor/vascular endothelial growth factor, microvascular hyperpermeability, and angiogenesis. *Am J Pathol* **146**, 1029-1039
51. Kliebenstein, D. J. (2004) Secondary metabolites and plant/environment interactions: a view through Arabidopsis thaliana tinged glasses. *Plant Cell Environ* **27**, 675-684
52. Karlovsky, P. (2008) Secondary metabolites in soil ecology. *Springer*, 1-19
53. Demain, A. L. (1999) Pharmaceutically active secondary metabolites of microorganisms. *Appl Microbiol Biotechnol* **52**, 455-463
54. Berdy, J. (2005) Bioactive microbial metabolites. *J Antibiot (Tokyo)* **58**, 1-26
55. Herrmann, J., Fayad, A. A., and Muller, R. (2017) Natural products from myxobacteria: novel metabolites and bioactivities. *Nat Prod Rep* **34**, 135-160
56. Newman, D. J., and Cragg, G. M. (2016) Natural Products as Sources of New Drugs from 1981 to 2014. *J Nat Prod* **79**, 629-661
57. Hamburger, M. H., K. (1991) 7. Bioactivity in plants: the link between phytochemistry and medicine. *Phytochemistry* **30**, 3864-3874
58. Demain, A. L. (2006) From natural products discovery to commercialization: a success story. *J Ind Microbiol Biotechnol* **33**, 486-495
59. Gerth, K., Bedorf, N., Irschik, H., Höfle, G., and Reichenbach, H. (1994) The soraphens: a family of novel antifungal compounds from Sorangium cellulosum (Myxobacteria). I. Soraphen A1 alpha: fermentation, isolation, biological properties. *J Antibiot (Tokyo)* **47**, 23-31
60. Reichenbach, H. (2001) Myxobacteria, producers of novel bioactive substances. *J Ind Microbiol Biotechnol* **27**, 149-156
61. Schneiker, S., Perlova, O., Kaiser, O., Gerth, K., Alici, A., Altmeyer, M. O., Bartels, D., Bekel, T., Beyer, S., Bode, E., Bode, H. B., Bolten, C. J., Choudhuri, J. V., Doss, S., Elnakady, Y. A., Frank, B., Gaigalat, L., Goesmann, A., Groeger, C., Gross, F., Jelsbak, L., Jelsbak, L., Kalinowski, J., Kegler, C., Knauber, T., Konietzny, S., Kopp, M., Krause, L., Krug, D., Linke, B., Mahmud, T., Martinez-Arias, R., McHardy, A. C., Merai, M., Meyer, F., Mormann, S., Munoz-Dorado, J., Perez, J., Pradella, S., Rachid, S., Raddatz, G., Rosenau, F., Ruckert, C., Sasse, F., Scharfe, M., Schuster, S. C., Suen, G., Treuner-Lange, A., Velicer, G. J., Vorholter, F. J., Weissman, K. J., Welch, R. D., Wenzel, S. C., Whitworth, D. E., Wilhelm, S., Wittmann, C., Blocker, H., Puhler, A., and Muller, R. (2007) Complete genome sequence of the myxobacterium Sorangium cellulosum. *Nat Biotechnol* **25**, 1281-1289
62. Land, M., Hauser, L., Jun, S. R., Nookaew, I., Leuze, M. R., Ahn, T. H., Karpinets, T., Lund, O., Kora, G., Wassenaar, T., Poudel, S., and Ussery, D. W. (2015) Insights from 20 years of bacterial genome sequencing. *Funct Integr Genomics* **15**, 141-161
63. Bode, H. B., and Muller, R. (2005) The impact of bacterial genomics on natural product research. *Angew Chem Int Ed Engl* **44**, 6828-6846

64. Kiskowski, M. A., Jiang, Y., and Alber, M. S. (2004) Role of streams in myxobacteria aggregate formation. *Phys Biol* **1**, 173-183
65. Gerth, K., Pradella, S., Perlova, O., Beyer, S., and Muller, R. (2003) Myxobacteria: proficient producers of novel natural products with various biological activities--past and future biotechnological aspects with the focus on the genus Sorangium. *J Biotechnol* **106**, 233-253
66. Wenzel, S. C., and Muller, R. (2009) The biosynthetic potential of myxobacteria and their impact in drug discovery. *Curr Opin Drug Discov Devel* **12**, 220-230
67. Bedorf, N., Schomburg, D., Gerth, K., Reichenbach, H., and Höfle, G. (1993) Antibiotics from gliding bacteria, LIV. Isolation and structure elucidation of soraphen A1α, a novel antifungal macrolide from Sorangium cellulosum. *J Org Chem*, 1017-1021
68. Shen, Y., Volrath, S. L., Weatherly, S. C., Elich, T. D., and Tong, L. (2004) A mechanism for the potent inhibition of eukaryotic acetyl-coenzyme A carboxylase by soraphen A, a macrocyclic polyketide natural product. *Mol Cell* **16**, 881-891
69. Ligon, J., Hill, S., Beck, J., Zirkle, R., Molnar, I., Zawodny, J., Money, S., and Schupp, T. (2002) Characterization of the biosynthetic gene cluster for the antifungal polyketide soraphen A from Sorangium cellulosum So ce26. *Gene* **285**, 257-267
70. Vahlensieck, H. F., Pridzun, L., Reichenbach, H., and Hinnen, A. (1994) Identification of the yeast ACC1 gene product (acetyl-CoA carboxylase) as the target of the polyketide fungicide soraphen A. *Curr Genet* **25**, 95-100
71. Tong, L., and Harwood, H. J., Jr. (2006) Acetyl-coenzyme A carboxylases: versatile targets for drug discovery. *J Cell Biochem* **99**, 1476-1488
72. Weatherly, S. C., Volrath, S. L., and Elich, T. D. (2004) Expression and characterization of recombinant fungal acetyl-CoA carboxylase and isolation of a soraphen-binding domain. *Biochem J* **380**, 105-110
73. Cho, Y. S., Lee, J. I., Shin, D., Kim, H. T., Jung, H. Y., Lee, T. G., Kang, L. W., Ahn, Y. J., Cho, H. S., and Heo, Y. S. (2010) Molecular mechanism for the regulation of human ACC2 through phosphorylation by AMPK. *Biochem Biophys Res Commun* **391**, 187-192
74. Harwood, H. J., Jr. (2005) Treating the metabolic syndrome: acetyl-CoA carboxylase inhibition. *Expert Opin Ther Targets* **9**, 267-281
75. Kim, K. H. (1997) Regulation of mammalian acetyl-coenzyme A carboxylase. *Annu Rev Nutr* **17**, 77-99
76. McGarry, J. D., Mannaerts, G. P., and Foster, D. W. (1977) A possible role for malonyl-CoA in the regulation of hepatic fatty acid oxidation and ketogenesis. *J Clin Invest* **60**, 265-270
77. Knowles, J. R. (1989) The mechanism of biotin-dependent enzymes. *Annu Rev Biochem* **58**, 195-221
78. Cronan, J. E., Jr., and Waldrop, G. L. (2002) Multi-subunit acetyl-CoA carboxylases. *Prog Lipid Res* **41**, 407-435
79. Tong, L. (2005) Acetyl-coenzyme A carboxylase: crucial metabolic enzyme and attractive target for drug discovery. *Cell Mol Life Sci* **62**, 1784-1803
80. Wakil, S. J., Stoops, J. K., and Joshi, V. C. (1983) Fatty acid synthesis and its regulation. *Annu Rev Biochem* **52**, 537-579
81. Barber, M. C., Price, N. T., and Travers, M. T. (2005) Structure and regulation of acetyl-CoA carboxylase genes of metazoa. *Biochim Biophys Acta* **1733**, 1-28
82. Nikolau, B. J., Ohlrogge, J. B., and Wurtele, E. S. (2003) Plant biotin-containing carboxylases. *Arch Biochem Biophys* **414**, 211-222
83. Abramson, H. N. (2011) The lipogenesis pathway as a cancer target. *J Med Chem* **54**, 5615-5638
84. Munday, M. R. (2002) Regulation of mammalian acetyl-CoA carboxylase. *Biochem Soc Trans* **30**, 1059-1064

85. McGarry, J. D., and Brown, N. F. (1997) The mitochondrial carnitine palmitoyltransferase system. From concept to molecular analysis. *Eur J Biochem* **244**, 1-14
86. Ramsay, R. R., Gandour, R. D., and van der Leij, F. R. (2001) Molecular enzymology of carnitine transfer and transport. *Biochim Biophys Acta* **1546**, 21-43
87. Foster, D. W. (2004) The role of the carnitine system in human metabolism. *Ann N Y Acad Sci* **1033**, 1-16
88. Bonnefont, J. P., Djouadi, F., Prip-Buus, C., Gobin, S., Munnich, A., and Bastin, J. (2004) Carnitine palmitoyltransferases 1 and 2: biochemical, molecular and medical aspects. *Mol Aspects Med* **25**, 495-520
89. Abu-Elheiga, L., Matzuk, M. M., Abo-Hashema, K. A., and Wakil, S. J. (2001) Continuous fatty acid oxidation and reduced fat storage in mice lacking acetyl-CoA carboxylase 2. *Science* **291**, 2613-2616
90. Schreurs, M., van Dijk, T. H., Gerding, A., Havinga, R., Reijngoud, D. J., and Kuipers, F. (2009) Soraphen, an inhibitor of the acetyl-CoA carboxylase system, improves peripheral insulin sensitivity in mice fed a high-fat diet. *Diabetes Obes Metab* **11**, 987-991
91. Harwood, H. J., Jr. (2004) Acetyl-CoA carboxylase inhibition for the treatment of metabolic syndrome. *Curr Opin Investig Drugs* **5**, 283-289
92. Stiede, K., Miao, W., Blanchette, H. S., Beysen, C., Harriman, G., Harwood, H. J., Jr., Kelley, H., Kapeller, R., Schmalbach, T., and Westlin, W. F. (2017) Acetyl-coenzyme A carboxylase inhibition reduces de novo lipogenesis in overweight male subjects: A randomized, double-blind, crossover study. *Hepatology* **66**, 324-334
93. Harriman, G., Greenwood, J., Bhat, S., Huang, X., Wang, R., Paul, D., Tong, L., Saha, A. K., Westlin, W. F., Kapeller, R., and Harwood, H. J., Jr. (2016) Acetyl-CoA carboxylase inhibition by ND-630 reduces hepatic steatosis, improves insulin sensitivity, and modulates dyslipidemia in rats. *Proc Natl Acad Sci U S A* **113**, E1796-1805
94. Swinnen, J. V., Brusselmans, K., and Verhoeven, G. (2006) Increased lipogenesis in cancer cells: new players, novel targets. *Curr Opin Clin Nutr Metab Care* **9**, 358-365
95. Milgraum, L. Z., Witters, L. A., Pasternack, G. R., and Kuhajda, F. P. (1997) Enzymes of the fatty acid synthesis pathway are highly expressed in in situ breast carcinoma. *Clin Cancer Res* **3**, 2115-2120
96. Yahagi, N., Shimano, H., Hasegawa, K., Ohashi, K., Matsuzaka, T., Najima, Y., Sekiya, M., Tomita, S., Okazaki, H., Tamura, Y., Iizuka, Y., Ohashi, K., Nagai, R., Ishibashi, S., Kadowaki, T., Makuuchi, M., Ohnishi, S., Osuga, J., and Yamada, N. (2005) Co-ordinate activation of lipogenic enzymes in hepatocellular carcinoma. *Eur J Cancer* **41**, 1316-1322
97. Berod, L., Friedrich, C., Nandan, A., Freitag, J., Hagemann, S., Harmrolfs, K., Sandouk, A., Hesse, C., Castro, C. N., Bahre, H., Tschirner, S. K., Gorinski, N., Gohmert, M., Mayer, C. T., Huehn, J., Ponimaskin, E., Abraham, W. R., Muller, R., Lochner, M., and Sparwasser, T. (2014) De novo fatty acid synthesis controls the fate between regulatory T and T helper 17 cells. *Nat Med* **20**, 1327-1333
98. Koutsoudakis, G., Romero-Brey, I., Berger, C., Perez-Vilaro, G., Monteiro Perin, P., Vondran, F. W., Kalesse, M., Harmrolfs, K., Muller, R., Martinez, J. P., Pietschmann, T., Bartenschlager, R., Bronstrup, M., Meyerhans, A., and Diez, J. (2015) Soraphen A: A broad-spectrum antiviral natural product with potent anti-hepatitis C virus activity. *J Hepatol* **63**, 813-821
99. Zhang, H., Tweel, B., Li, J., and Tong, L. (2004) Crystal structure of the carboxyltransferase domain of acetyl-coenzyme A carboxylase in complex with CP-640186. *Structure* **12**, 1683-1691
100. Ibarguren, M., Lopez, D. J., and Escriba, P. V. (2014) The effect of natural and synthetic fatty acids on membrane structure, microdomain organization, cellular functions and human health. *Biochim Biophys Acta* **1838**, 1518-1528

101. Vance, J. E. (2015) Phospholipid synthesis and transport in mammalian cells. *Traffic* **16**, 1-18
102. Spector, A. A., and Yorek, M. A. (1985) Membrane lipid composition and cellular function. *J Lipid Res* **26**, 1015-1035
103. Baum, S. J., Kris-Etherton, P. M., Willett, W. C., Lichtenstein, A. H., Rudel, L. L., Maki, K. C., Whelan, J., Ramsden, C. E., and Block, R. C. (2012) Fatty acids in cardiovascular health and disease: a comprehensive update. *J Clin Lipidol* **6**, 216-234
104. Lavie, C. J., Milani, R. V., Mehra, M. R., and Ventura, H. O. (2009) Omega-3 polyunsaturated fatty acids and cardiovascular diseases. *J Am Coll Cardiol* **54**, 585-594
105. Kapoor, R., and Huang, Y. S. (2006) Gamma linolenic acid: an antiinflammatory omega-6 fatty acid. *Curr Pharm Biotechnol* **7**, 531-534
106. Teres, S., Barcelo-Coblijn, G., Benet, M., Alvarez, R., Bressani, R., Halver, J. E., and Escriba, P. V. (2008) Oleic acid content is responsible for the reduction in blood pressure induced by olive oil. *Proc Natl Acad Sci U S A* **105**, 13811-13816
107. Das, U. N. (2006) Essential fatty acids: biochemistry, physiology and pathology. *Biotechnol J* **1**, 420-439
108. Lamalice, L., Le Boeuf, F., and Huot, J. (2007) Endothelial cell migration during angiogenesis. *Circ. Res.* **100**, 782-794
109. Michaelis, U. R. (2014) Mechanisms of endothelial cell migration. *Cell. Mol. Life Sci.* **71**, 4131-4148
110. Ades, E. W., Candal, F. J., Swerlick, R. A., George, V. G., Summers, S., Bosse, D. C., and Lawley, T. J. (1992) HMEC-1: establishment of an immortalized human microvascular endothelial cell line. *J Invest Dermatol* **99**, 683-690
111. Bouis, D., Hospers, G. A., Meijer, C., Molema, G., and Mulder, N. H. (2001) Endothelium in vitro: a review of human vascular endothelial cell lines for blood vessel-related research. *Angiogenesis* **4**, 91-102
112. Costantini, S., Di Bernardo, G., Cammarota, M., Castello, G., and Colonna, G. (2013) Gene expression signature of human HepG2 cell line. *Gene* **518**, 335-345
113. O'Brien, J., Wilson, I., Orton, T., and Pognan, F. (2000) Investigation of the Alamar Blue (resazurin) fluorescent dye for the assessment of mammalian cell cytotoxicity. *Eur J Biochem* **267**, 5421-5426
114. Nicoletti, I., Migliorati, G., Pagliacci, M. C., Grignani, F., and Riccardi, C. (1991) A rapid and simple method for measuring thymocyte apoptosis by propidium iodide staining and flow cytometry. *J Immunol Methods* **139**, 271-279
115. Riccardi, C., and Nicoletti, I. (2006) Analysis of apoptosis by propidium iodide staining and flow cytometry. *Nat Protoc* **1**, 1458-1461
116. Decker, T., and Lohmann-Matthes, M. L. (1988) A quick and simple method for the quantitation of lactate dehydrogenase release in measurements of cellular cytotoxicity and tumor necrosis factor (TNF) activity. *J Immunol Methods* **115**, 61-69
117. Nachlas, M. M., Margulies, S. I., Goldberg, J. D., and Seligman, A. M. (1960) The determination of lactic dehydrogenase with a tetrazolium salt. *Anal Biochem* **1**, 317-326
118. CytoTox 96®Non-Radioactive Cytotoxicity Assay - Instructions for Use of Product (G1780). Promega.
119. Koeberle, A., Shindou, H., Koeberle, S. C., Laufer, S. A., Shimizu, T., and Werz, O. (2013) Arachidonoyl-phosphatidylcholine oscillates during the cell cycle and counteracts proliferation by suppressing Akt membrane binding. *Proc Natl Acad Sci U S A* **110**, 2546-2551
120. Mohanty, J. G., Jaffe, J. S., Schulman, E. S., and Raible, D. G. (1997) A highly sensitive fluorescent micro-assay of H2O2 release from activated human leukocytes using a dihydroxyphenoxazine derivative. *J Immunol Methods* **202**, 133-141

121. Marczak, A. (2009) Fluorescence anisotropy of membrane fluidity probes in human erythrocytes incubated with anthracyclines and glutaraldehyde. *Bioelectrochemistry* **74**, 236-239
122. Liang, C. C., Park, A. Y., and Guan, J. L. (2007) In vitro scratch assay: a convenient and inexpensive method for analysis of cell migration in vitro. *Nat Protoc* **2**, 329-333
123. 2D and 3D Chemotaxis Assays Using µ-Slide Chemotaxis (Application Note 17). ibidi.
124. Livak, K. J., and Schmittgen, T. D. (2001) Analysis of relative gene expression data using real-time quantitative PCR and the 2(-Delta Delta C(T)) Method. *Methods* **25**, 402-408
125. Anders, S., and Huber, W. (2010) Differential expression analysis for sequence count data. *Genome Biol* **11**, R106
126. Smith, P. K., Krohn, R. I., Hermanson, G. T., Mallia, A. K., Gartner, F. H., Provenzano, M. D., Fujimoto, E. K., Goeke, N. M., Olson, B. J., and Klenk, D. C. (1985) Measurement of protein using bicinchoninic acid. *Anal Biochem* **150**, 76-85
127. Laemmli, U. K. (1970) Cleavage of structural proteins during the assembly of the head of bacteriophage T4. *Nature* **227**, 680-685
128. Littlehales, W. J. (1989) Electroblotting technique for transferring specimens from a polyacrylamide electrophoresis or like gel onto a membrane. Google Patents
129. Harada, N., Oda, Z., Hara, Y., Fujinami, K., Okawa, M., Ohbuchi, K., Yonemoto, M., Ikeda, Y., Ohwaki, K., Aragane, K., Tamai, Y., and Kusunoki, J. (2007) Hepatic de novo lipogenesis is present in liver-specific ACC1-deficient mice. *Mol Cell Biol* **27**, 1881-1888
130. Savage, D. B., Choi, C. S., Samuel, V. T., Liu, Z. X., Zhang, D., Wang, A., Zhang, X. M., Cline, G. W., Yu, X. X., Geisler, J. G., Bhanot, S., Monia, B. P., and Shulman, G. I. (2006) Reversal of diet-induced hepatic steatosis and hepatic insulin resistance by antisense oligonucleotide inhibitors of acetyl-CoA carboxylases 1 and 2. *J Clin Invest* **116**, 817-824
131. Fullerton, M. D., Galic, S., Marcinko, K., Sikkema, S., Pulinilkunnil, T., Chen, Z. P., O'Neill, H. M., Ford, R. J., Palanivel, R., O'Brien, M., Hardie, D. G., Macaulay, S. L., Schertzer, J. D., Dyck, J. R., van Denderen, B. J., Kemp, B. E., and Steinberg, G. R. (2013) Single phosphorylation sites in Acc1 and Acc2 regulate lipid homeostasis and the insulin-sensitizing effects of metformin. *Nat Med* **19**, 1649-1654
132. Baron, A., Migita, T., Tang, D., and Loda, M. (2004) Fatty acid synthase: a metabolic oncogene in prostate cancer? *J Cell Biochem* **91**, 47-53
133. Scott, K. E., Wheeler, F. B., Davis, A. L., Thomas, M. J., Ntambi, J. M., Seals, D. F., and Kridel, S. J. (2012) Metabolic regulation of invadopodia and invasion by acetyl-CoA carboxylase 1 and de novo lipogenesis. *PLoS One* **7**, e29761
134. Swinnen, J. V., Van Veldhoven, P. P., Timmermans, L., De Schrijver, E., Brusselmans, K., Vanderhoydonc, F., Van de Sande, T., Heemers, H., Heyns, W., and Verhoeven, G. (2003) Fatty acid synthase drives the synthesis of phospholipids partitioning into detergent-resistant membrane microdomains. *Biochem Biophys Res Commun* **302**, 898-903
135. Yeagle, P. L. (1985) Cholesterol and the cell membrane. *Biochim Biophys Acta* **822**, 267-287
136. Byfield, F. J., Aranda-Espinoza, H., Romanenko, V. G., Rothblat, G. H., and Levitan, I. (2004) Cholesterol depletion increases membrane stiffness of aortic endothelial cells. *Biophys J* **87**, 3336-3343
137. Zengel, P., Nguyen-Hoang, A., Schildhammer, C., Zantl, R., Kahl, V., and Horn, E. (2011) µ-Slide Chemotaxis: a new chamber for long-term chemotaxis studies. *BMC Cell Biol* **12**, 21
138. Baenke, F., Peck, B., Miess, H., and Schulze, A. (2013) Hooked on fat: the role of lipid synthesis in cancer metabolism and tumour development. *Dis Model Mech* **6**, 1353-1363
139. Liu, H., Liu, J. Y., Wu, X., and Zhang, J. T. (2010) Biochemistry, molecular biology, and pharmacology of fatty acid synthase, an emerging therapeutic target and diagnosis/prognosis marker. *Int J Biochem Mol Biol* **1**, 69-89

140. Mounier, C., Bouraoui, L., and Rassart, E. (2014) Lipogenesis in cancer progression (review). *Int J Oncol* **45**, 485-492
141. Wei, X., Schneider, J. G., Shenouda, S. M., Lee, A., Towler, D. A., Chakravarthy, M. V., Vita, J. A., and Semenkovich, C. F. (2011) De novo lipogenesis maintains vascular homeostasis through endothelial nitric-oxide synthase (eNOS) palmitoylation. *J Biol Chem* **286**, 2933-2945
142. Versari, D., Daghini, E., Virdis, A., Ghiadoni, L., and Taddei, S. (2009) Endothelial dysfunction as a target for prevention of cardiovascular disease. *Diabetes Care* **32 Suppl 2**, S314-321
143. Browne, C. D., Hindmarsh, E. J., and Smith, J. W. (2006) Inhibition of endothelial cell proliferation and angiogenesis by orlistat, a fatty acid synthase inhibitor. *FASEB J* **20**, 2027-2035
144. Seguin, F., Carvalho, M. A., Bastos, D. C., Agostini, M., Zecchin, K. G., Alvarez-Flores, M. P., Chudzinski-Tavassi, A. M., Coletta, R. D., and Graner, E. (2012) The fatty acid synthase inhibitor orlistat reduces experimental metastases and angiogenesis in B16-F10 melanomas. *Br J Cancer* **107**, 977-987
145. Patella, F., Schug, Z. T., Persi, E., Neilson, L. J., Erami, Z., Avanzato, D., Maione, F., Hernandez-Fernaud, J. R., Mackay, G., Zheng, L., Reid, S., Frezza, C., Giraudo, E., Fiorio Pla, A., Anderson, K., Ruppin, E., Gottlieb, E., and Zanivan, S. (2015) Proteomics-based metabolic modeling reveals that fatty acid oxidation (FAO) controls endothelial cell (EC) permeability. *Mol Cell Proteomics* **14**, 621-634
146. Schoors, S., Bruning, U., Missiaen, R., Queiroz, K. C., Borgers, G., Elia, I., Zecchin, A., Cantelmo, A. R., Christen, S., Goveia, J., Heggermont, W., Godde, L., Vinckier, S., Van Veldhoven, P. P., Eelen, G., Schoonjans, L., Gerhardt, H., Dewerchin, M., Baes, M., De Bock, K., Ghesquiere, B., Lunt, S. Y., Fendt, S. M., and Carmeliet, P. (2015) Fatty acid carbon is essential for dNTP synthesis in endothelial cells. *Nature* **520**, 192-197
147. De Bock, K., Georgiadou, M., Schoors, S., Kuchnio, A., Wong, B. W., Cantelmo, A. R., Quaegebeur, A., Ghesquiere, B., Cauwenberghs, S., Eelen, G., Phng, L. K., Betz, I., Tembuyser, B., Brepoels, K., Welti, J., Geudens, I., Segura, I., Cruys, B., Bifari, F., Decimo, I., Blanco, R., Wyns, S., Vangindertael, J., Rocha, S., Collins, R. T., Munck, S., Daelemans, D., Imamura, H., Devlieger, R., Rider, M., Van Veldhoven, P. P., Schuit, F., Bartrons, R., Hofkens, J., Fraisl, P., Telang, S., Deberardinis, R. J., Schoonjans, L., Vinckier, S., Chesney, J., Gerhardt, H., Dewerchin, M., and Carmeliet, P. (2013) Role of PFKFB3-driven glycolysis in vessel sprouting. *Cell* **154**, 651-663
148. Wakil, S. J., and Abu-Elheiga, L. A. (2009) Fatty acid metabolism: target for metabolic syndrome. *J Lipid Res* **50 Suppl**, S138-143
149. Bourbeau, M. P., and Bartberger, M. D. (2015) Recent advances in the development of acetyl-CoA carboxylase (ACC) inhibitors for the treatment of metabolic disease. *J Med Chem* **58**, 525-536
150. Abu-Elheiga, L., Matzuk, M. M., Kordari, P., Oh, W., Shaikenov, T., Gu, Z., and Wakil, S. J. (2005) Mutant mice lacking acetyl-CoA carboxylase 1 are embryonically lethal. *Proc Natl Acad Sci U S A* **102**, 12011-12016
151. Oh, W., Abu-Elheiga, L., Kordari, P., Gu, Z., Shaikenov, T., Chirala, S. S., and Wakil, S. J. (2005) Glucose and fat metabolism in adipose tissue of acetyl-CoA carboxylase 2 knockout mice. *Proc Natl Acad Sci U S A* **102**, 1384-1389
152. Choi, C. S., Savage, D. B., Abu-Elheiga, L., Liu, Z. X., Kim, S., Kulkarni, A., Distefano, A., Hwang, Y. J., Reznick, R. M., Codella, R., Zhang, D., Cline, G. W., Wakil, S. J., and Shulman, G. I. (2007) Continuous fat oxidation in acetyl-CoA carboxylase 2 knockout mice increases total energy expenditure, reduces fat mass, and improves insulin sensitivity. *Proc Natl Acad Sci U S A* **104**, 16480-16485

153. Hoehn, K. L., Turner, N., Swarbrick, M. M., Wilks, D., Preston, E., Phua, Y., Joshi, H., Furler, S. M., Larance, M., Hegarty, B. D., Leslie, S. J., Pickford, R., Hoy, A. J., Kraegen, E. W., James, D. E., and Cooney, G. J. (2010) Acute or chronic upregulation of mitochondrial fatty acid oxidation has no net effect on whole-body energy expenditure or adiposity. *Cell Metab* **11**, 70-76
154. Olson, D. P., Pulinilkunnil, T., Cline, G. W., Shulman, G. I., and Lowell, B. B. (2010) Gene knockout of Acc2 has little effect on body weight, fat mass, or food intake. *Proc Natl Acad Sci U S A* **107**, 7598-7603
155. Mao, J., DeMayo, F. J., Li, H., Abu-Elheiga, L., Gu, Z., Shaikenov, T. E., Kordari, P., Chirala, S. S., Heird, W. C., and Wakil, S. J. (2006) Liver-specific deletion of acetyl-CoA carboxylase 1 reduces hepatic triglyceride accumulation without affecting glucose homeostasis. *Proc Natl Acad Sci U S A* **103**, 8552-8557
156. Schrauwen, P., van Aggel-Leijssen, D. P., Hul, G., Wagenmakers, A. J., Vidal, H., Saris, W. H., and van Baak, M. A. (2002) The effect of a 3-month low-intensity endurance training program on fat oxidation and acetyl-CoA carboxylase-2 expression. *Diabetes* **51**, 2220-2226
157. Bandyopadhyay, G. K., Yu, J. G., Ofrecio, J., and Olefsky, J. M. (2006) Increased malonyl-CoA levels in muscle from obese and type 2 diabetic subjects lead to decreased fatty acid oxidation and increased lipogenesis; thiazolidinedione treatment reverses these defects. *Diabetes* **55**, 2277-2285
158. Musi, N., Hirshman, M. F., Nygren, J., Svanfeldt, M., Bavenholm, P., Rooyackers, O., Zhou, G., Williamson, J. M., Ljunqvist, O., Efendic, S., Moller, D. E., Thorell, A., and Goodyear, L. J. (2002) Metformin increases AMP-activated protein kinase activity in skeletal muscle of subjects with type 2 diabetes. *Diabetes* **51**, 2074-2081
159. Jump, D. B., Torres-Gonzalez, M., and Olson, L. K. (2011) Soraphen A, an inhibitor of acetyl CoA carboxylase activity, interferes with fatty acid elongation. *Biochem Pharmacol* **81**, 649-660
160. Lu, H., Li, X., Luo, Z., Liu, J., and Fan, Z. (2013) Cetuximab reverses the Warburg effect by inhibiting HIF-1-regulated LDH-A. *Mol Cancer Ther* **12**, 2187-2199
161. Luwor, R. B., Lu, Y., Li, X., Mendelsohn, J., and Fan, Z. (2005) The antiepidermal growth factor receptor monoclonal antibody cetuximab/C225 reduces hypoxia-inducible factor-1 alpha, leading to transcriptional inhibition of vascular endothelial growth factor expression. *Oncogene* **24**, 4433-4441
162. Semenza, G. L. (2010) HIF-1: upstream and downstream of cancer metabolism. *Curr Opin Genet Dev* **20**, 51-56
163. Warburg, O. (1956) On the origin of cancer cells. *Science* **123**, 309-314
164. Luo, J., Hong, Y., Lu, Y., Qiu, S., Chaganty, B. K., Zhang, L., Wang, X., Li, Q., and Fan, Z. (2017) Acetyl-CoA carboxylase rewires cancer metabolism to allow cancer cells to survive inhibition of the Warburg effect by cetuximab. *Cancer Lett* **384**, 39-49
165. Svensson, R. U., and Shaw, R. J. (2016) Lipid Synthesis Is a Metabolic Liability of Non-Small Cell Lung Cancer. *Cold Spring Harb Symp Quant Biol* **81**, 93-103
166. Beckers, A., Organe, S., Timmermans, L., Scheys, K., Peeters, A., Brusselmans, K., Verhoeven, G., and Swinnen, J. V. (2007) Chemical inhibition of acetyl-CoA carboxylase induces growth arrest and cytotoxicity selectively in cancer cells. *Cancer Res* **67**, 8180-8187
167. Griffith, D. A., Kung, D. W., Esler, W. P., Amor, P. A., Bagley, S. W., Beysen, C., Carvajal-Gonzalez, S., Doran, S. D., Limberakis, C., Mathiowetz, A. M., McPherson, K., Price, D. A., Ravussin, E., Sonnenberg, G. E., Southers, J. A., Sweet, L. J., Turner, S. M., and Vajdos, F. F. (2014) Decreasing the rate of metabolic ketone reduction in the discovery of a clinical acetyl-CoA carboxylase inhibitor for the treatment of diabetes. *J Med Chem* **57**, 10512-10526

168. Neuschwander-Tetri, B. A. (2010) Hepatic lipotoxicity and the pathogenesis of nonalcoholic steatohepatitis: the central role of nontriglyceride fatty acid metabolites. *Hepatology* **52**, 774-788
169. Saggerson, D. (2008) Malonyl-CoA, a key signaling molecule in mammalian cells. *Annu Rev Nutr* **28**, 253-272
170. Olsen, A. M., Eisenberg, B. L., Kuemmerle, N. B., Flanagan, A. J., Morganelli, P. M., Lombardo, P. S., Swinnen, J. V., and Kinlaw, W. B. (2010) Fatty acid synthesis is a therapeutic target in human liposarcoma. *Int J Oncol* **36**, 1309-1314
171. Stoiber, K., Naglo, O., Pernpeintner, C., Zhang, S., Koeberle, A., Ulrich, M., Werz, O., Muller, R., Zahler, S., Lohmuller, T., Feldmann, J., and Braig, S. (2017) Targeting de novo lipogenesis as a novel approach in anti-cancer therapy. *Br J Cancer*
172. Teuwen, L. A., Draoui, N., Dubois, C., and Carmeliet, P. (2017) Endothelial cell metabolism: an update anno 2017. *Curr Opin Hematol* **24**, 240-247
173. Galbraith, C. G., Yamada, K. M., and Galbraith, J. A. (2007) Polymerizing actin fibers position integrins primed to probe for adhesion sites. *Science* **315**, 992-995
174. Seano, G., and Primo, L. (2015) Podosomes and invadopodia: tools to breach vascular basement membrane. *Cell Cycle* **14**, 1370-1374
175. Gimona, M., Buccione, R., Courtneidge, S. A., and Linder, S. (2008) Assembly and biological role of podosomes and invadopodia. *Curr Opin Cell Biol* **20**, 235-241
176. Gimona, M., and Buccione, R. (2006) Adhesions that mediate invasion. *Int J Biochem Cell Biol* **38**, 1875-1892
177. Yamaguchi, H., and Oikawa, T. (2010) Membrane lipids in invadopodia and podosomes: key structures for cancer invasion and metastasis. *Oncotarget* **1**, 320-328
178. Yamaguchi, H., Yoshida, S., Muroi, E., Kawamura, M., Kouchi, Z., Nakamura, Y., Sakai, R., and Fukami, K. (2010) Phosphatidylinositol 4,5-bisphosphate and PIP5-kinase Ialpha are required for invadopodia formation in human breast cancer cells. *Cancer Sci* **101**, 1632-1638
179. Berro, J., Michelot, A., Blanchoin, L., Kovar, D. R., and Martiel, J. L. (2007) Attachment conditions control actin filament buckling and the production of forces. *Biophys J* **92**, 2546-2558
180. Vander Heiden, M. G. (2013) Exploiting tumor metabolism: challenges for clinical translation. *J Clin Invest* **123**, 3648-3651
181. Sukharev, S. (1999) Mechanosensitive channels in bacteria as membrane tension reporters. *FASEB J* **13 Suppl**, S55-61
182. Maeda, T., Wurgler-Murphy, S. M., and Saito, H. (1994) A two-component system that regulates an osmosensing MAP kinase cascade in yeast. *Nature* **369**, 242-245
183. Tokishita, S., Yamada, H., Aiba, H., and Mizuno, T. (1990) Transmembrane signal transduction and osmoregulation in Escherichia coli: II. The osmotic sensor, EnvZ, located in the isolated cytoplasmic membrane displays its phosphorylation and dephosphorylation abilities as to the activator protein, OmpR. *J Biochem* **108**, 488-493
184. Sugiura, A., Hirokawa, K., Nakashima, K., and Mizuno, T. (1994) Signal-sensing mechanisms of the putative osmosensor KdpD in Escherichia coli. *Mol Microbiol* **14**, 929-938
185. Los, D. A., and Murata, N. (2000) Regulation of enzymatic activity and gene expression by membrane fluidity. *Sci STKE* **2000**, pe1
186. Haidekker, M. A., L'Heureux, N., and Frangos, J. A. (2000) Fluid shear stress increases membrane fluidity in endothelial cells: a study with DCVJ fluorescence. *Am J Physiol Heart Circ Physiol* **278**, H1401-1406
187. Gudi, S., Nolan, J. P., and Frangos, J. A. (1998) Modulation of GTPase activity of G proteins by fluid shear stress and phospholipid composition. *Proc Natl Acad Sci U S A* **95**, 2515-2519

188. Rawicz, W., Olbrich, K. C., McIntosh, T., Needham, D., and Evans, E. (2000) Effect of chain length and unsaturation on elasticity of lipid bilayers. *Biophys J* **79**, 328-339
189. Pritchard, K. A., Jr., Schwarz, S. M., Medow, M. S., and Stemerman, M. B. (1991) Effect of low-density lipoprotein on endothelial cell membrane fluidity and mononuclear cell attachment. *Am J Physiol* **260**, C43-49
190. Braig, S., Schmidt, B. S., Stoiber, K., Händel, C., Möhn, T., Werz, O., Müller, R., Zahler, S., Koeberle, A., and Käs, J. A. (2015) Pharmacological targeting of membrane rigidity: implications on cancer cell migration and invasion. *New J Phys* **17**, 083007

7 APPENDIX

7.1 Abbreviations

Table 15: List of abbreviations

Abbreviations	Full name
% (v/v)	Volume percentage rate
% (w/v)	Weight per volume
Å	Ångström
ACC	Acetyl-CoA carboxylase
AMPK	Adenosine monophosphate-activated protein kinase
Aqua dest.	Aqua destillata
BC	Biotin carboxylase
BCCP	Biotin carboxyl-carrier protein
bFGF	Basic fibroblast growth factor
Bkg	Background
BSA	Bovine serum albumin
CAPS	3-(Cyclohexylamino)-1-propanesulfonic acid
cDNA	Complementary DNA
CT	Carboxyltransferase
DMEM	Dulbecco's modified Eagle's medium
DMSO	Dimethyl sulfoxide
DNA	Deoxyribonucleic acid
DOPG	Dioleoylphosphatidylglycerol
EC	Endothelial cell
ECGM	Endothelial cell growth medium
ECL	Enhanced chemiluminescence
EGF	Epidermal growth factor
eNOS	Endothelial nitric oxide synthase
FACS	Fluorescence-activated cell sorting
FAS	Fatty acid synthase
FBS	Fetal bovine serum
FGF-2	Fibroblast growth factor
FMI:Y	Forward migration index
Gf	Grating factor

Table 15: continue list of abbreviations

Abbreviations	Full name
HBSS	Hanks' balanced salt solution
HFS	Hypotonic fluorochrome solution
HGF	Hepatocyte growth factor
HMEC	Human microvascular endothelial cell
HRP	Horseradish peroxidase
HUVEC	Human umbilical vein endothelial cell
IC_{50}	Half maximal inhibitory concentration
LDH	Lactate dehydrogenase
log	Logarithm
MUFA	Ponounsaturated fatty acid
PAF	Platelet-activating factor
PAGE	Polyacrylamide gel electrophoresis
PBS	Phosphate buffered saline
PC	Phosphatidylcholine
PDGF	Platelet-derived growth factor
PE	Phosphatidylethanolamine
PG	Phosphatidylglycerol
PI	Phosphatidylinositol
PIPES	1,4-Piperazinediethanesulfonic acid
PL	Phospholipid
PS	Phosphatidylserine
PUFA	Polyunsaturated fatty acid
PVDF	Polyvinylidene difluoride
qPCR	Quantitative polymerase chain reaction
RNA	Ribonucleic acid
RT	Room temperature
S.E.M	Standard error of the mean
SDS	Sodium dodecyl sulfate
SFA	Saturated fatty acids
siRNA	Small interfering RNA
SorA	Soraphen A

Table 15: continue list of abbreviations

Abbreviations	Full name
STS	Staurosporine
TBS	Tris-buffered saline
TBS-T	Tris-buffered saline with Tween 20
TGF-β	Transforming growth factor-β
TMA-DPH	Trimethylammonium diphenylhexatriene
TNF-α	Tumor necrosis factor-α
TOFA	5-Tetradecyloxy-2-furonic acid
UPLC-MS/MS	Ultra-performance liquid chromatography-coupled electrospray ionization tandem mass spectrometry
VEGF	Vascular endothelial growth factor

7.2 List of figures

7.3 List of tables

7.4 Publications

7.4.1 Articles

Daniel K. Glatzel, Andreas Koeberle, Helmut Pein, Konstantin Loeser, Anna Stark, Nelli Keksel, Oliver Werz, Rolf Müller, Iris Bischoff, Robert Fürst. "**Acetyl-CoA carboxylase 1 regulates endothelial cell migration by shifting the phospholipid composition.**" *Journal of Lipid Resarch* (2017) [Epub ahead of print].

Gulen I. Kaya, Kubra Uzun, Buket Bozkurt, Mustafa A Onur, Nehir U Somer, Daniel K. Glatzel, Robert Fürst. "**Chemical characterization and biological activity of an endemic Amaryllidaceae species: Galanthus cilicicus**." *South African Journal of Botany* 108 (2017): 256-260.

Karin Meirer, Daniel Glatzel, Simon Kretschmer, Sandra K. Wittmann, Markus Hartmann, René Blöcher, Carlo Angioni, Gerd Geisslinger, Dieter Steinhilber, Bettina Hofmann, Robert Fürst, Ewgenij Proschak. "**Design, Synthesis and Cellular Characterization of a Dual Inhibitor of 5-Lipoxygenase and Soluble Epoxide Hydrolase**." *Molecules* 22.1 (2016): 45.

Oliver G. Rössler, Daniel Glatzel, Gerald Thiel. "**Resveratrol upregulates Egr-1 expression and activity involving extracellular signal-regulated protein kinase and ternary complex factors**." *Experimental cell research* 332.1 (2015): 116-127.

7.4.2 Oral and poster presentation

Daniel K. Glatzel; **Acetyl-CoA Carboxylase (ACC) Regulates the Migration of Primary Endothelial Cells,** 29. Irseer Naturstofftage, February 23, 2017, Irsee, Germany. (Short Talk)

Daniel K. Glatzel, Nelli Keksel, Andreas Koeberle, Oliver Werz, Mukul Ashtikar, Rolf Müller, Robert Fürst; **The acetyl-CoA carboxylase (ACC) inhibitor soraphen A blocks the migration of primary endothelial cells by shifting the cell membranes' composition of fatty acids**; 29. Irseer Naturstofftage, February 22-24, 2017, Irsee, Germany. (Poster presentation)

Daniel Glatzel, Rolf Müller, Andreas Koeberle, Oliver Werz, Robert Fürst; **The acetyl-CoA carboxylase (ACC) inhibitor soraphen blocks the proliferation and migration of primary endothelial cells**; 82nd Annual Meeting of the German Society for Experimental and Clinical Pharmacology and Toxicology (DGPT), February 29-March 3, 2016, Berlin, Germany. (Poster presentation)

Daniel Glatzel, Rolf Müller, Andreas Koeberle, Oliver Werz, Robert Fürst; **The acetyl-CoA carboxylase (ACC) inhibitor soraphen blocks the proliferation and migration of primary endothelial cells**; Deutsche Pharmazeutische Gesellschaft (DPhG) Jahrestagung 2015 / German Pharmaceutical Society, Annual meeting, September 23-25, 2015, Düsseldorf, Germany. (Poster presentation)

Daniel K. Glatzel, Iris Bischoff, Rolf Müller, Andreas Koeberle, Robert Fürst; **The acetyl-CoA carboxylase (ACC) inhibitor soraphen A blocks the proliferation and migration of primary endothelial cells**; German Pharm-Tox Summit, 81nd Annual Meeting of the German Society for Experimental and Clinical Pharmacology and Toxicology (DGPT), March 9-13, 2015, Kiel, Germany. (Poster presentation)

7.5 Danksagung

Zuerst möchte ich mich bei Prof. Robert Fürst bedanken. Vielen Dank für die Möglichkeit an diesem Lehrstuhl zu promovieren, für die professionelle Unterstützung und die erstklassige Betreuung während meiner gesamten Zeit. Im großen Maß schätze ich den wissenschaftlichen Input, die aufschlussreichen Diskussionen und das stets motivierende Vertrauen, das du mir und meinen Ideen entgegengebracht hast. Danke für die Möglichkeit an zahlreichen wissenschaftlichen Konferenzen teilzunehmen, um dort meine Arbeit der Fachwelt zu präsentieren und danke für die Gelegenheit mit vielen anderen Instituten zusammenzuarbeiten, wodurch ich meine wissenschaftliche Expertise stets ausbauen konnte. Ich bin sehr stolz darauf, dass ich ein Teil der Arbeitsgruppe Fürst sowie der Pharmazeutischen Biologie und der Goethe Universität Frankfurt werden konnte.

Ein nicht minder großer Dank geht an Prof. Rolf Marschalek für die aufgebrachte Zeit und Arbeit als Zweitgutachter meiner Dissertation sowie für die vielen interessanten Ideen zu meinem Projekt. Danke auch allen anderen Mitgliedern der Prüfungskommission.

Ein besonderer Dank geht auch an meine Kooperationspartner für ihre wissenschaftliche Unterstützung und die hilfreichen Ideen, die meine Arbeit in einem besonderen Maße bereichert haben. Vielen Dank an Dr. Andreas Koeberle für die tatkräftige experimentelle Unterstützung und die wissenschaftliche Hilfestellung. Mein Dank geht auch an Prof. Oliver Werz, Helmut Pein, Konstantin Löser sowie Prof. Hanns Häberlein, Nelli Keksel, Dr. Mukul Ashtikar und Prof. Rolf Müller. Ich danke der Deutschen Forschungsgemeinschaft (FOR 1406, FU 691/9-2) für die Finanzierung des Projektes.

Vielen Dank an Dr. Iris Bischoff für die Zusammenarbeit, Unterstützung und die unterhaltsame Zeit auf vielen Konferenzen. Ich möchte mich auch für die Hilfe von Dr. Ilse Zündorf, Dr. Claus Meyer und Dr. Simone Braig bedanken.

Ebenfalls vielen Dank an alle ehemaligen und aktuellen Mitglieder des Arbeitskreises für die erfolgreiche Zusammenarbeit am Institut: Alessa, Anna Lena, Annemarie, Betty, Freia, Jacqueline, Jenni, Laura, Melissa, Mona, Rebecca, Silvia, Valerie und allen nicht namentlich genannten Mitarbeitern. Danke Mareike für die tatkräftige Unterstützung besonderes gegen Ende meiner Doktorarbeit. Auch vielen Dank an Frieder dafür, dass du als Masterrand mit deiner

fleißigen und positiven Einstellung Teil des Soraphen-Projektes geworden bist. Ein ganz besonderer Dank gilt Anna und Ashkan. Ihr habt mich stets unterstützt, an mich geglaubt und mir eine schöne Zeit bereitet. Ich bin froh euch kennen gelernt zu haben und hoffe, dass unsere Freundschaft auch weiterhin bestehen bleibt.

Ich danke auch meinen Freunden. Danke, dass ich zum Ausgleich gegenüber stressigen Zeiten viel Spaß mit euch haben konnte. Yvonne, dir möchte ich im besonderen Maße danken. Du hast mich unterstützt, wann immer es möglich war. Vielen Dank für deine kritischen Kommentare, deine großzügige Hilfe und deinen wissenschaftlichen Rat.

Zu guter Letzt danke ich meiner ganzen Familie. Ihr seid die beste Familie, die man sich vorstellen kann. Von Kindesbeinen an habt ihr mir die Welt erklärt und all meine Fragen beantwortet. Auch noch heute schätze ich euren Rat und eure Meinung. Die tiefe Dankbarkeit gegenüber meinen Eltern, die mich nicht nur finanziell und moralisch unterstützt haben, lässt sich kaum in Worte fassen: Mama, Papa, Dominik, ich danke euch für Alles! Ihr wart und seid stets der wichtigste Ankerpunkt in meinem Leben und meine besten und größten Motivatoren. Ich danke euch von tiefsten Herzen für die viele Liebe und das Lachen. Ohne euch wäre dies alles nicht möglich gewesen. Danke!